

Diploma Thesis

**Spectral Densities of the  $\tau$  Lepton in a  
Global  $U(2)_L \times U(2)_R$  Linear Sigma Model  
with Electroweak Interaction**

**Anja Habersetzer**

Johann Wolfgang Goethe-Universität  
Frankfurt am Main

19 September 2011

# Contents

<b>1</b>	<b>Introduction</b>	<b>1</b>
1.1	Standard Model . . . . .	2
1.2	Quantum Chromodynamics . . . . .	7
1.3	Chiral Symmetry . . . . .	10
1.3.1	Chiral Currents and Symmetry Breaking . . . . .	12
1.3.2	Spontaneously Broken Chiral Symmetry . . . . .	17
1.4	Glashow-Weinberg-Salam Theory . . . . .	21
<b>2</b>	<b>Linear Sigma Model and Electroweak Interaction</b>	<b>29</b>
2.1	The Linear Sigma Model . . . . .	29
2.1.1	Spontaneous Symmetry Breaking, Field Renormalisation, and Mass Terms . . . . .	34
2.2	$SU(2)_L \times U(1)_Y$ and Weak Interaction . . . . .	45
2.2.1	$U(1)_Y$ Transformation . . . . .	45
2.2.2	Vector Meson Dominance . . . . .	48
2.2.3	Electroweak Interactions . . . . .	50
2.2.4	Weinberg Mixing, Field Strength Tensors $L^{\mu\nu}, R^{\mu\nu}$ . . . . .	53
2.2.5	The $W\rho$ Vertex . . . . .	55
2.2.6	The Lagrange Density with Electroweak Interactions . . . . .	56
<b>3</b>	<b>Tree-Level Vertices</b>	<b>58</b>
3.1	$\tau \rightarrow W\nu_\tau$ Vertex . . . . .	59
3.2	Vector Channel . . . . .	60
3.2.1	$2\pi$ Vector Channel . . . . .	60
3.2.2	$4\pi$ Vector Channel . . . . .	65
3.3	Axial-Vector Channel . . . . .	66
3.3.1	$3\pi$ Axial-Vector Channel . . . . .	67
3.3.2	$5\pi$ Axial-Vector Channel . . . . .	69
<b>4</b>	<b>Decay Widths and Spectral Functions</b>	<b>70</b>
4.1	Källén-Lehmann Representation and Optical Theorem . . . . .	70
4.2	Interacting Lagrangian and Spectral Functions . . . . .	71

4.3	ALEPH Spectral Functions and their Parametrisation within the Linear Sigma Model . . . . .	73
<b>5</b>	<b>Vector Channel Spectral Function</b>	<b>76</b>
5.1	First Estimate of the Parameter $\delta$ . . . . .	77
5.1.1	The Breit-Wigner Spectral Density and the fully $s$ -Dependent Spectral Density . . . . .	78
5.2	Breit-Wigner Spectral Density . . . . .	79
5.3	Spectral Density based on the $s$ -Dependent Decay Width $\Gamma_{\rho^- \rightarrow \pi^- \pi^0}(s)$ from the Linear Sigma Model . . . . .	81
5.3.1	Fitted Spectral Function based on $\Gamma_{\rho^- \rightarrow \pi^- \pi^0}(s)$ . . . . .	82
5.3.2	Comparison to Breit-Wigner with fitted Parameters $\delta$ and $m_\rho$ . . . . .	85
5.4	Comparison to other Parametrisations for the $W\rho$ Vertex and the $s$ -Dependent $\rho$ Decay Width . . . . .	86
5.4.1	Momentum-Independent $W\rho$ Mixing . . . . .	86
5.4.2	Two other Parametrisations of the $\rho$ Decay Width . . . . .	89
<b>6</b>	<b>Axial-Vector Channel Spectral Function</b>	<b>93</b>
6.1	Breit-Wigner Spectral Density . . . . .	93
6.2	Estimates of the Parameters $Z$ and $\delta$ . . . . .	97
6.2.1	Pion Renormalisation Constant $Z$ . . . . .	98
6.2.2	Vector Coupling $\delta$ . . . . .	101
6.3	Axial-Vector Spectral Density based on the Elastic Decay Width $a_1 \rightarrow \rho\pi$ from the Linear Sigma Model . . . . .	103
6.4	Fitted Axial-Vector Spectral Density . . . . .	105
<b>7</b>	<b>Conclusions and Outlook</b>	<b>109</b>
<b>A</b>	<b>Field Strength Tensors <math>L^{\mu\nu}</math> and <math>R^{\mu\nu}</math></b>	<b>112</b>
<b>B</b>	<b><math>W\rho</math> Vertex</b>	<b>115</b>
<b>C</b>	<b>Invariant Mass-Squared Distribution</b>	<b>116</b>
<b>D</b>	<b><math>\tau \rightarrow W\nu_\tau</math> Decay Width</b>	<b>118</b>
	<b>Bibliography</b>	<b>122</b>

# Chapter 1

## Introduction

This work is dedicated to the study of the vector and axial-vector spectral functions of the  $\tau$  lepton within the framework of a  $U(2)_L \times U(2)_R$  Linear Sigma Model with electroweak interaction. As an effective field theory the Linear Sigma Model describes hadronic degrees of freedom based on the symmetries of the Standard Model of Particle Physics. Therefore, the following section aims at giving a general and concise introduction to the Standard Model and the meaning of symmetries for contemporary elementary particle physics. In the next section the  $SU(3)_C$  symmetry group will be discussed in short, followed by an introduction to chiral symmetry  $SU(2)_L \times SU(2)_R$ . In the last section of this chapter the Glashow-Weinberg-Salam theory of the local group  $SU(2)_L \times U(1)_Y$  is presented. Important concepts of the theoretical framework of the Standard Model, such as the Noether Theorem, the Gauge Principle, Spontaneous Symmetry Breaking, and the Higgs Mechanism will be introduced in the context of these three symmetry groups. In Chapter 2 it will be first shown how the symmetries of the Standard Model are realised within the global  $U(2)_L \times U(2)_R$  Linear Sigma Model and how electroweak interactions can be introduced to the model on the basis of local  $SU(2)_L \times U(1)_Y$  symmetry transformations of the hadronic degrees of freedom. The vertices that are relevant for the vector and axial-vector decay channels in weak  $\tau$  decay are extracted from the Lagrangian with electroweak interaction in Chapter 3. This is followed by a short introduction to the Källén-Lehmann Representation of spectral functions and how these can be parametrised within the framework of this model (Chapter 4). The results of the vector and axial-vector spectral functions are presented in Chapter 5 and 6.

## 1.1 Standard Model

The forces that create and act on matter can be brought down to four fundamental interaction types; gravitation, electromagnetism, weak interaction and strong interaction. The attempt to unify these interactions within one theory has been a difficult task during the last century.

Electromagnetic phenomena were seen to be materialisations of two different forces; electricity and magnetism and it is already about 150 years ago since it is known that magnetism and electricity can actually be traced back to the same source. In 1865 James Clerk Maxwell explained with the Maxwell equations the relations between the spatial and time dependencies of the electric and magnetic fields  $\vec{E}$  and  $\vec{B}$  [1]. Since then, the question what kind of phenomena, electricity or magnetism, is observed, has become solely a question of the reference frame. After the formulation of Einstein's special relativity in the framework of the four-dimensional Minkowski space, it was discovered that the Maxwell equations were already covariant under Lorentz transformations. They could now be written in a profound, yet simple way

$$\begin{aligned}\partial_\mu F^{\mu\nu} &= \mu_0 j^\nu, & F^{\mu\nu} &= \partial^\mu A^\nu - \partial^\nu A^\mu, \\ \partial^\lambda F^{\mu\nu} + \partial^\mu F^{\nu\lambda} + \partial^\nu F^{\lambda\mu} &= 0,\end{aligned}\tag{1.1}$$

where  $F^{\mu\nu}$  is the field strength tensor of the electromagnetic four potential  $A^\mu = (\varphi, \vec{A})$ .

In the late 1940s Richard Feynman, Freeman Dyson and Julian Schwinger developed Quantum Electrodynamics (QED) as a Lagrangian-derived quantum field theory for the electromagnetic phenomena. The electromagnetic potential  $A^\mu$  is now associated with the photon field and arises naturally as the gauge boson of a theory with local  $U(1)$  symmetry.

Now, ever since the success of QED as a local quantum field theory, based on the group  $U(1)$ , many physicists believe that all of the known four fundamental interactions ought to be described in the framework of local quantum field theories, where the interaction between matter fields is generated through the presence of gauge fields. So far, that has been successfully achieved for weak and strong interactions while the development of a theory of quantum gravity still faces problems.

The *Standard Model of Particle Physics* describes all matter and its interactions on a microscopic scale where the effects of gravity are negligible. It is based on a Lagrange density whose degrees of freedom are fields that, after canonical quantisation, represent wave functions of particles in space time and a local  $SU(3)_C \times SU(2)_L \times U(1)_Y$  symmetry group. To each symmetry group correspond interaction fields (gauge bosons) and matter fields

(fermions). The fermions itself are divided in six quarks and six leptons and they are organised with increasing masses in three *flavour* families each (see Table 1.1).

Quarks			Leptons		
Flavour	Mass	electric charge $e$	Flavour	Mass	electric charge $e$
u	1.5 to 3.3 MeV	2/3	$\nu_e$		0
d	3.5 to 6.0 MeV	-1/3	$e^-$	0.51 MeV	-1
s	105 MeV	-1/3	$\nu_\mu$		0
c	1.27 GeV	2/3	$\mu^-$	105.66 MeV	-1
b	4.20 GeV	-1/3	$\nu_\tau$		0
t	171.3 GeV	2/3	$\tau^-$	1.78 GeV	-1

Table 1.1: Fermion families

While quarks carry the quantum numbers *colour*, *electromagnetic charge* and *weak isospin* and are thus subject to all three fundamental interactions, leptons only carry electromagnetic charge and weak isospin. The *Glashow-Weinberg-Salam Theory of Weak Interaction* (GWS) describes electromagnetic and weak interactions among quarks and leptons by means of a local  $SU(2)_L \times U(1)_Y$  symmetry group. *Quantum Chromodynamics* (QCD) describes the strong interaction between quarks on the base of a local  $SU(3)_C$  group. Both, GWS and QCD, are so-called gauge theories where the interaction fields arise from the requirement of invariance of the Lagrangian under the transformations of the fields. An additional term in the Lagrange density, the properly normalized square of the field strength tensor, generates the gauge field self interactions.

The electroweak phenomena of  $SU(2)_L \times U(1)_Y$  are created by three massive weak bosons ( $W^\pm$ ,  $Z^0$ ) and the massless photon. The requirement that the Lagrangian should remain invariant under local  $SU(2)_Y$  gauge transformations was challenged by the observed masses of the weak bosons, since a mass term would violate the symmetry. The skilful use of the concept of Spontaneous Symmetry Breaking plus the introduction of a scalar background field, the Higgs field, solved that problem.

For  $SU(3)_C$  there are eight massless gluons that generate the force holding the coloured quarks confined. Due to confinement, neither quarks nor gluons exist as single particle states. They only appear in colour-neutral bound states of, e.g., mesons ( $\bar{q}q$ ) and baryons ( $qqq$ ). The existence of other colour-neutral bound states, such as *glueballs* and *tetraquarks*, is currently under research. Although lattice calculations yield strong evidence for its existence, the glueball has not yet been unambiguously identified.

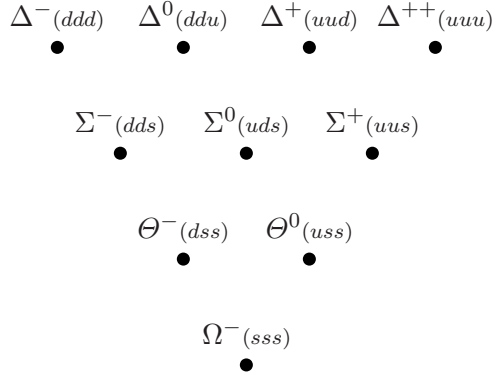


Figure 1.1: The  $SU(N_F = 3)$  baryon decuplet with  $I^P = 3/2^+$ .

While the leptonic fermions were already known and partly proven experimentally, quarks were introduced as auxiliary degrees of freedom<sup>1</sup> that allowed to organise the growing number of observed particles and resonances during the second half of last century. On the base of Wigner's group theory developments hadrons could now be understood as multiplets of states whose properties were explained by their quark content. For example the baryon decuplet (Fig. 1.1) and the meson octet (Fig. 1.2) can be organised as the 10, resp. 8, representations of  $SU(N_f = 3)$ , with  $N_f$  referring to the number of quark flavours. Based on the assumption that the quarks might become massless for very high energies, the flavour group describes the quarks as a degenerate multiplet under  $U(N_f)$  flavour transformations.

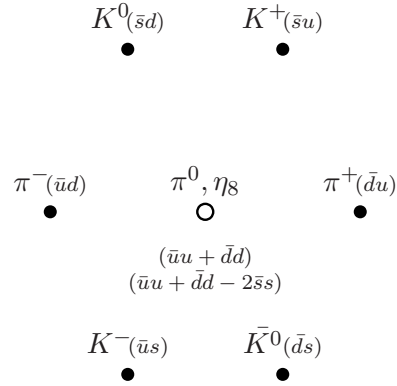


Figure 1.2: The  $SU(N_F = 3)$  pseudoscalar meson octet.

---

<sup>1</sup>Gell-Mann discusses a unitary symmetry group on the base of a set of *fictitious* "leptons" which [are degenerate in their mass and] *may have nothing to do with real leptons but help to fix the physical ideas in a rather graphic way*. He also proposed the algebraic structure of the internal space of the quarks (colour space) and although he did not explicitly mention the gluons as carrier of strong interaction he pointed out that there might be an interacting vector field analogously to the  $U(1)$  gauge field of QED [2].

Although, at first, this idea was heavily disputed, experimental evidence for quarks as fundamental building blocks of hadrons was given only few years later by results of pion nucleon collisions at Brookhaven National Laboratory in 1970 [3]. These were explained by Drell and Yan in terms of partons (nucleon constituents) that carry only a fraction of the charge of the electron. Two partons, a quark of the nucleon and an antiquark of the pion annihilate into a photon which in turn decays into a lepton pair  $\mu^+\mu^-$  with the cross section being proportional to the squared quark charge. For collisions of  $\pi^- = \bar{u}d$  ( $\pi^+ = u\bar{d}$ ) with  ${}^{12}C = 18u + 18d$  the theoretical prediction for the ratio of the two cross sections is

$$\begin{aligned}\sigma(\pi^+N \rightarrow \mu^+\mu^-) &\simeq 18Q_d^2 = 18\left(\frac{1}{9}\right), \\ \sigma(\pi^-N \rightarrow \mu^+\mu^-) &\simeq 18Q_u^2 = 18\left(\frac{4}{9}\right) \\ R_{\text{th.}} &= \frac{\sigma(\pi^+N \rightarrow \mu^+\mu^-)}{\sigma(\pi^-N \rightarrow \mu^+\mu^-)} = \frac{1}{4}.\end{aligned}\tag{1.2}$$

This agrees with the results from the experiment<sup>2</sup> where the ratio for the two cross sections is

$$R_{\text{exp}} = \frac{1}{4}.$$

However, some resonances (e.g.,  $\Delta^{++}$ ) could only be explained as bound states of three quarks with same flavour and spin. But as spin 1/2 particles quarks have to obey Fermi-Dirac-Statistics and thus, follow Pauli's exclusion principle. For  $\Delta^{++} = u\uparrow u\uparrow u\uparrow$  Pauli's exclusion principle seemed to be clearly violated and enforced the necessity of another additional degree of freedom, colour.

The idea of colour as a new charge of the quarks was supported by the results of  $e^+e^-$  annihilations at high energies as they were performed since 1967 at Stanford Linear Accelerator Center (SLAC). The ratio of the cross sections  $\sigma(e^+e^- \rightarrow \bar{q}q)$  and  $\sigma(e^+e^- \rightarrow \mu^+\mu^-)$  could only be explained by a factor  $N_C$ , accounting for the three additional colour degrees of freedom;

$$R = \frac{\sigma(e^+e^- \rightarrow \text{hadrons})}{\sigma(e^+e^- \rightarrow \mu^+\mu^-)} = N_C \sum Q_q^2 = 3\left(\frac{4}{9} + \frac{1}{9} + \frac{1}{9}\right) = 2.\tag{1.3}$$

Another reason for the success of the Standard model were predictions made about the existence of new particles that up to that time had not been dis-

---

<sup>2</sup>This example is, e.g., found in [4].



covered<sup>3</sup>. Chapter IV in [5] gives a comprehensive overview about experiments that led to broad acceptance of the idea of quarks being coloured constituents of matter carrying fractional electromagnetic charges.

Furthermore, reflections on symmetries do not only allow for organising particles within multiplets or describing interactions as exchange of gauge bosons. They also give insight into the profound nature of conservation laws. In the theoretical framework of the Standard Model (*Quantum Field Theory*, QFT) the symmetry properties of the particle multiplets are reflected in the associated Lagrange density which then itself has to be invariant under transformations of the fields. Invariance of a Lagrangian under certain transformations then automatically leads to symmetric equations of motion. Now, the *Noether Theorem* states that to each independent symmetry transformation of the degrees of freedom corresponds a conserved quantity, the *Noether Current* and that to each conserved current corresponds a conserved charge.

There are external symmetries, described by the Poincare group<sup>4</sup>, and internal symmetries that refer to intrinsic particle properties as, e.g., strong and weak isospin and electric charge. Global internal symmetries lead to the classification of particles within multiplets, while local internal symmetries lead to gauge bosons that generate interactions.

A transformation is called global if its parameter is constant and local if the parameter is space-time dependent. Requiring invariance of the Lagrangian under local transformations of the matter fields then deduces the existence of massless spin-1 fields, the gauge bosons that couple to the conserved charges. The result is a new, covariant derivative that transforms as the fields themselves so that the Lagrangian remains invariant and the dynamics between fermions and gauge bosons is generated in the covariant derivative<sup>5</sup>.

Thus, examining the symmetry properties does not only yield important constraints on the Lagrangian and the allowed interactions between particles, but also yields observable conserved currents and the interactions among them.

---

<sup>3</sup>For example on page 31 in the *Eightfold Way* Gell-Mann and Murray predicted the  $\eta$  meson as a pseudoscalar resonance  $\chi^0$ , which should decay into  $2\gamma$  like  $\pi^0$ , unless it is heavy enough to yield  $\pi^+ + \pi^- + \gamma$  with appreciable probability[2].

<sup>4</sup>The group of Lorentz transformations is a subgroup of the larger-10 dimensional Poincare group which is the symmetry group underlying such fundamental physical insights as energy and momentum conservation which result from invariance under time and space translations. Also, angular momentum conservation can be ascribed to invariance under the rotation group  $O(3)$  which is also a subgroup of the Poincare group.

<sup>5</sup>This procedure is also called minimal coupling, since only those interaction terms between gauge and matter field are introduced that are necessary to retain gauge invariance.

## 1.2 Quantum Chromodynamics

Quantum Chromodynamics is the theory of the strong interaction based on a local  $SU(3)_C$  symmetry group whose fundamental representation is given by the  $SU(3)_C$  quark vector

$$q_f = \begin{pmatrix} q_f^r \\ q_f^g \\ q_f^b \end{pmatrix}, \quad f = u, d, s, c, t, b. \quad (1.4)$$

Each entry  $q^r, q^g, q^b$  is a four-dimensional Dirac spinor and red, green, blue denote the colour degrees of freedom. They are the charges of strong interaction. The interactions among the charged quarks are transmitted via gluons, the gauge fields of  $SU(3)_C$ .

The Dirac Lagrangian

$$\mathcal{L}_{\text{Dirac}} = \sum_f \bar{q}_f (i\gamma_\mu \partial^\mu - m_f) q_f \quad (1.5)$$

is symmetric under global  $SU(3)$  colour transformations. The transformations are performed by unitary  $(3 \times 3)$  matrices  $U$  with

$$UU^\dagger = U^\dagger U = \mathbb{1} \quad (1.6)$$

and

$$\det(U) = 1. \quad (1.7)$$

They act on  $q$  according to

$$\begin{aligned} q \longrightarrow q' &= Uq = \exp\left(-i \sum_{a=1}^8 \theta_a \frac{\lambda^a}{2}\right) q \\ &\simeq \left(\mathbb{1} - i \sum_{a=1}^8 \theta_a \frac{\lambda^a}{2}\right) q. \end{aligned} \quad (1.8)$$

The Gell-Mann matrices  $\lambda_a$  are one representation of the  $N_C^2 - 1 = 8$  generators of  $SU(3)$  and obey the commutation relations

$$[\lambda_a, \lambda_b] = 2if_{abc}\lambda_c, \quad \text{with } (a, b, c = 1, \dots, 8), \quad (1.9)$$

where  $f_{abc}$  are the antisymmetric structure constants of  $SU(3)$ . Under local  $SU(3)$  transformations ( $\theta \rightarrow \theta(x^\mu)$ ) the quark vector transforms as

$$q \longrightarrow q' = \exp\left(-i \sum_{a=1}^8 \theta_a(x^\mu) \frac{\lambda^a}{2}\right) q \simeq \left(\mathbb{1} - i \sum_{a=1}^8 \theta_a(x^\mu) \frac{\lambda^a}{2}\right) q. \quad (1.10)$$

A symmetry-violating term arises from the partial derivative because of the space-time dependence of the transformation parameter. In order to resolve this the partial derivative is promoted to a covariant derivative via the introduction of gauge boson fields  $\mathcal{A}^\mu$

$$\partial^\mu q_f \rightarrow \mathcal{D}^\mu q_f = \partial^\mu q_f + ig_{\text{QCD}} \mathcal{A}_a^\mu \frac{\lambda^a}{2} q_f , \quad (1.11)$$

where the gluon matrix  $\mathcal{A}^\mu = \mathcal{A}_a^\mu \frac{\lambda^a}{2}$  transforms under the adjoint representation of  $SU(3)_C$  as

$$\mathcal{A}^\mu \rightarrow U \mathcal{A}^\mu U^\dagger - \frac{i}{g_{\text{QCD}}} U \partial^\mu U^\dagger . \quad (1.12)$$

From  $U$  being unitary matrices it follows that

$$\partial_\mu (UU^\dagger) = U \partial_\mu U^\dagger + (\partial_\mu U) U^\dagger = 0 . \quad (1.13)$$

It can then be shown that the terms from the partial derivative acting on  $U$  are cancelled by the terms that arise from the transformation of the gauge fields. Then the quark covariant derivative  $\mathcal{D}^\mu q_f$  transforms as  $q_f$ ,

$$\begin{aligned} \mathcal{D}^\mu q_f \longrightarrow (\mathcal{D}^\mu q_f)' &= \partial^\mu q'_f + ig_{\text{QCD}} \mathcal{A}^{\mu'} \frac{\lambda_a}{2} q'_f \\ &= U(x^\mu) \partial^\mu q'_f + [\partial^\mu U(x^\mu)] q_f \\ &\quad + ig_{\text{QCD}} [U(x^\mu) \mathcal{A}^\mu U^\dagger(x^\mu) - \frac{i}{g_{\text{QCD}}} U(x^\mu) \partial^\mu U^\dagger(x^\mu)] U(x^\mu) q_f \\ &= U(x^\mu) \mathcal{D}^\mu q_f , \end{aligned} \quad (1.14)$$

and thus maintains the symmetry of the Lagrangian under local  $SU(3)_C$  transformations.

QCD is flavour-blind - gluonic fields do not distinguish between different quark flavours and  $SU(3)_C$  transformations act on the colour degrees of freedom only - but in nature the quarks are not degenerate in flavour space, so the fermionic term in the Lagrangian becomes a sum over all flavours. And the QCD Lagrangian finally can be defined as [6]

$$\mathcal{L}_{\text{QCD}} = \sum_{f=1}^{N_f} \bar{q}_f (i\gamma_\mu \mathcal{D}^\mu - m_f) q_f - \frac{1}{4} \sum_{a=1}^8 \mathcal{F}_{\mu\nu}^a \mathcal{F}_a^{\mu\nu} \quad (1.15)$$

where

$$\mathcal{F}_a^{\mu\nu} = \partial^\mu \mathcal{A}_a^\nu - \partial^\nu \mathcal{A}_a^\mu - g_{\text{QCD}} f_{abc} \mathcal{A}_b^\mu \mathcal{A}_c^\nu \quad (1.16)$$

is the field strength tensor of the gauge bosons and  $f_{abc}$  are the antisymmetric  $SU(3)$  structure constants<sup>6</sup>. From (1.15) the equations of motion for quark and gluonic fields are then obtained as

$$(i\gamma_\mu \mathcal{D}^\mu - m_f)q_f = 0 , \quad (1.17)$$

$$D^\mu \mathcal{F}_{\mu\nu}^a = g_{\text{QCD}} \sum_f \bar{q}_f \frac{\lambda_a}{2} \gamma_\nu q_f . \quad (1.18)$$

The equations of motion for the gauge field show that the covariant derivative acting on the field strength tensor is proportional to the matter current

$$J_{\nu a} = \sum_f \bar{q}_f \frac{\lambda_a}{2} \gamma_\nu q_f . \quad (1.19)$$

In the absence of matter the current on the right-hand side of (1.18) vanishes

$$D^\mu \mathcal{F}_{\mu\nu}^a = 0 . \quad (1.20)$$

In the QED analogue one obtains in the absence of matter  $\partial_\alpha F^{\alpha\beta} = 0$  for the inhomogeneous Maxwell equations. Thus the photon field itself does not carry charge and does not act as a source for itself. In Yang-Mills theories, on the contrary, due to the non-Abelian nature of the group  $SU(3)$ , the result is

$$\partial_\nu \mathcal{F}_a^{\mu\nu} = -g_{\text{QCD}} f_{abc} \mathcal{A}_{b\nu} \mathcal{F}_c^{\mu\nu} . \quad (1.21)$$

This accounts for the fact that gluons also carry colour and act as sources for strong interaction themselves. The self-interaction of the gauge fields arises from the commutator in the field strength tensor and is a general feature of non-Abelian field theories.

From the Lagrangian one can directly read off the so-called *tree-level* vertices, that allow for a perturbative QCD calculation of physical observables such as decay widths. Quantities that are explicitly contained in the Lagrangian, as here for example the coupling constant  $g_{\text{QCD}}$  in (1.12) and the quark masses  $m_f$  in (1.15) are referred to as *bare* masses or couplings, respectively. In order to obtain the physical values of these bare quantities, also the interactions need to be considered. This leads to diverging contributions and thus each theory has to be renormalised so that the physically relevant values can be extracted.

In the case of the QCD Lagrangian, renormalisation results in an energy-dependent coupling constant

$$\alpha_S(q^2) = \frac{g_{\text{QCD}}^2(q^2)}{4\pi} , \quad (1.22)$$

---

<sup>6</sup>For an explicit representation of the  $SU(3)$  structure constants see refs. [7] or [8].

also called the *running coupling*  $\alpha_S$ . The energy dependence of  $\alpha_S$  is given by the following relation

$$\alpha_S(q^2) = \frac{4\pi}{(11 - \frac{2N_f}{3})\ln(q^2/\Lambda^2)} \quad (1.23)$$

where  $\Lambda$  refers to the Yang-Mills scale. From Equation (1.23) follows that, for  $N_f < (11 \cdot 3)/2$ , as it is realised in nature,  $\alpha_S$  decreases with increasing energy. For low energies  $q^2 \lesssim 1 \text{ GeV}^2$  the value of the running coupling constant increases, suggesting one possible explanation for the well-known feature of confined quarks and gluons. Quarks and gluons cannot be observed as single particle states, but as colour-neutral (white) objects only. For high energies a new phase of matter is expected, the *quark gluon plasma* in which quarks and gluons are deconfined, since for high energies the value of the running coupling decreases (*asymptotic freedom*).

### 1.3 Chiral Symmetry

In the limit of massless quarks, the QCD Lagrangian reveals another fundamental symmetry: global  $U(N_f)_L \times U(N_f)_R$  transformations of the quark spinors

$$q \xrightarrow{U(N_f)_L} U_L q, \quad q \xrightarrow{U(N_f)_R} U_R q. \quad (1.24)$$

where  $q$  denotes an  $N_f$ -dimensional vector in flavour space with each entry being a four-component Dirac spinor field.

The  $U(N_f)$  matrices  $U_L$  and  $U_R$  act on the Dirac as well as on the flavour space. They are defined as

$$U_L = \exp\left\{-i\frac{1-\gamma^5}{2} \sum_{a=0}^{N_f^2-1} \theta_L^a t_a\right\}, \quad U_R = \exp\left\{-i\frac{1+\gamma^5}{2} \sum_{a=0}^{N_f^2-1} \theta_R^a t_a\right\}. \quad (1.25)$$

From now on, for any Lie group  $U(N_f)$  the generators are denoted by  $t_a$  and  $a = 0, 1, 2, \dots, N_f^2 - 1$  while the  $N_f^2 - 1$  generators of  $SU(N_f)$  are denoted by  $t_i$  and  $i = 1, 2, \dots, N_f^2 - 1$ . As in the QCD case they obey the  $SU(N_f)$  commutation relations

$$[t_i, t_j] = if_{ijk} t_k. \quad (1.26)$$

The field  $q$  can be decomposed in its left- and right-handed<sup>7</sup> components by the chiral projectors

$$P_L = \frac{1 - \gamma_5}{2}, \quad P_R = \frac{1 + \gamma_5}{2} \quad (1.27)$$

$$\implies q = (P_L + P_R)q = q_L + q_R,$$

where  $\gamma^5$  is defined as

$$\gamma^5 = i\gamma^0\gamma^1\gamma^2\gamma^3 = \gamma_5, \quad (1.28)$$

and  $\gamma^\mu$  are the Dirac matrices. In chiral representation<sup>8</sup>  $\gamma^5$  is diagonal

$$\gamma^5 = \begin{pmatrix} 1 & 0 \\ 0 & -1 \end{pmatrix}, \quad (1.29)$$

such that  $q_R, q_L$  are eigenvectors of  $\gamma^5$  with eigenvalues  $L, R$  ( $\pm 1$  resp.).

For the decomposed fields  $q_L, q_R$  the QCD Lagrangian reads

$$\begin{aligned} \mathcal{L}_{\text{QCD}} = & \sum_{f=1}^{N_f} i(\bar{q}_{L,f}\gamma_\mu\mathcal{D}^\mu q_{L,f} + \bar{q}_{R,f}\gamma_\mu\mathcal{D}^\mu q_{R,f}) \\ & - \sum_{f=1}^{N_f} (\bar{q}_{R,f}m_f q_{L,f} + \bar{q}_{L,f}m_f q_{R,f}) - \frac{1}{4} \sum_{a=1}^8 \mathcal{F}_{\mu\nu}^a \mathcal{F}_a^{\mu\nu}. \end{aligned} \quad (1.30)$$

---

<sup>7</sup>For massless particles chirality corresponds to positive or negative helicity, defined as the projection of the spin onto the momentum vector

$$h_\pm = \frac{\vec{\sigma} \cdot \vec{p}}{p} = \pm 1.$$

After a Fourier transformation into momentum space ( $\partial^\mu \rightarrow p^\mu$ ) the equation of motion for free, massive fermions reads

$$(\gamma^\mu p_\mu - m)q = (\gamma^\mu p_\mu - m) \left( \frac{1 - \gamma_5}{2} q + \frac{1 + \gamma_5}{2} q \right).$$

For massless fermions in chiral representation the Dirac equation above decouples into the Weyl equations. In literature, however, the distinction between chirality and helicity is often not made clear. As the weak interaction couples to chiral left-handed fields being represented by the eigenvalues of  $\gamma_5$  it seems important to make this differentiation here.

<sup>8</sup>In the chiral representation the 4-spinors are defined as

$$q_f^c = \begin{pmatrix} (q_f^c)_R \\ (q_f^c)_L \end{pmatrix}$$

and the Dirac matrices are defined as

$$\gamma^0 = \begin{pmatrix} 0 & \mathbf{1} \\ \mathbf{1} & 0 \end{pmatrix}, \quad \gamma^i = \begin{pmatrix} 0 & -\sigma^i \\ \sigma^i & 0 \end{pmatrix}.$$

In the chiral limit where all quarks masses vanish, the above Lagrangian is clearly invariant under chiral transformations (1.24). In nature, however, chiral symmetry is not exact. While on the hadronic mass scale of 1 GeV the masses of up and down quark and even the strange quark can be considered to be still small enough ( $m_u \simeq 0.0015$  GeV,  $m_d \simeq 0.0035$  GeV,  $m_s = 0.105$  GeV) to allow for the assumption of a chiral symmetry, the charm mass  $m_c = 1.27$  GeV is already of the order of the hadronic masses, while  $m_b = 4.20$  GeV and  $m_t = 171.3$  GeV clearly exceed the scale where they could be approximated as "vanishing". Considering the  $2 \times N_f^2$  chiral currents, derived from the Lagrangian with the quark mass terms included, reveals the pattern of chiral symmetry breaking, according to the different possibilities of mass degeneracy.

### 1.3.1 Chiral Currents and Symmetry Breaking

After the transformation defined in (1.24)

$$\mathcal{L}_{\text{QCD}} \longrightarrow \mathcal{L}_{\text{QCD}} + \delta\mathcal{L}_{\text{QCD}} , \quad (1.31)$$

$$\begin{aligned} \delta\mathcal{L}_{\text{QCD}} = & \bar{q}_L t_a \gamma_\mu q_L \partial^\mu \theta_L^a + \bar{q}_R t_a \gamma_\mu q_R \partial^\mu \theta_R^a \\ & - i\theta_L^a (\bar{q}_L t_a M q_R - \bar{q}_R t_a M q_L) - i\theta_R^a (\bar{q}_R t_a M q_L - \bar{q}_L t_a M q_R) , \end{aligned} \quad (1.32)$$

where  $M$  is the diagonal quark mass matrix of rank  $N_f$

$$M = \text{diag}(m_u, m_d, m_s, m_c, m_b, m_t) . \quad (1.33)$$

Now the Noether theorem states that if a Lagrangian

$$\mathcal{L} = \mathcal{L}(\phi_a(x^\mu), \partial_\mu \phi_a(x^\mu)) \quad (1.34)$$

is invariant under the transformations

$$x^\mu \rightarrow x^\mu + \delta x^\mu , \quad \phi_a \rightarrow \phi'_a = \phi + \delta\phi_a^\mu , \quad (1.35)$$

then there exist the conserved *Noether currents*

$$\mathcal{J}_a^\mu = \frac{\partial \mathcal{L}}{\partial (\partial_\mu \phi_a)} \delta\phi_a - \delta x^\mu \mathcal{L} , \quad \partial_\mu \mathcal{J}_a^\mu = 0 , \quad (1.36)$$

and that to each conserved current corresponds a conserved charge

$$Q_a = \int J_a^0 d^3x . \quad (1.37)$$

The right-handed and left-handed currents can now be obtained by considering the variation of  $\delta\mathcal{L}_{\text{QCD}}$  with respect to the parameters  $\delta\theta_L$  and  $\delta\theta_R$  [9]

$$\mathcal{J}_{a(L,R)}^\mu = \frac{\delta\mathcal{L}_{\text{QCD}}}{\delta(\partial^\mu\theta_{L,R}^a)} . \quad (1.38)$$

The  $2N_f^2$  independent parameters  $\theta_{Va}$  and  $\theta_{Aa}$  are defined by the relations:

Vector transformation:

$$\begin{aligned} \theta_{La} &= \theta_{Ra} , \\ \theta_{Va} &= \frac{\theta_{La} + \theta_{Ra}}{2} . \end{aligned} \quad (1.39)$$

Axial-vector transformation:

$$\begin{aligned} \theta_{La} &= -\theta_{Ra} , \\ \theta_{Aa} &= \frac{-\theta_{La} + \theta_{Ra}}{2} . \end{aligned} \quad (1.40)$$

Letting the  $U(N_f)_L \times U(N_f)_R$  transformations act simultaneously on left-handed and right-handed quark fields one can define global vector and axial-vector transformations<sup>9</sup> according to

$$q \xrightarrow{U(N_f)^V} q' = U_L U_R q = \exp\{-i\theta_V^a t_a\} q , \quad (1.41)$$

$$q \xrightarrow{U(N_f)^A} q' = U_L U_R q = \exp\{-\gamma^5 \theta_A^a t_a\} q . \quad (1.42)$$

The currents corresponding to vector and axial-vector transformations are then

$$V_a^\mu = \frac{\delta\mathcal{L}_{\text{QCD}}}{\delta(\partial^\mu\theta_L^a)} + \frac{\delta\mathcal{L}_{\text{QCD}}}{\delta(\partial^\mu\theta_R^a)} = \bar{q}\gamma^\mu t_a q , \quad (1.43)$$

$$A_a^\mu = \frac{\delta\mathcal{L}_{\text{QCD}}}{\delta(\partial^\mu\theta_L^a)} - \frac{\delta\mathcal{L}_{\text{QCD}}}{\delta(\partial^\mu\theta_R^a)} = \bar{q}\gamma^\mu\gamma^5 t_a q , \quad (1.44)$$

with divergences

$$\partial_\mu V_a^\mu = \frac{\partial\delta\mathcal{L}_{\text{QCD}}}{\partial\theta_L^a} + \frac{\partial\delta\mathcal{L}_{\text{QCD}}}{\partial\theta_R^a} = i\bar{q}[M, t_a]q , \quad (1.45)$$

$$\partial_\mu A_a^\mu = \frac{\partial\delta\mathcal{L}_{\text{QCD}}}{\partial\theta_L^a} - \frac{\partial\delta\mathcal{L}_{\text{QCD}}}{\partial\theta_R^a} = i\bar{q}\{t_a, M\}\gamma^5 q . \quad (1.46)$$

---

<sup>9</sup>Because of  $\gamma^5$  in (1.42) the axial-vector transformations do not build a group, since closure is not satisfied.



Now the manifestations of chiral symmetry breaking and some of the experimentally verified predictions made from the resulting constraints will be described. Analogously to the irreducible representations of  $U(N_f)_L \times U(N_f)_R$  the  $2N_f^2$  currents in (1.43) and (1.44) can be split into two singlet currents and two currents belonging to the adjoint representation of the group ( $U(N_f) = U(1) \times SU(N_f)$ ).

One can anticipate the following scenarios of mass degeneracy:

- all quarks are massless  $m_f = 0$ ,
- all quarks are massive, but degenerate  $m_u = m_d = m_s = m_c = m_t = m_b = m$ ,
- all quarks are massive and not degenerate.

Within these scenarios one can analyse chiral symmetry from Equations (1.45) and (1.46).

The  $U(1)_V$  symmetry corresponds to the conservation of the quark number; its generator is proportional to the unit matrix and thus commutes with all other generators. From (1.43) the  $U(1)_V$  current can be read off as

$$V_0^\mu = \bar{q}\gamma^\mu t_0 q \quad (1.47)$$

and its divergence is

$$\partial_\mu V_0^\mu = i\bar{q}[M, t_0]q = 0 . \quad (1.48)$$

Thus, even for massive quarks, the  $U(1)_V$  vector symmetry remains unbroken and baryon number is always conserved.

While  $SU(N_f)_V$  is broken in the case of massive and non-degenerate quarks it is clearly preserved, if  $m_u = m_d = \dots = m_f$ . Then the quark mass matrix  $M$  commutes with all other generators

$$\partial_\mu V_i^\mu = im_f \bar{q}[1, t_i]q = 0, \quad i = 1, 2, 3 . \quad (1.49)$$

The  $N_f^2 - 1$  vector currents are then conserved individually and  $SU(N_f)_V$  remains intact<sup>10</sup>.  $SU(N_f)_V$  is the standard flavour symmetry (isospin for  $N_f = 2$ ), as, for example, for the nucleon isospin doublet of  $SU(2)_f$ .

---

<sup>10</sup>Electromagnetic interactions break the vector symmetry explicitly which, e.g., results in the Gell-Mann-Nishijima relation. A closer analysis of the electroweak interaction and its symmetry breaking will be given in the following section about the Glashow-Salam-Weinberg model.

The  $SU(N_f)$  axial-vector currents  $A_i^\mu$  are only conserved if the quark masses are identically zero since

$$\partial_\mu A_i^\mu = \bar{q}\{t_i, M\}\gamma^5 t_i q . \quad (1.50)$$

The divergence of the  $U(1)$  axial current  $A_0^\mu$  is obtained as

$$\partial_\mu A_0^\mu = 2i\bar{q}M\gamma^5 q . \quad (1.51)$$

and also vanishes in the chiral limit. This is, however, only true on the classical level. Calculations to first order of perturbation theory of the amplitude of an axial current coupled to two vector currents coupled to gluons reveal that the Ward identities can only be respected for either the vector or the axial-vector current [7]. Since the symmetry under vector transformations corresponds to conservation of baryon number, one chooses the  $U(1)$  axial symmetry to be explicitly broken<sup>11</sup>. For massless quarks and  $N_c = 3$  the not conserved singlet current, corresponding to the  $\eta$  meson, then reads

$$\partial_\mu A_0^\mu = \frac{\alpha_S N_C}{8\pi} F_{\mu\nu}^a \tilde{F}^{a\mu\nu} \text{ with } (\tilde{F}_{\mu\nu}^a = \varepsilon^{\mu\nu\alpha\beta} F_{\alpha\beta}^a). \quad (1.52)$$

The anomalous axial singlet current yields the explanation of the massive  $\eta$  meson which otherwise would be a massless Goldstone boson of the spontaneously broken axial-vector symmetry.

The contribution from the anomaly to the current corresponding to the neutral  $\pi$  is

$$\partial_\mu A_3^\mu = \frac{\alpha N_C}{12\pi} \mathcal{F}_{\mu\nu}^a \tilde{\mathcal{F}}^{a\mu\nu} \quad (1.53)$$

and yields a great confirmation of the chiral anomaly in the axial-vector current in the presence of an electromagnetic field; the  $\pi^0 \rightarrow \gamma\gamma$  decay rate was predicted in agreement with the experimental result to be

$$\Gamma_{\pi^0 \rightarrow \gamma\gamma} = \left( \frac{\alpha N_c}{3\pi f_\pi} \right)^2 \frac{m_\pi^3}{64\pi} \simeq 7.7 \text{ eV}$$

by Adler, Bell and Jackiw [12]. Equations (1.52) and (1.53) show that the symmetry breaking term depends on the number of quark colours  $N_c$  but is independent on assumptions about the degeneracy of the quarks in flavour space<sup>12</sup>.

---

<sup>11</sup>On the physical side this “true” breaking of the axial chiral symmetry is also attributed to instanton effects as it has been shown by t’Hooft [10]. Detailed discussion on the subject of the chiral anomaly can be found, e.g., in Chapter III-3 of [7] and Chapter 18 in [11].

<sup>12</sup>Bouchiat, Iliopoulos and Meyer [13] showed that for three generations of quarks and leptons the anomalies cancel out separately for quarks carrying fractional electromagnetic charges and if the number of colours is  $N_c = 3$  [11]. This remarkably substantiates quark colour as additional degree of freedom. Only when the anomalous contributions cancel each other out, theories that are based on a local symmetry with anomalous currents will be renormalisable and produce experimentally verifiable predictions.

Both vector and axial-vector isospin currents of the chiral model reflect strong isospin symmetry which is for example seen in the almost exact degeneracy of the hadronic mass spectra for the pion triplet ( $N_f = 2$ ) or the kaon quadruplet ( $N_f = 3$ ). They are also in accordance with the currents that are observed in electroweak, strangeness preserving semileptonic interactions. Their relation is seen for example in the Goldberger-Treiman relation

$$g_{\pi NN} = g_A \frac{M_N}{f_\pi} \simeq 12.5 \quad (1.54)$$

which connects the effective strong-interaction coupling between pions and nucleons  $g_{\pi NN}$  and the pion decay constant  $f_\pi$  extracted from the weak decay of the pion. The constant  $g_A$  describes the ratio of the vector and axial-vector couplings as they are measured in weak  $\beta$  decay. Since the weak interaction is a purely  $V-A$  interaction one would expect this ratio to be one. But as a consequence of the broken axial symmetry the ratio is  $g_A = \frac{G_A}{G_V} \simeq 1.22$ . The experimental value from pion-nucleon scattering is given by

$$\frac{g_{\pi NN}^2}{4\pi} \simeq 13.5 \Rightarrow g_{\pi NN} \simeq 13.03 .$$

which agrees with the theoretical prediction to about 4% [7, 14].

The Goldberger-Treiman relation can be derived from an assumption called partial conservation of the axial current (PCAC). In  $SU(2)_f$  the weak decay of  $\pi \rightarrow \mu\nu_\tau$  is dominated by the axial current  $A_i^\mu$ . The amplitude  $\mathcal{M}_{\pi \rightarrow \mu\nu}$ , derived from the weak interaction Lagrangian of strangeness-conserving semileptonic processes, is of current-current type and proportional to

$$\langle 0 | \bar{q} \gamma^\mu (1 - \gamma^5) t_i q | \pi_j \rangle = \langle 0 | V_i^\mu | \pi_j \rangle - \langle 0 | A_i^\mu | \pi_j \rangle .$$

In order to describe the transition between the vacuum  $J^P = 0^+$  and the pion  $J^P = 0^-$  it is necessary to demand a non-zero matrix element for the axial current

$$\langle 0 | \bar{q} \gamma^\mu \gamma^5 t_i q | \pi_j \rangle = i p^\mu f_\pi \delta_{ij} e^{-i p \cdot x} . \quad (1.55)$$

The decay rate for the process  $\pi \rightarrow \mu\nu_\tau$  is then calculated to

$$\Gamma_{\pi \rightarrow \mu\nu} = \frac{G_F^2 m_\mu^2 f_\pi^2 (m_\pi^2 - m_\mu^2)^2}{4\pi m_\pi^3} \cos^2 \theta_C . \quad (1.56)$$

$G_F$  denotes the effective weak Fermi coupling and is defined as

$$G_F = \frac{g^2}{2\sqrt{2}M_W^2} . \quad (1.57)$$

From (1.56) the vacuum decay constant of the pion  $f_\pi$  can be determined by experiment and its value is given by  $f_\pi = 92.4$  MeV.

Taking the divergence of (1.55) results in

$$\langle 0 | \partial_\mu A_i^\mu(x) | \pi_j(p) \rangle = -p_\mu p^\mu f_\pi \delta_{ij} e^{-ip \cdot x} = -m_\pi^2 f_\pi \delta_{ij} e^{-ip \cdot x} . \quad (1.58)$$

With a pion mass of  $m_{\pi^\pm} = 0.139$  GeV the divergence of the axial current can clearly be approximated by zero on hadronic mass scales of  $\sim 1$  GeV. Thus, at least for  $N_f = 2$  and massive quarks, the axial chiral symmetry is considered to be approximately conserved on the classical level.

### 1.3.2 Spontaneously Broken Chiral Symmetry

For  $N_f = 2$  the irreducible representations of  $U(N_f)_L \times U(N_f)_R$  for mesons are obtained as external products of their fundamental representations. The mesonic states are then considered to be the bilinear combinations

$$\begin{aligned} \text{scalar:} & \quad \sigma_a = \bar{q} t_a q , \\ \text{pseudoscalar:} & \quad \pi_a = i \bar{q} t_a \gamma^5 q , \\ \text{vector:} & \quad V_a^\mu = \bar{q} t_a \gamma^\mu q , \\ \text{axial vector:} & \quad A_a^\mu = \bar{q} t_a \gamma^\mu \gamma^5 q . \end{aligned}$$

With the unitary matrices  $U_V, U_A$  as they are given in (1.41) and (1.42) the quark fields transform under  $SU(2)$  vector and axial-vector transformations<sup>13</sup> according to

$$\begin{aligned} q & \xrightarrow{V} U_V q \simeq (1 - i \theta_V^i t_i) q , \\ q & \xrightarrow{A} U_A q \simeq (1 - i \gamma_5 \theta_A^i t_i) q . \end{aligned} \quad (1.59)$$

Under  $SU(2)_V$  transformations the scalar, pseudoscalar, vector, and axial-vector triplets therefore transform as

$$\begin{aligned} \text{scalar:} & \quad \bar{q} t_i q & \longrightarrow & \quad \bar{q} t_i q + \bar{q} \varepsilon_{ijk} \theta_{Vj} t_k q , \\ \text{pseudoscalar:} & \quad i \bar{q} t_i \gamma^5 q & \longrightarrow & \quad i \bar{q} t_i \gamma^5 q + i \bar{q} \varepsilon_{ijk} \theta_{Vj} t_k \gamma^5 q , \\ \text{vector:} & \quad \bar{q} t_i \gamma^\mu q & \longrightarrow & \quad \bar{q} t_i \gamma^\mu q + \bar{q} \varepsilon_{ijk} \theta_{Vj} t_k \gamma^\mu q , \\ \text{axial vector:} & \quad \bar{q} t_i \gamma^\mu \gamma^5 q & \longrightarrow & \quad \bar{q} t_i \gamma^\mu \gamma^5 q + \bar{q} \varepsilon_{ijk} \theta_{Vj} t_k \gamma^\mu \gamma^5 q . \end{aligned} \quad (1.60)$$

<sup>13</sup>The following discussion of the chiral transformation of the mesons is based on the introduction to chiral symmetry written by Volker Koch [14].

This is only a rotation in strong isospace, e.g., one obtains for the pseudoscalar triplet

$$\vec{\pi} \xrightarrow{V} \vec{\pi} + \vec{\theta}_V \times \vec{\pi} . \quad (1.61)$$

The results for a vector transformation acting on scalar, vector, and axial-vector fields can be written down analogously.

Now, under axial-vector transformations, the adjoint field transforms as  $\bar{q} \rightarrow \bar{q}' \simeq \bar{q}(1 - i\gamma^5\theta_{Ai}t_i)$ , because  $\gamma^5$  anticommutes with  $\gamma_0$ . Together with the anticommutation relations  $\{t_i, t_j\} = \delta_{ij}$  the pion triplet transforms as

$$\begin{aligned} i\bar{q}\gamma^5t_iq &\longrightarrow i\bar{q}'\gamma^5t_iq' \simeq i\bar{q}(\mathbb{1} - i\gamma^5\theta_{Aj}t_j)\gamma^5t_i(\mathbb{1} - i\gamma^5\theta_{Aj}t_j)q \\ &= i\bar{q}\gamma^5t_iq + \theta_{Aj}(\bar{q}t_j\gamma^5\gamma^5t_iq + \bar{q}\gamma^5t_i t_j\gamma^5q) + O[\theta_A]^2 \\ &= i\bar{q}\gamma^5t_iq + \theta_{Aj}\bar{q}\{t_i, t_j\}q \\ &= i\bar{q}\gamma^5t_i\psi + \theta_{Ai}\bar{q}q . \end{aligned} \quad (1.62)$$

The purely pseudoscalar like state ( $\sim \gamma_5$ ) obtained an additional scalar contribution ( $\sim \mathbb{1}$ ); the axial transformation performs a rotation of the pseudoscalar states into the scalar states as for example

$$\vec{\pi} \xrightarrow{A} \vec{\pi} + \vec{\theta}_A\sigma \quad (1.63)$$

and analogously for vectors and axial vectors

$$\vec{\rho}^\mu \xrightarrow{A} \vec{\rho}^\mu + \vec{\theta}_A \times \vec{a}_1^\mu . \quad (1.64)$$

Since mesons are colourless bound quark-antiquark states, the symmetry properties of QCD are expected to be also reflected in the hadronic spectrum. Under axial transformations scalars and pseudoscalars, as well as vectors and axial vectors appear to be partners and should thus have the same eigenvalues. As it was already noted, the symmetry corresponding to vector transformations is related to conservation of strong isospin and is reflected in the spectrum of the pion triplet. But from hadron spectroscopy it is also known that the difference between the  $\rho$  and the  $a_1$  mass is already of the order of the  $\rho$  mass itself ( $m_\rho = 0.776$  GeV,  $m_{a_1} = 1.23$  GeV) and the expected symmetry property, the degeneracy under axial transformations, is not observed in experiment. On the other side, PCAC and the Goldberger Treiman relation indicate that it is justified to assume that the axial symmetry is at least approximately conserved. The resolution to this contradiction is the spontaneous breaking of the axial symmetry.

Apart from the symmetry properties of the Lagrangian, the ground state of the potential of a system (vacuum) also possesses symmetries. Provided

that the ground state is not unique but consists of an infinite number of degenerate ground states, the symmetry is spontaneously broken, if one of these degenerate ground states is explicitly ascribed to the vacuum. The ground state is then only invariant under transformations performed by the broken generators.

For a  $O(N)$  symmetric Lagrangian of the form

$$\mathcal{L} = \frac{1}{2}(\partial^\mu \Phi_i)^2 - \frac{1}{2}\mu^2(\Phi_i)^2 - \frac{\lambda}{4}[(\Phi_i)^2]^2 \quad (1.65)$$

and  $\mu^2 > 0$  there is exactly one ground state at position  $\phi_0 = 0$  and the ground state has the same symmetries under  $O(N)$  transformations of the fields  $\phi_i \rightarrow O_{ij}\phi_j$ ,  $i, j = 0, 1, \dots, N-1$  as the Lagrangian. The number of symmetries of the ground state is then the same as the dimension of the symmetry group of the Lagrangian, and all  $\frac{N(N-1)}{2}$  generators of  $O(N)$  annihilate the ground state

$$\Phi'_0 = U\Phi_0 = 0. \quad (1.66)$$

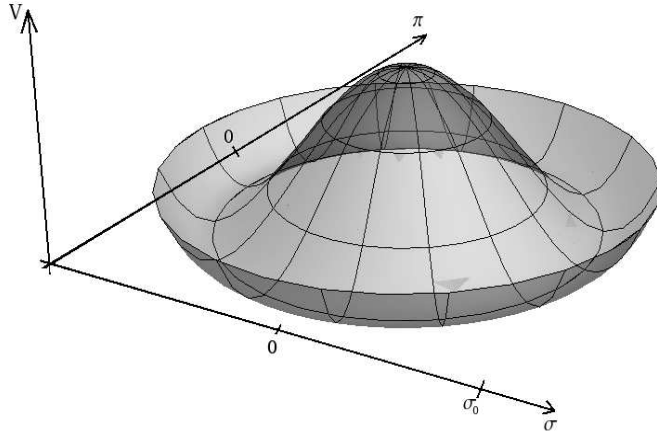


Figure 1.3: Mexican hat potential of a  $O(N = 2)$  Linear Sigma Model with  $\Phi = (\sigma, \pi)^T$  and  $\mathcal{L} = \frac{1}{2}(\partial^\mu \Phi)^2 - \frac{1}{2}\mu^2(\Phi)^2 - \frac{\lambda}{4}[(\Phi)^2]^2$ .

Now, if  $\mu^2 < 0$ , the ground state is moved to a constant distance  $\phi_0$  from the origin (Figure 1.3). At first, the ground state is still invariant under rotations in the  $N$  dimensional plane spanned by the fields  $\phi_i$ ,  $i = 0, 1, \dots, N-1$ , but as soon as one ascribes this vacuum expectation value to one specific field

$$\Phi_0 = (\phi_0, 0, 0, \dots, 0), \quad (1.67)$$

the symmetry is spontaneously broken. The ground state is now only symmetric under transformations of a subgroup of the original symmetry group and only the generators in the direction of  $\Phi_0$  annihilate the ground state.

Goldstone's Theorem [15] states that, if a continuous symmetry is spontaneously broken, there arise as many massless scalar fields as there are broken generators in the ground state, or more precisely; if a Lagrangian is invariant under a continuous symmetry group  $G$  and the number of generators of  $G$  is  $N$ , while the ground state is only invariant under a subset  $H$ , with dimension  $M$ , then, there are  $N - M$  massless spin 0 particles. Expanding the potential about its minimum gives rise to the mass term of the field corresponding to the unbroken symmetry, while the fields corresponding to the broken symmetries are massless.

Now, looking at the  $O(2)$  example in Figure 1.3, one can understand the  $\sigma$  field as the radial component of  $\Phi$  and  $\pi$  as the tangential component. Then, radial excitations of  $\Phi$  along the  $\sigma$  axis do cost energy ( $m_\sigma \neq 0$ ), while excitations of  $\Phi$  in the tangential direction are along the trough of the potential and do not cost energy ( $m_\pi = 0$ ). Thus, the pions are considered to be the massless Goldstone bosons of the spontaneously broken axial-vector symmetry.

For the  $SU(2)_L \times SU(2)_R$  scalar and pseudoscalar mesons this means that the potential is invariant under axial-vector rotations in the plane of the chiral partners  $\sigma$  and  $\pi$ .

Since the  $\sigma$  meson carries the quantum numbers of the vacuum ( $0^+$ ) it can be chosen to take on the expectation value of the ground state  $\phi_0$

$$\sigma \rightarrow \sigma + \phi_0 .$$

Then the symmetry is spontaneously broken and the three pions ( $J^P = 0^+$ ) are considered to be the Goldstone bosons. In the Lagrangian, there are now new contributions to the mass terms that are proportional to the square of the vacuum expectation value. Thus, the mass difference between the pion and  $\sigma$  resonances is explained by means of a spontaneously broken chiral symmetry. The same mechanism gives rise to the mass difference between  $\rho$  and  $a_1$ . In the chiral limit, where chiral symmetry is exact,  $a_1$  and  $\rho$  become degenerate in mass after the chiral phase transition ( $T > T_C$ ).

## 1.4 Glashow-Weinberg-Salam Theory

Besides its symmetry under local  $SU(3)_C$  and global  $SU(2)_L \times SU(2)_R$  the QCD Lagrangian without mass term<sup>14</sup>

$$\mathcal{L}_{\text{Dirac}} = \sum_f \bar{q}_f i \gamma_\mu \partial^\mu q_f . \quad (1.69)$$

is also invariant under  $SU(2)_L \times U(1)_Y$  gauge transformations. The indices  $L$  and  $Y$  refer to the groups generated by the weak isospin and hypercharge operators  $I_3$  and  $Y$ . These two groups provide the framework to describe electromagnetism and weak interaction within a unified gauge theory.

Electric charge  $Q$  as immediately experimentally observable quantum number is related to hypercharge  $Y$  and the third component of weak isospin  $I_3$  by the Gell-Mann-Nishijima relation of the weak interaction

$$Q = I_3 + \frac{Y}{2} . \quad (1.70)$$

All fermions - leptons and quarks - are subject to electroweak interactions. Weak interaction bosons couple only to fields with weak isospin  $I_3$ , e.g., either left-handed particles or right-handed antiparticles, and thus weak interaction violates the symmetry under charge  $C$  and parity  $P$  conjugation individually, while it preserves combined  $CP$  transformations (Figure 1.4).

In the two flavour case the  $SU(2)_L$  fundamental representation for up and down quark is given by a left-handed doublet state  $q_1$  describing the fields that transform under  $SU(2)_L$  and two right-handed isosinglets  $q_2, q_3$  that do not transform under  $SU(2)_L$

$$q_1 = \begin{pmatrix} u_L \\ d_L \end{pmatrix}, \quad q_2 = u_R, \quad q_3 = d_R . \quad (1.71)$$

As for chiral symmetry left-handedness and right-handedness are defined by the eigenvalues  $\pm 1$  of  $\gamma^5$  in chiral representation. The quantities  $q_R, q_L$  are the eigenvectors of  $\gamma^5$ . They are obtained by the chiral projectors given in (1.27).

Another important peculiarity about the weak interaction eigenstates is that they are not the eigenstates of the strong interaction, but a rotation among

---

<sup>14</sup>For fermionic fields such a mass term would read

$$\mathcal{L}_m = m(\bar{q}_L q_R + \bar{q}_R q_L) . \quad (1.68)$$

Since it mixes the left- and right-handed fields it is not invariant under  $SU(2)_L \times U(1)_Y$  transformations of  $q_L, q_R$ . A closer description of the fermionic masses and their gauge invariant generation in the Lagrangian can be found for example in Chapter 20.2 of [16].



$$\begin{array}{ccc}
\begin{array}{l} u_L, c_L, t_L \\ I_3 = \frac{1}{2}, Y = \frac{1}{3} \end{array} & \xrightarrow{C} & \begin{array}{l} \bar{u}_L, \bar{c}_L, \bar{t}_L \\ I_3 = 0, Y = -\frac{2}{3} \end{array} \\
\begin{array}{l} u_L, c_L, t_L \\ I_3 = \frac{1}{2}, Y = \frac{1}{3} \end{array} & \xrightarrow{P} & \begin{array}{l} u_R, c_R, t_R \\ I_3 = 0, Y = \frac{4}{3} \end{array} \\
\begin{array}{l} u_L, c_L, t_L \\ I_3 = \frac{1}{2}, Y = \frac{1}{3} \end{array} & \xrightarrow{CP} & \begin{array}{l} \bar{u}_R, \bar{c}_R, \bar{t}_R \\ I_3 = -\frac{1}{2}, Y = \frac{1}{3} \end{array}
\end{array}$$

Figure 1.4: Charge and parity transformations of up, charm and top quark.

those. Denoting the weak eigenstates with  $d', s', b'$  their relation to the chiral (strong isospin) eigenstates is described by the Cabibbo-Kobayashi-Maskawa matrix  $V_{\text{CKM}}$

$$\begin{pmatrix} d' \\ s' \\ b' \end{pmatrix} = V_{\text{CKM}} \begin{pmatrix} d \\ s \\ b \end{pmatrix} . \quad (1.72)$$

For three flavours this reduces to a rotation about the Cabibbo angle  $\theta_C$

$$\begin{pmatrix} d' \\ s' \end{pmatrix} = \begin{pmatrix} \cos\theta_C & \sin\theta_C \\ -\sin\theta_C & \cos\theta_C \end{pmatrix} \begin{pmatrix} d \\ s \end{pmatrix} . \quad (1.73)$$

The following introduction into the Glashow-Weinberg-Salam Theory will be only applied to the quarks of the first family  $u$  and  $d$ , where  $d$  is now already defined as the weak quark spinor, so that the prime, referring to the prefactor  $\cos\theta_C$  of  $u$ , can be omitted.

Now, in terms of the weak eigenstates<sup>15</sup> the non-interacting Lagrangian can be written as

$$\mathcal{L}_0 = i\bar{q}_1\gamma^\mu\partial_\mu q_1 + i\bar{q}_2\gamma^\mu\partial_\mu q_2 + i\bar{q}_3\gamma^\mu\partial_\mu q_3 . \quad (1.75)$$

---

<sup>15</sup>The GWS model is trivially extended to all lepton families by adding the corresponding terms. Since the neutrinos are considered to be their own antiparticles there is only one right-handed singlet in each family

$$\begin{pmatrix} \nu_{l,L} \\ l_L \end{pmatrix}, \quad l_R . \quad (1.74)$$

In Section 1.3 it was shown that the Lagrangian in (1.75) is invariant under global  $SU(2)_L$  transformations. Since any  $U(1)$  transformation is proportional to a phase factor only,  $\mathcal{L}_0$  is also invariant under combined  $SU(2)_L \times U(1)_Y$  transformations according to

$$\begin{aligned} q_1 &\rightarrow q'_1 = U_Y U_L q_1 , \\ q_2 &\rightarrow q'_2 = U_Y q_2 , \\ q_3 &\rightarrow q'_3 = U_Y q_3 . \end{aligned} \tag{1.76}$$

Now, invariance of the Lagrangian (1.75) under local  $SU(2)_L$  transformations of the doublet

$$q_1 \rightarrow q'_1 = U_L(x^\mu) q_1 = e^{-i\theta^i(x^\mu) t_i} q_1 \tag{1.77}$$

is again obtained via a covariant derivative. If the weak gauge bosons  $W^\mu(x^\mu) = W_i^\mu(x^\mu) t^i$  transform under local  $SU(2)_L$  adjoint representation as

$$W^\mu(x^\mu) \xrightarrow{SU(2)_L} U_L(x^\mu) W^\mu(x^\mu) U_L^\dagger(x^\mu) - \frac{i}{g} \partial^\mu U_L(x^\mu) U_L^\dagger(x^\mu) , \tag{1.78}$$

the covariant derivative reads

$$\partial^\mu \rightarrow \mathcal{D}^\mu = \partial^\mu - ig W^\mu(x^\mu) , \tag{1.79}$$

and the weakly interacting Lagrangian reads

$$\mathcal{L}_{\text{weak}} = i\bar{q}_1 \gamma_\mu \mathcal{D}^\mu q_1 . \tag{1.80}$$

Both, left- and right-handed quarks, are subject to electroweak interactions and should therefore transform under local  $U(1)_Y$ . Generally, the gauge bosons couple to the charges of the symmetry group; while left-handed fields carry weak isospin and right-handed fields do not, both, left- and right-handed fields, carry electromagnetic charge. Also, provided that due to the Anderson-Higgs mechanism the weak gauge bosons are massive, the third component of the physical weak interaction boson  $Z^0$  is a mixed state of the  $U(1)_Y$  and  $SU(2)_L$  gauge fields  $B^\mu$  and  $W_3^\mu$ . This gave rise to the Gell-Mann-Nishijima relation of the weak interaction, describing the relation between the quantum numbers of bare and physical fields.

Now, in order to incorporate the fact that the neutral currents  $B^\mu$  and  $W_3^\mu$  couple differently to left- and right-handed fields, the transformations of the doublet and the singlets have to be proportional to the corresponding  $U(1)_Y$  eigenvalues  $y_1, y_2$ , and  $y_3$ . Thus, for  $U(1)_Y$  the transformation law is

$$q_1 \longrightarrow q'_1 = U_{Y_1} q_1 = e^{iy_1 \theta(x^\mu)} q_1 ,$$

$$\begin{aligned}
q_3 &\longrightarrow q'_2 = U_{Y_2} q_2 = e^{iy_2\theta(x^\mu)} q_2 , \\
q_3 &\longrightarrow q'_3 = U_{Y_3} q_3 = e^{iy_3\theta(x^\mu)} q_3 .
\end{aligned} \tag{1.81}$$

The gauge field corresponding to the gauge group  $U(1)_Y$  is denoted by  $B^\mu$  and transforms as

$$B^\mu \xrightarrow{U(1)_Y} B^{\mu'} = B^\mu + \frac{1}{g'} \partial^\mu \theta(x^\mu) . \tag{1.82}$$

For each quark state  $q_i$  one obtains a covariant derivative according to the transformation properties of  $q_i$  under  $SU(2)_L \times U(1)_Y$

$$\begin{aligned}
D_1^\mu &= \partial^\mu - igW^\mu(x^\mu) - ig'y_1 B^\mu(x^\mu) , \\
D_2^\mu &= \partial^\mu - ig'y_2 B^\mu(x^\mu) , \\
D_3^\mu &= \partial^\mu - ig'y_3 B^\mu(x^\mu) .
\end{aligned} \tag{1.83}$$

With the transformations (1.78) and (1.82) of the gauge bosons  $W^\mu$  and  $B^\mu$  the covariant derivatives transform as the quark fields themselves and thus maintain the local symmetry of (1.80), where  $D$  is replaced with  $D_i$ ,  $i = 1, 2, 3$ . The dynamical contribution of the gauge fields is contained in the field strength tensors. For the abelian  $U(1)_Y$  field  $B^\mu$  it reads

$$B^{\mu\nu} = \partial^\mu B^\nu - \partial^\nu B^\mu \tag{1.84}$$

and is invariant under  $SU(2)_L \times U(1)_Y$  transformations. For the non-abelian gauge bosons

$$W^{\mu\nu} = \partial^\mu W^\nu - \partial^\nu W^\mu - ig[W^\mu, W^\nu], \quad W^{\mu\nu} = W_i^{\mu\nu} t^i \tag{1.85}$$

is obtained, with  $W^{\mu\nu}$  transforming as the adjoint representation

$$W^{\mu\nu} \xrightarrow{SU(2)_L \times U(1)_Y} U_L W^{\mu\nu} U_L^\dagger . \tag{1.86}$$

The weakly interacting quark Lagrangian can be written down as

$$\mathcal{L}_{\text{int}} = \sum_{i=1}^3 i\bar{q}_i \gamma_\mu D_i^\mu q_i - \frac{1}{4} B_{\mu\nu} B^{\mu\nu} - \frac{1}{4} W_{\mu\nu} W^{\mu\nu} . \tag{1.87}$$

In order to maintain gauge invariance the gauge bosons of Yang-Mills theories have to be massless. While this holds for the photon  $\gamma$ , the interaction field of Quantum Electrodynamics, the weak interaction bosons actually are massive. They carry a mass of  $m_{W^\pm} = 80.399$  GeV and  $m_{Z^0} = 91.188$  GeV

[6]<sup>16</sup>. The contradiction of the massive gauge bosons  $W^\pm, Z^0$  was resolved by spontaneous symmetry breaking, this time applied to a isospinor scalar field  $\xi$  implemented by a  $\phi^4$  interaction Lagrangian

$$\mathcal{L}_\xi = (\partial^\mu \xi^\dagger)(\partial^\mu \xi) - \mu^2 \xi^\dagger \xi - \frac{\lambda}{4} (\xi^\dagger \xi)^2 . \quad (1.88)$$

This so-called Higgs field carries weak isospin  $I = \frac{1}{2}$  and hypercharge  $Y = 1$ . It transforms under the electroweak symmetry group like the left-handed fermion fields,

$$\xi = \begin{pmatrix} \xi^+ \\ \xi^0 \end{pmatrix} , \quad (1.89)$$

$$\xi \xrightarrow{SU(2) \times U(1)} \xi' = U_L U_Y \xi . \quad (1.90)$$

Both fields,  $\xi^+$  and  $\xi^0$ , are complex-valued

$$\xi^+ = \frac{1}{\sqrt{2}} (\xi_3 + i \xi_4) , \quad (1.91)$$

$$\xi^0 = \frac{1}{\sqrt{2}} (\xi_1 + i \xi_2) . \quad (1.92)$$

To render the symmetry of  $\mathcal{L}_\xi$  local, the partial derivative in (1.88) is again replaced by a covariant derivative according to the one acting on the left-handed doublet

$$D^\mu \xi = \partial^\mu \xi - ig W^\mu \xi - ig' B^\mu \xi . \quad (1.93)$$

Thus the weakly interacting Lagrangian for the Higgs field reads

$$\mathcal{L}_\xi^{\text{int}} = (D^\mu \xi^\dagger)(D^\mu \xi) - V(\xi) , \quad (1.94)$$

with the potential defined as

$$V(\xi) = \mu^2 \xi^\dagger \xi + \frac{\lambda}{4} (\xi^\dagger \xi)^2 . \quad (1.95)$$

In the Goldstone mode where  $\mu^2 < 0$  the minima of the potential lie on a circle with

$$\langle 0 | \xi | 0 \rangle = \sqrt{\frac{-2\mu^2}{\lambda}} = \sqrt{2} \xi_0 .$$

---

<sup>16</sup>Since usually the exchanged momenta in an interaction process are much smaller than the  $W$  bosons masses, their propagator reduces to  $1/M_W^2$  and thus explains the short range or “weakness” of the weak interaction. It was not obvious from the beginning that it is only of short range and not weak in terms of its coupling strength which is actually of the order of the electromagnetic coupling.

Now the real part  $\text{Re}[\xi_0] = \xi_1$  is chosen to take on the expectation value of the ground state. Then, the minimum of  $V(\xi)$  is not degenerate anymore and is defined to be

$$\begin{aligned} \langle 0|\xi_1|0\rangle &= \sqrt{2}\xi_0, \\ \text{and } \langle 0|\xi_2|0\rangle &= \langle 0|\xi_3|0\rangle = \langle 0|\xi_4|0\rangle = 0. \end{aligned} \quad (1.96)$$

The local symmetry of  $\mathcal{L}_\xi^{int}$  enables different isospin transformations of  $\xi$  at each point in space time, this freedom to choose a distinct orientation for  $\xi$  in isospace has to be removed by a gauge-fixing procedure. In unitary gauge where  $\xi$  is set to be in the  $t_3$  direction only, all fluctuations of the ground state that would affect the fields  $\xi_2, \xi_3$ , and  $\xi_4$  vanish and thus  $\xi(x^\mu)$  for each point in space-time is defined as

$$\xi(x^\mu) = \begin{pmatrix} 0 \\ \xi_0 + \frac{\varsigma(x^\mu)}{\sqrt{2}} \end{pmatrix}. \quad (1.97)$$

The interaction of  $\xi$  with the electroweak bosons is then derived from the covariant derivative (1.93) according to

$$D^\mu \xi = \begin{pmatrix} 0 \\ \frac{\partial^\mu \varsigma}{\sqrt{2}} \end{pmatrix} - i\frac{g}{2}W^\mu \begin{pmatrix} 0 \\ \xi_0 + \frac{\varsigma}{\sqrt{2}} \end{pmatrix} - i\frac{g'}{2}B^\mu \begin{pmatrix} 0 \\ \xi_0 + \frac{\varsigma}{\sqrt{2}} \end{pmatrix} \quad (1.98)$$

and

$$\begin{aligned} (D^\mu \xi^\dagger)(D^\mu \xi) &= \frac{1}{2}(\partial^\mu \varsigma)^2 + \frac{g^2 \xi_0^2}{4}[(W_1^\mu)^2 + (W_2^\mu)^2] + \frac{\xi_0^2}{4}(gW_3^\mu - g'B^\mu)^2 \\ &\quad + \text{products of higher order}. \end{aligned} \quad (1.99)$$

The Higgs field kinetics are now described by the first term in (1.99). The degrees of freedom  $\xi_2, \xi_3$ , and  $\xi_4$  in the definition (1.92) are now the massless modes of the scalar field, while the vacuum expectation value of  $\xi$  gives rise to self-interaction terms of the gauge fields. So to say, the three Goldstone modes are eaten by the three  $SU(2)_L$  gauge bosons so that they become massive.

Now, the charged physical fields are identified as

$$W^{\mu\pm} = \frac{W_1^\mu \mp iW_2^\mu}{\sqrt{2}} \quad (1.100)$$

and the physical neutral weak boson  $Z^0$  is associated with a linear combination of the gauge bosons of the  $SU(2)_L \times U(1)_Y$  local symmetry. It mixes the  $t_0$  and  $t_3$  components of the bare gauge fields (Weinberg mixing)

$$Z^\mu = \frac{1}{\sqrt{g'^2 + g^2}}(gW_3^\mu - g'B^\mu).$$

The boson masses are then obtained as

$$m_{W^\pm} = \frac{g\xi}{\sqrt{2}}, \quad m_{Z^0} = \sqrt{g'^2 + g^2} \frac{\xi}{\sqrt{2}}. \quad (1.101)$$

The remaining degree of freedom is used to construct the massless photon field orthogonal to  $Z^0$

$$A^\mu = \frac{1}{\sqrt{g'^2 + g^2}} (gW_3^\mu + g'B^\mu). \quad (1.102)$$

This is nothing else than a change of basis from the vector space that spans the  $SU(2)_L \times U(1)_Y$  bare gauge fields  $W^\mu, B^\mu$  into the basis of the physical fields  $W^\pm, Z^0, A^\mu$ . This mixing of the bare gauge fields is also described by a rotation about an angle  $\theta_W$

$$\begin{pmatrix} A^\mu \\ Z^\mu \end{pmatrix} = \begin{pmatrix} \cos\theta_W & \sin\theta_W \\ -\sin\theta_W & \cos\theta_W \end{pmatrix} \begin{pmatrix} B^\mu \\ W_3^\mu \end{pmatrix}. \quad (1.103)$$

The Weinberg angle  $\theta_W$  is defined by the relations

$$\frac{g}{\sqrt{g^2 + g'^2}} = \cos\theta_W, \quad \frac{g'}{g} = \tan\theta_W \quad (1.104)$$

and one obtains  $e = g' \sin\theta_W = g \cos\theta_W$ . The Weinberg angle has been experimentally determined by the ratio of the weak boson masses to be

$$\sin^2\theta_W = 1 - \frac{M_W^2}{M_Z^2} = 0.222. \quad (1.105)$$

The Weinberg mixing has no influence on the charged currents. The flavour-changing interactions between the charged bosons  $W^\pm$  and the left-handed quark doublets are thus given by

$$\begin{aligned} \mathcal{L}_{W^\pm} &= g(\bar{u}_L, \bar{d}_L)\gamma_\mu(W_1^\mu t^1 + W_2^\mu t^2) \begin{pmatrix} u_L \\ d_L \end{pmatrix} \\ &= g(\bar{u}_L, \bar{d}_L)\gamma_\mu \begin{pmatrix} 0 & \frac{W_1^\mu - iW_2^\mu}{\sqrt{2}} \\ \frac{W_1^\mu + iW_2^\mu}{\sqrt{2}} & 0 \end{pmatrix} \begin{pmatrix} u_L \\ d_L \end{pmatrix} \\ &= \frac{g}{\sqrt{2}} \left( \bar{u}\gamma_\mu \frac{1 - \gamma^5}{2} W^{\mu+} d + \bar{d}\gamma_\mu \frac{1 - \gamma^5}{2} W^{\mu-} u \right). \end{aligned} \quad (1.106)$$

The above Lagrangian will be exactly the same for the lepton fields as they have been defined in (1.74). Figure 1.5 also gives an example for lepton flavour- changing processes.

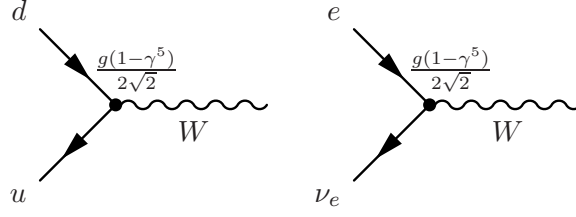


Figure 1.5: Flavour-changing weak processes

The interactions with the neutral bosons have to be calculated from

$$\mathcal{L}_{B,W_3} = g\bar{q}_1\gamma_\mu W_3^\mu t^3 q_1 + \frac{g'}{2} \sum_{i=1}^3 y_i \bar{q}_i \gamma_\mu B^\mu q_i . \quad (1.107)$$

From there one can already see that interactions generated by the neutral currents are between the fermions and antifermions of both chiralities. After rotating the bare fields into their physical counterparts this becomes

$$\mathcal{L}_{A,Z^0} = \sum_{i=1}^3 e\bar{q}_i\gamma_\mu Q_i A^\mu q_i + \frac{e}{2\sin\theta_W\cos\theta_W} \sum_{i=1}^3 \bar{q}_i\gamma_\mu(v - a\gamma^5)Z^\mu q_i . \quad (1.108)$$

The factor  $v - a\gamma^5$  describes the  $V-A$  structure of weak interaction. The neutral-current couplings  $v_f$  and  $a_f$  are, according to [17], found in Table 1.4.

The first term in (1.108) is the well-known QED interaction Lagrangian, where  $Q_i$  denotes the electromagnetic charge operators

$$Q_1 = \begin{pmatrix} \frac{2}{3} & 0 \\ 0 & -\frac{1}{3} \end{pmatrix}, \quad Q_2 = \frac{2}{3}, \quad Q_3 = -\frac{1}{3}. \quad (1.109)$$

The second term contains the interaction vertices between the neutral  $Z$  boson and the left- and right-handed quarks.

	$e$	$\nu_e$	$u$	$d$
$2v_f$	$-1 + 4\sin^2\theta_W$	1	$1 - \frac{8}{3}\sin^2\theta_W$	$-1 + \frac{4}{3}\sin^2\theta_W$
$2a_f$	-1	1	1	-1

Table 1.2: Neutral-current vector and axial-vector couplings

Now, the most important characteristics of weak interactions have been presented. The next chapter will describe the Linear Sigma Model, followed by an introduction of weak interactions according to the GWS model of electroweak interactions.

## Chapter 2

# Linear Sigma Model and Electroweak Interaction

### 2.1 The Linear Sigma Model

Linear sigma models are effective quantum field theories, where the principles of the Standard Model are applied to the hadronic degrees of freedom. In the energy region of  $\approx 1$  GeV quarks are still confined and their bound states can be observed as the light mesonic resonances. The Linear Sigma Model with  $U(N_f = 2)_L \times U(N_f = 2)_R$  symmetry attempts to describe the phenomenology of the scalar  $(\sigma, \vec{a}_0)$ , pseudoscalar  $(\eta, \vec{\pi})$ , vector  $(\omega, \vec{\rho})$ , and axialvector resonances  $(f_1, \vec{a}_1)$ . They are parametrised by direct products of the quark vectors in  $U(2)_L \times U(2)_R$  fundamental representation for up and down quarks. Then from Standard Model symmetry considerations a Lagrangian

$$\mathcal{L} = \mathcal{L}(\Phi, L^\mu, R^\mu)$$

is constructed.

Now, in this  $U(2)_L \times U(2)_R$  Linear Sigma Model,  $\Phi$  is defined as the external product of the quark spinors in the fundamental representation

$$\Phi_{ij} \simeq \langle q_L \bar{q}_R \rangle_{ij} . \quad (2.1)$$

In the above equation  $i$  and  $j$  denote the flavour indices  $i, j = 1, 2$  and the quark vectors are defined as

$$q_L = \begin{pmatrix} u_L \\ d_L \end{pmatrix}, \quad q_R = \begin{pmatrix} u_R \\ d_R \end{pmatrix} . \quad (2.2)$$



Thus, for mass-degenerate up and down quarks, the matrix-valued field  $\Phi$  reads explicitly

$$\Phi_{ij} \simeq \sqrt{2}\bar{q}_{j,R} q_{i,L}, \quad i, j = 1, 2. \quad (2.3)$$

Since  $\Phi$  is an object in the product space of the  $U(2)_L$  and  $U(2)_R$  irreducible representations, the left-hand side and right-hand side in (2.3) are not the same. However, the matrix-valued field  $\Phi$  and the external product of the flavour vectors obey the same transformation law under chiral transformations. The same holds for the left- and right-handed fields that are discussed below.

The  $[\bar{2} \otimes 2]$  irreducible representations of  $U(2)_L \times U(2)_R$  are given by one left-handed and one right-handed doublet, hence the field  $\Phi$  transforms under  $U(2)_L \times U(2)_R$  as

$$\Phi \rightarrow \Phi' = U_L \Phi U_R^\dagger. \quad (2.4)$$

The transformation is generated by the unitary matrices

$$U_L = e^{-i\theta_L^a t_a}, \quad U_R = e^{-i\theta_R^a t_a} \quad (2.5)$$

with  $t_a$  being the  $U(2)$  generators.

Using the left-handed chiral projector  $P_L$ , defined in Equation (1.27),  $\Phi_{ij}$  can be decomposed into its scalar and pseudoscalar contributions according to

$$\begin{aligned} \Phi_{ij} &\simeq \sqrt{2}\bar{q}_{j,R} q_{i,L} = \sqrt{2}\bar{q}_j P_L^2 q_i = \sqrt{2}\bar{q}_j P_L q_i \\ &= \frac{1}{\sqrt{2}}\bar{q}_j (1 - \gamma^5) q_i = \frac{1}{\sqrt{2}}(\bar{q}_j q_i - \bar{q}_j \gamma^5 q_i), \quad i, j = u, d. \end{aligned} \quad (2.6)$$

For left- and right-handed fields  $L^\mu$  and  $R^\mu$  the analogue procedure, this time applied to direct products of the fundamental and “anti”-fundamental representations of  $U(2)_L$  and  $U(2)_R$  respectively, yields the definition for vector and axial-vector fields

$$L_{ij}^\mu \simeq \sqrt{2}\bar{q}_{j,L} \gamma^\mu q_{i,L} = \frac{1}{\sqrt{2}}(\bar{q}_j \gamma^\mu q_i + \bar{q}_j \gamma^\mu \gamma^5 q_i), \quad (2.7)$$

$$R_{ij}^\mu \simeq \sqrt{2}\bar{q}_{j,R} \gamma^\mu q_{i,R} = \frac{1}{\sqrt{2}}(\bar{q}_j \gamma^\mu q_i - \bar{q}_j \gamma^\mu \gamma^5 q_i). \quad (2.8)$$

They transform separately under the adjoint representations of  $U(2)_L$  and  $U(2)_R$  as

$$L^\mu \longrightarrow U_L L^\mu U_L^\dagger, \quad R^\mu \longrightarrow U_R R^\mu U_R^\dagger. \quad (2.9)$$

Now, according to the strong isospin eigenvalues  $I_3$  of their constituents the fields are embedded into the algebra of strong isospin by means of the  $U(2)_V$  generators

$$t_0 = \frac{1}{2} \begin{pmatrix} 1 & 0 \\ 0 & 1 \end{pmatrix}, \quad t_1 = \frac{1}{2} \begin{pmatrix} 0 & 1 \\ 1 & 0 \end{pmatrix}, \quad t_2 = \frac{1}{2} \begin{pmatrix} 0 & -i \\ i & 0 \end{pmatrix}, \quad t_3 = \frac{1}{2} \begin{pmatrix} 1 & 0 \\ 0 & -1 \end{pmatrix} \quad (2.10)$$

and

$$\Phi = \Phi_a t^a, \quad L^\mu = L_a^\mu t^a, \quad R^\mu = R_a^\mu t^a. \quad (2.11)$$

The generator  $t_0$  corresponds to  $U(1)$  and  $t_i$  ( $i = 1, 2, 3$ ) correspond to the subgroup  $SU(2)$  with commutation relations

$$[t_i, t_j] = i \varepsilon_{ijk} t_k.$$

The  $SU(2)$  structure constants are given by

$$\varepsilon_{ijk} = \begin{cases} 1, & \text{for even permutations of } 123 \\ -1, & \text{for odd permutations of } 123 \\ 0, & \text{otherwise.} \end{cases}$$

Finally, the scalar,  $\sigma_a$ , and pseudoscalar degrees of freedom,  $\pi_a$ , are represented in  $\Phi$  by

$$\Phi = (\sigma + i\eta)t_0 + (\vec{a}_0 + i\vec{\pi}) \cdot \vec{t} = (\sigma_a + i\pi_a) t_a. \quad (2.12)$$

Vector,  $V^\mu$ , and axial-vector mesons,  $A^\mu$ , are introduced by left-handed and right-handed fields

$$\begin{aligned} L^\mu &= (V_a^\mu + A_a^\mu) t_a = (\omega^\mu + f_1^\mu) t_0 + (\vec{\rho}^\mu + \vec{a}_1^\mu) \cdot \vec{t}, \\ R^\mu &= (V_a^\mu - A_a^\mu) t_a = (\omega^\mu - f_1^\mu) t_0 + (\vec{\rho}^\mu - \vec{a}_1^\mu) \cdot \vec{t}. \end{aligned} \quad (2.13)$$

Again, the index  $a = 0, 1, 2, 3$  denotes the generators of  $U(2)$ , while the index  $i = 1, 2, 3$  denotes the  $SU(2)$  generators.

Having thus attributed the light mesonic states to their representation in  $\Phi$ ,  $L^\mu$ , and  $R^\mu$ , the Lagrangian of the model can be constructed. It is based on a free Klein-Gordon Lagrangian for scalar and pseudoscalar fields with a  $\Phi^4$  potential

$$\mathcal{L}_0 = \text{Tr}[(\partial^\mu \Phi^\dagger)(\partial^\mu \Phi)] - m_0^2 \text{Tr}[\Phi^\dagger \Phi] - \lambda_1 \text{Tr}[(\Phi^\dagger \Phi)^2] - \lambda_2 (\text{Tr}[\Phi^\dagger \Phi])^2. \quad (2.14)$$

The Lagrangian  $\mathcal{L}_0$  is invariant under global  $U(2)_L \times U(2)_R$  transformations (2.4) of  $\Phi$ .

The parameters of a global transformation are space-time independent and together with the invariance of the trace under cyclic permutations of its arguments the invariance of the derivative term in  $\mathcal{L}_0$  can be seen from

$$\begin{aligned}\text{Tr}[(\partial^\mu \Phi'^\dagger)(\partial^\mu \Phi')] &= \text{Tr}[(\partial^\mu U_R \Phi U_L^\dagger)(\partial^\mu U_L \Phi U_R^\dagger)] \\ &= \text{Tr}[U_R(\partial^\mu \Phi)U_L^\dagger U_L(\partial^\mu \Phi)U_R^\dagger] = \text{Tr}[(\partial^\mu \Phi^\dagger)(\partial^\mu \Phi)] .\end{aligned}$$

The same holds for all other terms in  $\mathcal{L}_0$  as they contain only products of  $\Phi$  with its hermitian conjugate  $\Phi^\dagger$ .

When vector and axial-vector fields were, in a variety of ways [18, 19, 20], introduced into the Linear Sigma Model they were first treated as massive Yang-Mills fields of a local chiral symmetry. They transform as the adjoint representation of the chiral group and they are spin 1 fields. Thus, it seems obvious to construct a chirally invariant Lagrangian based on the assumption that the left- and right-handed fields are the gauge bosons of a local  $U(2)_L \times U(2)_R$  symmetry. Consequently, the global  $U(2)_L \times U(2)_R$  symmetry was set to a local one as it has been done by [18, 19, 20] for an  $O(4)$  model and by [21] for the  $U(2)$  model. However, there is no local chiral symmetry in the QCD Lagrangian and the present Linear Sigma Model is also based on a global chiral symmetry. But, the local model is still the basis on which the chirally invariant terms for vector and axial-vector mesons were constructed and the restraint of a local symmetry was lifted only later.

At first, the partial derivative in (2.14) is replaced by a covariant one and generates the dynamics between scalar and vector mesons

$$\begin{aligned}D^\mu \Phi &= \partial^\mu \Phi - ig_1 (L^\mu \Phi - \Phi R^\mu) , \\ (D^\mu \Phi)^\dagger &= \partial^\mu \Phi^\dagger + ig_1 (R^\mu \Phi^\dagger - \Phi^\dagger L^\mu)\end{aligned}\tag{2.15}$$

and (2.14) becomes

$$\mathcal{L}_\Phi = \text{Tr}[(D^\mu \Phi^\dagger)(D^\mu \Phi)] - m_0^2 \text{Tr} [\Phi^\dagger \Phi] - \lambda_1 \text{Tr} [(\Phi^\dagger \Phi)^2] - \lambda_2 (\text{Tr} [\Phi^\dagger \Phi])^2 .\tag{2.16}$$

The Lagrangian is invariant under local transformations if the left-handed and right-handed fields transform as

$$L^\mu \longrightarrow U_L L^\mu U_L^\dagger + \frac{i}{g_1} U_L \partial^\mu U_L^\dagger ,\tag{2.17}$$

$$R^\mu \longrightarrow U_R R^\mu U_R^\dagger + \frac{i}{g_1} U_R \partial^\mu U_R^\dagger .\tag{2.18}$$

In the global model, the second term in (2.18) becomes zero and the transformation laws in Equation (2.9) are obtained.

While maintaining gauge invariance by constructing a covariant derivative on the basis of a local chiral symmetry is effortless, introducing a mass term for the vector and axial-vector fields already breaks chiral gauge invariance. One could also think about introducing a scalar field, similar to the Higgs mechanism for the electroweak interactions, but the main advantage of a local chiral symmetry would be that the gauge field couplings could all be described by the same coupling constant  $g_1$  in (2.15).

However, most important is that the models based on a local chiral symmetry cannot describe the phenomenology of vector and axial-vector mesons [20]. Thus, one reduces chiral symmetry to a global one and can then simply add a mass term according to

$$\frac{m_1^2}{2} \text{Tr} \left[ (L^\mu)^2 + (R^\mu)^2 \right] . \quad (2.19)$$

The invariance of the partial derivative term under global chiral transformations can be seen from

$$\begin{aligned} D^\mu \Phi &\longrightarrow (D^\mu \Phi)' = U_L (\partial^\mu \Phi) U_R^\dagger - ig_1 \left( U_L L^\mu U_L^\dagger U_L \Phi U_R^\dagger - U_L \Phi U_R^\dagger U_R R^\mu U_R^\dagger \right) \\ &= U_L (\partial^\mu \Phi) U_R^\dagger - ig_1 \left( U_L L^\mu \Phi U_R^\dagger - U_L \Phi R^\mu U_R^\dagger \right) \\ &= U_L D^\mu \Phi U_R^\dagger \end{aligned} \quad (2.20)$$

and for the mass term from

$$\begin{aligned} &\frac{m_1}{2} \text{Tr} (L'_\mu L^{\mu'} + R'_\mu R^{\mu'}) \\ &= \frac{m_1}{2} \text{Tr} [U_L L_\mu U_L^\dagger U_L L^\mu U_L^\dagger + U_R R_\mu U_R^\dagger U_R R^\mu U_R^\dagger] \\ &= \frac{m_1}{2} \text{Tr} [L_\mu L^\mu + R_\mu R^\mu] . \end{aligned} \quad (2.21)$$

Again, only the invariance of the trace under cyclic permutations was used.

The dynamics of the Yang-Mills bosons is encoded in the field strength tensors for left- and right-handed fields

$$L^{\mu\nu} = \partial^\mu L^\nu - \partial^\nu L^\mu , \quad R^{\mu\nu} = \partial^\mu R^\nu - \partial^\nu R^\mu . \quad (2.22)$$

They transform covariantly under  $U(N_f)_L$  and  $U(N_f)_R$

$$L^{\mu\nu} \longrightarrow U_L L^{\mu\nu} U_L^\dagger , \quad R^{\mu\nu} \longrightarrow U_R R^{\mu\nu} U_R^\dagger . \quad (2.23)$$

They are generally obtained from the commutator of the covariant derivative and thus should also contain non-Abelian contributions from the left- and right-handed fields. With a local chiral symmetry, these non-Abelian

contributions would then be proportional to the coupling constant  $g_1$ . Since this model is only invariant under global transformations, one can define new additional couplings for each contribution that would arise from the commutator in the field strength tensors. Thus,  $L^{\mu\nu}$  and  $R^{\mu\nu}$  have been redefined and contain the derivative terms only.

The non-Abelian contributions to the field strength tensors appear together with other chirally invariant higher-order interaction vertices with couplings  $g_2, g_3, g_4, g_5$  and  $g_6$  in  $\mathcal{L}_3$  and  $\mathcal{L}_4$

$$\mathcal{L}_3 = -2ig_2(\text{Tr}[L_{\mu\nu}[L_\mu, L_\nu]] + \text{Tr}[R_{\mu\nu}, [R_\mu, R_\nu]]) , \quad (2.24)$$

$$\begin{aligned} \mathcal{L}_4 = & g_3\{\text{Tr}[L^\mu L^\nu L_\mu L_\nu] + \text{Tr}[R^\mu R^\nu R_\mu R_\nu]\} \\ & + g_4\{\text{Tr}[L^\mu L_\mu L^\nu L_\nu] + \text{Tr}[R^\mu R_\mu R^\nu R_\nu]\} \\ & + g_5\text{Tr}[R^\mu R_\nu]\text{Tr}[L^\mu L_\nu] \\ & + g_6\{\text{Tr}[L_\mu, L^\mu]\text{Tr}[L_\nu, L^\nu] + \text{Tr}[R_\mu, R^\mu]\text{Tr}[R_\nu, R^\nu]\} . \end{aligned} \quad (2.25)$$

Because the field strength tensors are obtained as the commutators of the covariant derivatives, they inevitably transform covariantly by definition. Thus, the Lagrangian for  $L^\mu$  and  $R^\mu$  finally reads

$$\mathcal{L}_{LR} = \frac{1}{4}\text{Tr}[(L^{\mu\nu})^2 + (R^{\mu\nu})^2] + \frac{m_1}{2}\text{Tr}[(L^\mu)^2 + (R^\mu)^2] + \mathcal{L}_3 + \mathcal{L}_4 . \quad (2.26)$$

Additional chirally invariant terms between the scalar, pseudoscalar and vector and axial-vector fields are added as

$$\begin{aligned} \mathcal{L}_5 = & \frac{h_1}{2}\text{Tr}(\Phi^\dagger\Phi)\text{Tr}[L_\mu L^\mu + R_\mu R^\mu] + h_2\text{Tr}[\Phi^\dagger L_\mu L^\mu \Phi + \Phi^\dagger R_\mu R^\mu \Phi] \\ & + 2h_3\text{Tr}[\Phi R_\mu \Phi^\dagger L^\mu] . \end{aligned} \quad (2.27)$$

They generate other possible interactions and will also modify the equations for the physical vector and axial-vector masses.

### 2.1.1 Spontaneous Symmetry Breaking, Field Renormalisation, and Mass Terms

In Chapter 1.3 the chiral symmetry of the QCD Lagrangian has been discussed. It was shown that chiral symmetry is broken explicitly by the quark masses and spontaneously by the non-vanishing vacuum expectation value of the chiral condensate. Moreover, even for vanishing quark masses the global

axial symmetry is broken by the  $U(1)_A$  anomaly. For massive but degenerate quarks the symmetry under axial transformations is completely violated and for non-degenerate massive quarks  $SU(2)_V$  is broken, too, leaving  $U(1)_V$  as the only unbroken symmetry.

To emulate this pattern of explicit chiral symmetry breaking two additional terms are introduced into the model

$$\mathcal{L}_{eSB} + \mathcal{L}_A = \text{Tr}[H(\Phi^\dagger + \Phi)] + c(\det\Phi + \det\Phi^\dagger). \quad (2.28)$$

The first term

$$\mathcal{L}_{eSB} = \text{Tr}[H(\Phi^\dagger + \Phi)] \quad (2.29)$$

emulates the explicit breaking of the  $SU(2)$  vector symmetry corresponding to the different possibilities of quark-mass degeneracy. The matrix  $H$  is diagonal in flavour space and defined as

$$H = h_a t^a, \quad (2.30)$$

where the elements  $h_a$  correspond to the quark masses and  $t_a$  to the  $U(2)$  generators. The explicit symmetry breaking term affects the vacuum by tilting the ground state towards the direction of the respective generators. Because the chiral condensate must carry the quantum numbers of the vacuum, only the generators that correspond to the non-charged particles ( $t_0$  and  $t_3$  for  $N_f = 2$ ) are used to simulate the explicit breaking of chiral symmetries and the matrix  $H$  is defined to be diagonal ( $h_1 = h_2 = 0$ ), in order not to violate the symmetry under charge conjugation by off-diagonal terms.

Vanishing quark masses correspond to an unbroken chiral symmetry, thus all coefficients  $h_a$  would be set to zero and the  $U(2)_V$  as well as the symmetry under axial transformations remains unharmed. For  $h_0 \neq 0$  and all other  $h_{1,2,3} = 0$  the explicit symmetry breaking term represents the case of non-vanishing but degenerate quark masses where  $SU(2)_V$  is still intact. For non-vanishing and non-degenerate quark masses one would also set  $h_3 \neq 0$  to break  $SU(2)_V$  explicitly.

The present Linear Sigma Model is based on the assumption of massive but mass-degenerate up and down quarks. On the hadronic mass scale, the mass difference between up and down quark is small enough to be neglected. Hence,  $m_u = m_d$  and therefore  $h_0 \neq 0$  and  $h_3 = 0$ . This also corresponds to the fact that after the symmetry has been spontaneously broken, only the sigma field has a vacuum expectation value. Thus, the ground state is tilted towards the  $t_0$  direction. More information about how explicit symmetry breaking of QCD in nature is realised in Linear Sigma Models with different numbers of quark flavours is, e.g., found in [22].

The second term in (2.28)

$$\mathcal{L}_A = c(\det\Phi + \det\Phi^\dagger)$$

corresponds to the  $U(1)_A$  anomaly and breaks the symmetry explicitly to  $U(2)_V \times SU(2)_A$ . According to the transformation of  $\Phi$  as given in (2.4) the term yielding the  $U(1)_A$  anomaly becomes

$$\begin{aligned} \mathcal{L}_A \rightarrow c[\det\Phi' + \det\Phi'^\dagger] &= c \left[ \det(U_L\Phi U_R^\dagger) + \det(U_R\Phi^\dagger U_L^\dagger) \right] \\ &= c \left[ \det \left( e^{-i\theta_L^a t_a} \Phi e^{i\theta_R^a t_a} \right) + \det \left( e^{-i\theta_R^a t_a} \Phi^\dagger e^{i\theta_L^a t_a} \right) \right] \\ &= c \left[ \det \left( e^{-i\frac{1}{2}(\theta_V^a t_a + \theta_A^a t_a)} \Phi e^{i\frac{1}{2}(\theta_V^a t_a - \theta_A^a t_a)} \right) \right. \\ &\quad \left. + \det \left( e^{-i\frac{1}{2}(\theta_V^a t_a - \theta_A^a t_a)} \Phi^\dagger e^{i\frac{1}{2}(\theta_V^a t_a + \theta_A^a t_a)} \right) \right] \\ &= c \left[ \det \left( e^{-i\theta_A^a t_a} \Phi \right) + \det \left( e^{i\theta_A^a t_a} \Phi^\dagger \right) \right] \\ &= c \left[ \det \left( e^{-i\theta_A^0 t_0 - i\theta_A^i t_i} \Phi \right) + \det \left( e^{i\theta_A^0 t_0 + i\theta_A^i t_i} \Phi^\dagger \right) \right] \\ &= c \left[ \det \left( e^{-i\theta_A^i t_i} \right) \det \left( e^{-i\theta_A^0 t_0} \Phi \right) \right. \\ &\quad \left. + \det \left( e^{i\theta_A^i t_i} \right) \det \left( e^{i\theta_A^0 t_0} \Phi^\dagger \right) \right] \\ &= c \left[ \exp(\text{Tr}[-i\theta_A^i t_i]) \det \left( e^{-i\theta_A^0 t_0} \Phi \right) \right. \\ &\quad \left. + \exp(\text{Tr}[i\theta_A^i t_i]) \det \left( e^{i\theta_A^0 t_0} \Phi^\dagger \right) \right] \\ &= \mathcal{L}'_A \neq \mathcal{L}_A, \end{aligned} \tag{2.31}$$

hence, because the  $SU(2)$  generators  $t_i, i \neq 0$ , are traceless matrices,  $\mathcal{L}_A$  transforms into

$$\mathcal{L}'_A = c \left[ \det \left( e^{-i\theta_A^0 t_0} \Phi \right) + \det \left( e^{i\theta_A^0 t_0} \Phi^\dagger \right) \right] \tag{2.32}$$

and thus breaks, as it has been shown above, the axial symmetry  $U(1)_A$ .

Finally, the full Lagrange density for the global  $U(2)_L \times U(2)_R$  Linear Sigma Model with scalar, pseudoscalar, vector, and axial-vector degrees of freedom is

$$\begin{aligned} \mathcal{L} &= \mathcal{L}_\Phi + \mathcal{L}_{LR} + \mathcal{L}_{eSB} + \mathcal{L}_A + \mathcal{L}_3 + \mathcal{L}_4 + \mathcal{L}_5 \\ &= \text{Tr}[(D^\mu\Phi^\dagger)(D^\mu\Phi)] - m_0^2 \text{Tr}[\Phi^\dagger\Phi] - \lambda_1 \text{Tr}[(\Phi^\dagger\Phi)^2] - \lambda_2 (\text{Tr}[\Phi^\dagger\Phi])^2 \\ &\quad - \frac{1}{4} \text{Tr}[(L^{\mu\nu})^2 - (R^{\mu\nu})^2] + \frac{m_1}{2} \text{Tr}[(L^\mu)^2 + (R^\mu)^2] \\ &\quad + \text{Tr}[H(\Phi^\dagger + \Phi)] + c(\det\Phi + \det\Phi^\dagger) + \mathcal{L}_3 + \mathcal{L}_4 + \mathcal{L}_5. \end{aligned} \tag{2.33}$$

In terms of its mesonic components the Lagrangian without the higher-order terms  $\mathcal{L}_{3,4,5}$  reads

$$\begin{aligned}
\mathcal{L} = & \frac{1}{2}[\partial^\mu \sigma + g_1(\eta f_1^\mu + \vec{\pi} \cdot \vec{a}_1^\mu)]^2 + \frac{1}{2}[\partial^\mu \eta - g_1(\sigma f_1^\mu + \vec{a}_0 \cdot \vec{a}_1^\mu)]^2 \\
& + \frac{1}{2}[\partial^\mu \vec{a}_0 + g_1(\vec{\rho}^\mu \times \vec{a}_0 + \eta \vec{a}_1^\mu + \vec{\pi} f_1^\mu)]^2 \\
& + \frac{1}{2}[\partial_\mu \vec{\pi} - g_1(\vec{\pi} \times \vec{\rho}^\mu + \sigma \vec{a}_1^\mu + \vec{a}_0 f_1^\mu)]^2 \\
& - \frac{m_0^2}{2}(\sigma^2 + \eta^2 + \vec{a}_0^2 + \vec{\pi}^2) - \frac{\lambda_1}{4}(\sigma^2 + \eta^2 + \vec{a}_0^2 + \vec{\pi}^2)^2 \\
& - \frac{\lambda_2}{2} \left[ \frac{1}{4}(\sigma^2 + \eta^2 + \vec{a}_0^2 + \vec{\pi}^2)^2 + (\sigma \vec{a}_0 + \eta \vec{\pi})^2 + (\vec{a}_0 \times \vec{\pi})^2 \right] \\
& - \frac{1}{4}(\partial^\mu \omega^\nu - \partial^\nu \omega^\mu)^2 - \frac{1}{4}(\partial^\mu f_1^\nu - \partial^\nu f_1^\mu)^2 \\
& - \frac{1}{4}[\partial^\mu \vec{\rho}^\nu - \partial^\nu \vec{\rho}^\mu + g_1(\vec{\rho}^\mu \times \vec{\rho}^\nu + \vec{a}_1^\mu \times \vec{a}_1^\nu)]^2 \\
& - \frac{1}{4}[\partial^\mu \vec{a}_1^\nu - \partial^\nu \vec{a}_1^\mu + g_1(\vec{\rho}^\mu \times \vec{a}_1^\nu + \vec{a}_1^\mu \times \vec{\rho}^\nu)]^2 \\
& + \frac{m_1^2}{2}(\omega^\mu{}^2 + \vec{\rho}^\mu{}^2 + f_1^\mu{}^2 + \vec{a}_1^\mu{}^2) + \frac{1}{2}c(\sigma^2 - \vec{a}_0^2 - \eta^2 + \vec{\pi}^2) + h_0\sigma .
\end{aligned} \tag{2.34}$$

The Lagrangian  $\mathcal{L}_5$  also contains vector and axial-vector self-interactions and thus affects the equations describing their physical masses. In terms of its mesonic fields one obtains

$$\begin{aligned}
\mathcal{L}_5 = & \frac{h_1}{2} \text{Tr}[\Phi^\dagger \Phi] \text{Tr}[L_\mu L^\mu + R_\mu R^\mu] + h_2 \text{Tr}[\Phi^\dagger L_\mu L^\mu \Phi + \Phi^\dagger R_\mu R^\mu \Phi] \\
& + 2h_3 \text{Tr}[\Phi R_\mu \Phi^\dagger L_\mu] \\
= & \frac{h_1}{4} (\sigma^2 + \eta^2 + \vec{a}_0^2 + \vec{\pi}^2) (f_{1\mu}^2 + \omega_\mu^2 + \vec{a}_{1\mu}^2 + \vec{\rho}_\mu^2) \\
& + \frac{h_2}{4} \left[ (\sigma^2 + \eta^2 + \vec{a}_0^2 + \vec{\pi}^2) (f_{1\mu}^2 + \omega_\mu^2 + \vec{a}_{1\mu}^2 + \vec{\rho}_\mu^2) \right. \\
& \quad \left. + 4(f_{1\mu} \vec{a}_{1\mu} + \omega_\mu \vec{\rho}_\mu) \cdot (\eta \vec{\pi} + \sigma \vec{a}_0 + (\vec{a}_0 \times \vec{\pi})) \right] \\
& + \frac{1}{4} h_3 \left\{ 2[(\vec{a}_{1\mu} \times \vec{\pi})^2 - (\vec{a}_{1\mu} \cdot \vec{\pi})^2 - (\vec{\rho}_\mu \times \vec{\pi})^2 + (\vec{\rho}_\mu \cdot \vec{\pi})^2 \right. \\
& \quad + (\vec{a}_{1\mu} \times \vec{a}_0)^2 - (\vec{a}_{1\mu} \cdot \vec{a}_0)^2 - (\vec{\rho}_\mu \times \vec{a}_0)^2 + (\vec{\rho}_\mu \cdot \vec{a}_0)^2] \\
& \quad - (f_{1\mu}^2 - \omega_\mu^2)(\eta^2 + \sigma^2 + \vec{a}_0^2 + \vec{\pi}^2) - (\eta^2 + \sigma^2)(\vec{a}_{1\mu}^2 - \rho_\mu^2) \\
& \quad - 4f_{1\mu}[\sigma \vec{a}_{1\mu} \cdot \vec{a}_0 + \eta \vec{a}_{1\mu} \cdot \vec{\pi} - \vec{\rho}_\mu \cdot (\vec{\pi} \times \vec{a}_0)] \\
& \quad \left. + 4\omega_\mu[\sigma \vec{\rho}_\mu \cdot \vec{a}_0 + \eta \vec{\rho}_\mu \cdot \vec{\pi} - \vec{a}_{1\mu} \cdot (\vec{\pi} \times \vec{a}_0)] \right\}
\end{aligned}$$



The analysis of the mass spectra of the scalar resonances  $\sigma$  and  $\pi$  indicates (Section 1.3) that chiral symmetry is dynamically broken by a non-vanishing vacuum expectation value of the ground state.

In the hadronic sector of QCD spontaneous breaking of chiral symmetry is realised by shifting the  $\sigma$  field by its non-vanishing constant vacuum expectation value  $\langle 0|\bar{q}_R q_L|0\rangle \simeq \phi_0$  such that the excitations of the field  $\Phi$  around its ground state can be studied. Since the  $\sigma$  resonance is the only scalar resonance that is equipped with the quantum numbers of the vacuum ( $J^P = 0^+$ ) it is considered to take on the role of the chiral condensate. The potential for  $\sigma$  can be read off from the Lagrangian (2.34) as

$$V(\sigma) = \frac{1}{2}(m_0^2 - c)\sigma^2 + \frac{1}{4}\left(\lambda_1 + \frac{\lambda_1}{2}\right)\sigma^4 - h_0\sigma . \quad (2.35)$$

The effect of the explicit symmetry breaking term  $\mathcal{L}_{\text{eSB}}$  is clearly seen in the potential above. By means of  $-h_0\sigma$  the ground state is tilted towards the positive  $\sigma$  direction and the vacuum loses its symmetry under axial rotations.

Setting  $m_0^2 - c < 0$  results, before explicit symmetry breaking ( $h_0 = 0$ ), in an infinite number of degenerate ground states along a circle in the plane of the chiral partners at<sup>1</sup>  $\sigma = \phi_0$ . The vacuum expectation value  $\phi_0$  is defined as the value that minimises the potential

$$\begin{aligned} \left. \frac{dV(\sigma)}{d\sigma} \right|_{\sigma=\phi_0} &= 0 , \\ \Rightarrow (m_0^2 - c)\phi_0 + \left(\lambda_1 + \frac{\lambda_2}{2}\right)\phi_0^3 - h_0 &= 0 . \end{aligned} \quad (2.36)$$

At this point ( $h_0 = 0$ ) the vacuum is still invariant under rotations in the plane of the chiral partners. The symmetry is spontaneously broken if sigma is shifted about its vacuum expectation value

$$\sigma(x^\mu) \longrightarrow \sigma(x^\mu) + \phi_0 . \quad (2.37)$$

Applying (2.37) to the Lagrange density results in the following additional terms for  $\mathcal{L}_\Phi$

$$\frac{1}{2} \left[ -2g_1\phi_0\partial^\mu\eta f_1^\mu + g_1^2\phi_0^2 f_1^\mu{}^2 + 2\phi_0 g_1^2(\sigma f_1^\mu{}^2 + f_1^\mu\vec{a}_0 \cdot \vec{a}_1^\mu) \right]$$

---

<sup>1</sup>An explicit expression for  $\phi_0$ , dependent on the bare parameters  $m_0, \lambda_1, \lambda_2, c, h_0$ , can be obtained by Cardano's method and has been explicitly calculated in [23]. In the following discussion  $\phi_0$  is simply taken as a constant. It will be expressed in terms of the physical, observable masses for  $\rho$  and  $a_1$  and the pion decay constant  $f_\pi$ .

$$\begin{aligned}
& + \frac{1}{2} [-2g_1\phi_0\partial^\mu\vec{\pi}\cdot\vec{a}_1^\mu + g_1^2\phi_0^2\vec{a}_1^{\mu 2} + 2\phi_0g_1^2(\sigma\vec{a}_1^{\mu 2} + f_1^\mu\vec{a}_0\cdot\vec{a}_1^\mu + (\vec{\pi}\times\vec{\rho}^\mu)\cdot\vec{a}_1^\mu)] \\
& - \frac{m_0^2}{2}(\phi_0^2 + 2\phi_0\sigma) \\
& - \frac{\lambda_1}{4} [\phi_0^4 + 4\phi_0^3\sigma + 6\phi_0^2\sigma^2 + 4\phi_0\sigma^3 + 2\phi_0^2\eta^2 + 4\phi_0\sigma\eta^2 + 2\phi_0^2\vec{a}_0^2 \\
& \quad + 4\phi_0\sigma\vec{a}_0^2 + 2\phi_0^2\vec{\pi}^2 + 4\phi_0\sigma\vec{\pi}^2] \\
& - \frac{\lambda_2}{2} \left[ \frac{1}{4} (\phi_0^4 + 4\phi_0^3\sigma + 6\phi_0^2\sigma^2 + 4\phi_0\sigma^3 + 2\phi_0^2\eta^2 + 4\phi_0\sigma\eta^2 + 2\phi_0^2\vec{a}_0^2 \right. \\
& \quad \left. + 4\phi_0\sigma\vec{a}_0^2 + 2\phi_0^2\vec{\pi}^2 + 4\phi_0\sigma\vec{\pi}^2) + (\phi_0^2\vec{a}_0^2 + 2\phi_0\sigma\vec{a}_0^2 + 2\phi_0\eta\vec{a}_0\cdot\vec{\pi}) \right] \\
& + h_0\phi_0 + \frac{1}{2}c(\phi_0^2 + 2\phi_0\sigma) . \tag{2.38}
\end{aligned}$$

For  $\mathcal{L}_5$  one obtains the following additional terms

$$\begin{aligned}
& \frac{h_1}{2}\phi_0\sigma(f_{1\mu}^2 + \omega_\mu^2 + \vec{a}_{1\mu}^2 + \vec{\rho}_{1\mu}^2) + \frac{h_1}{4}\phi_0^2(f_{1\mu}^2 + \omega_\mu^2 + \vec{a}_{1\mu}^2 + \vec{\rho}_{1\mu}^2) \\
& + \frac{h_2}{2}\phi_0\sigma(f_{1\mu}^2 + \omega_\mu^2 + \vec{a}_{1\mu}^2 + \vec{\rho}_{1\mu}^2) + \frac{h_2}{4}\phi_0^2(f_{1\mu}^2 + \omega_\mu^2 + \vec{a}_{1\mu}^2 + \vec{\rho}_{1\mu}^2) \\
& + h_2\phi_0(f_{1\mu}\vec{a}_0\cdot\vec{a}_{1\mu} + \omega_\mu\vec{a}_0\cdot\vec{\rho}) \\
& + \frac{h_3}{2}\phi_0\sigma(-f_{1\mu}^2 + \omega_\mu^2 - \vec{a}_{1\mu}^2 + \vec{\rho}_{1\mu}^2) + \frac{h_3}{4}\phi_0^2(-f_{1\mu}^2 + \omega_\mu^2 - \vec{a}_{1\mu}^2 + \vec{\rho}_{1\mu}^2) \\
& + h_3\phi_0[\omega_\mu\vec{a}_0\cdot\vec{\rho} - f_{1\mu}\vec{a}_0\cdot\vec{a}_{1\mu} + \vec{\pi}\cdot(\vec{a}_{1\mu}\times\vec{\rho})] . \tag{2.39}
\end{aligned}$$

The blue terms, being proportional to the field self-interactions, give additional contributions to the quadratic scalar, pseudoscalar, vector, and axial-vector meson terms

$$\begin{aligned}
& \frac{3}{2}\left(\lambda_1 + \frac{\lambda_2}{2}\right)\phi_0^2\sigma^2 , & \frac{1}{2}\left(\lambda_1 + \frac{\lambda_2}{2}\right)\phi_0^2\vec{\pi}^2 , \\
& \frac{1}{2}\left(\lambda_1 + \frac{\lambda_2}{2}\right)\phi_0^2\eta^2 , & \frac{1}{2}\left(\lambda_1 + \frac{3\lambda_2}{2}\right)\phi_0^2\vec{a}_0^2 , \\
& \left[g_1^2 + \frac{1}{2}(h_1 + h_2 - h_3)\right]\phi_0^2f_1^{\mu 2} , & \left[g_1^2 + \frac{1}{2}(h_1 + h_2 - h_3)\right]\phi_0^2\vec{a}_1^{\mu 2} .
\end{aligned}$$

Together with the symmetry breaking terms arising from the  $U(1)_A$  anomaly

$$c(\det\Phi + \det\Phi^\dagger) = \frac{1}{2}c(\sigma^2 + \vec{\pi}^2 - \eta^2 - \vec{a}_0^2) ,$$

the meson masses are obtained as

$$m_\sigma^2 = m_0^2 + 3\left(\lambda_1 + \frac{\lambda_2}{2}\right)\phi_0^2 - c , \tag{2.40}$$

$$m_{a_0}^2 = m_0^2 + \left(\lambda_1 + 3\frac{\lambda_2}{2}\right)\phi_0^2 + c , \tag{2.41}$$

$$m_\eta^2 = Z^2 \left[ m_0^2 + \left( \lambda_1 + \frac{\lambda_2}{2} \right) \phi_0^2 + c \right], \quad (2.42)$$

$$m_\pi^2 = Z^2 \left[ m_0^2 + \left( \lambda_1 + \frac{\lambda_2}{2} \right) \phi_0^2 - c \right] = \frac{h_0}{\phi_0}, \quad (2.43)$$

$$m_\omega^2 = m_\rho^2 = m_1^2 + \frac{\phi_0^2}{2} (h_1 + h_2 + h_3), \quad (2.44)$$

$$m_{f_1}^2 = m_{a_1}^2 = m_1^2 + (g_1 \phi_0)^2 + \frac{\phi_0^2}{2} (h_1 + h_2 - h_3). \quad (2.45)$$

The constants  $h_1, h_2, h_3$  arise from  $\mathcal{L}_5$  and not from the explicit symmetry breaking term  $\mathcal{L}_{\text{eSB}}$ , where apart from  $h_0$  all other  $h_a = 0$ . As it will be shown later, the factor  $Z^2$  in the mass terms of the pseudoscalar states is due to a wave-function renormalisation that will take place in the course of the procedure that removes the unphysical, bilinears marked in red in (2.38). Without spontaneous symmetry breaking  $Z$  would be equal to one. The above equations clearly show that spontaneous symmetry breaking prompts the mass difference between the chiral partners  $\sigma, \pi$  and  $\eta, \vec{a}_0$ . The mass degeneracy between the vector and axial-vector chiral partners is lifted by a commensurate shift of the axial-vector mass terms.

Shifting  $\sigma$  about its constant vacuum expectation value has broken the  $SU(2)_A$  symmetry spontaneously and gave rise to  $N_f^2 - 1 = 3$  Goldstone bosons, the pions. The scalar  $\sigma$  took on the role of the Higgs field in the electroweak Lagrangian. Its vacuum expectation value  $\phi_0$  couples to the scalar and pseudoscalar singlets and gives rise to additional mass terms which, even without explicit chiral symmetry breaking ( $h_0 = 0$ ), realize the mass difference between the chiral partners  $\sigma_0$  and  $\pi$ , as well as between  $\rho$  and  $a_1$ . In nature the pions are indeed massive ( $h_0 > 0$ ), but from PCAC one can also conclude that the explicit breaking of the axial symmetry is only small. The pions are thus considered to be the quasi-Goldstone bosons of the spontaneously broken axial symmetry.

The bilinear terms marked in red in (2.38)

$$2g_1 \phi_0 \partial^\mu \eta f_{1\mu}^\mu, \quad 2g_1 \phi_0 \partial^\mu \vec{\pi} \cdot \vec{a}_1^\mu$$

appear as off-diagonal couplings of the pseudoscalar and axial-vector fields and then the bare fields in the Lagrangian would not be the eigenvectors of the interaction Hamiltonian, but mixed  $\vec{\pi} \vec{a}_{1\mu}$  and  $\eta f_{1\mu}$  states.

Now, if chiral symmetry was local, these bilinear contributions could be removed by a 't Hooft gauge-fixing term [21] according to

$$\mathcal{L}_{GF} = -\frac{1}{2\xi} (\partial_\mu \omega^\mu)^2 - \frac{1}{2\xi} (\partial_\mu f_1^\mu + \xi g_1 \phi_0 \eta)^2$$

$$-\frac{1}{2\xi}(\partial_\mu \vec{\rho}^\mu)^2 - \frac{1}{2\xi}(\partial_\mu \vec{a}_1^\mu - \xi g_1 \phi_0 \vec{\pi})^2 . \quad (2.46)$$

If now as for the GWS model the vacuum is set to the  $t_3$  component only and  $\xi \rightarrow \infty$  (unitary gauge), then  $\mathcal{L}_{GF}$  would reduce to

$$-g_1 \phi_0 \partial_\mu f_1^\mu \eta - \frac{1}{2} \xi g_1^2 \phi_0^2 \eta^2 - g_1 \phi_0 \partial_\mu \vec{a}_1^\mu \cdot \vec{\pi} - \frac{1}{2} \xi g_1^2 \phi_0^2 \vec{\pi}^2$$

and cancel the bilinear terms in (2.38). Using the 't Hooft gauge fixing would be desirable as it maintains renormalisability. However, chiral symmetry is only global and applying the 't Hooft gauge fixing does not remove the unphysical mixing terms moreover, effective theories do not have to be renormalisable and gauge symmetry is already broken by the vector and axial-vector masses.

Another possibility is to redefine the axial-vector fields,  $f_{1\mu}$  and  $\vec{a}_{1\mu}$ , and consider the bare fields as mixed states of their physical composites. The axial-vector bare fields are then replaced by

$$A_a^\mu \longrightarrow A_a^\mu + w \partial^\mu \pi_a . \quad (2.47)$$

It should be remembered that  $\pi_a t^a = \eta t_0 + \vec{\pi} \cdot \vec{t}$ . In order to remove the bilinear terms in (2.38),  $w$  is defined as

$$w = \frac{g_1 \phi_0}{m_{a_1}^2} . \quad (2.48)$$

Now, in order to examine the procedure of removing the unphysical bilinear terms, only

$$\mathcal{L}_\Phi + \mathcal{L}_{YM} + \mathcal{L}_{\phi_0} \quad (2.49)$$

will be considered, where  $\mathcal{L}_\Phi$  is the scalar Lagrangian with the contributions from SSB being separated into  $\mathcal{L}_{\phi_0}$  and  $\mathcal{L}_{YM}$  that are affected by the shift of the axial-vector fields.

After the shift of the axial-vector fields, the scalar Lagrangian without the contributions from spontaneous symmetry breaking reads

$$\begin{aligned} \mathcal{L}_\Phi = & \frac{1}{2} \{ (\partial^\mu \sigma)^2 + 2g_1 (\partial^\mu \sigma) [\eta (f_1^\mu + w \partial^\mu \eta) + \vec{\pi} \cdot (\vec{a}_1^\mu + w \partial^\mu \vec{\pi})] \\ & + g_1^2 [\eta (f_1^\mu + w \partial^\mu \eta) + \vec{\pi} \cdot (\vec{a}_1^\mu + w \partial^\mu \vec{\pi})]^2 \} \\ & + \frac{1}{2} \{ (\partial^\mu \eta)^2 - 2g_1 (\partial^\mu \eta) [\sigma (f_1^\mu + w \partial^\mu \eta) + \vec{a}_0 \cdot (\vec{a}_1^\mu + w \partial^\mu \vec{\pi})] \\ & + g_1^2 [\sigma (f_1^\mu + w \partial^\mu \eta) + \vec{a}_0 \cdot (\vec{a}_1^\mu + w \partial^\mu \vec{\pi})]^2 \} \\ & + \frac{1}{2} \{ (\partial^\mu \vec{a}_0)^2 + 2g_1 (\partial^\mu \vec{a}_0) \cdot [\vec{\rho}^\mu \times \vec{a}_0 + \eta (\vec{a}_1^\mu + w \partial^\mu \vec{\pi}) + \vec{\pi} (f_1^\mu + w \partial^\mu \eta)] \} \end{aligned}$$

$$\begin{aligned}
& +g_1^2[\bar{\rho}^\mu \times \bar{a}_0 + \eta(\bar{a}_1^\mu + w\partial^\mu \bar{\pi}) + \bar{\pi}(f_1^\mu + w\partial^\mu \eta)]^2\} \\
& + \frac{1}{2} \{ (\partial_\mu \bar{\pi})^2 - 2g_1(\partial_\mu \bar{\pi}) \cdot [\bar{\pi} \times \bar{\rho}^\mu + \sigma(\bar{a}_1^\mu + w\partial^\mu \bar{\pi}) + \bar{a}_0(f_1^\mu + w\partial^\mu \eta)] \\
& \quad + g_1^2[\bar{\pi} \times \bar{\rho}^\mu + \sigma(\bar{a}_1^\mu + w\partial^\mu \bar{\pi}) + \bar{a}_0(f_1^\mu + w\partial^\mu \eta)]^2\} \\
& - \frac{m_0^2}{2}(\sigma^2 + \eta^2 + \bar{a}_0^2 + \bar{\pi}^2) - \frac{\lambda_1}{4}(\sigma^2 + \eta^2 + \bar{a}_0^2 + \bar{\pi}^2)^2 \\
& - \frac{\lambda_2}{2} \left[ \frac{1}{4} (\sigma^2 + \eta^2 + \bar{a}_0^2 + \bar{\pi}^2)^2 + (\sigma\bar{a}_0 + \eta\bar{\pi})^2 + (\bar{a}_0 \times \bar{\pi})^2 \right] \\
& + \frac{1}{2} c(\sigma^2 - \bar{a}_0^2 - \eta^2 + \bar{\pi}^2) + h_0\sigma. \tag{2.50}
\end{aligned}$$

For the Lagrangian of the vector and axial-vector fields one obtains

$$\begin{aligned}
\mathcal{L}_{YM} = & -\frac{1}{4}(\partial^\mu \omega^\nu - \partial^\nu \omega^\mu)^2 - \frac{1}{4}[\partial^\mu(f_1^\nu + w\partial^\nu \eta) - \partial^\nu(f_1^\mu + w\partial^\mu \eta)]^2 \\
& - \frac{1}{4}[(\partial^\mu \bar{\rho}^\nu - \partial^\nu \bar{\rho}^\mu)^2 + 2g_1(\partial^\mu \bar{\rho}^\nu - \partial^\nu \bar{\rho}^\mu) \cdot \\
& \quad (\bar{\rho}^\mu \times \bar{\rho}^\nu + \bar{a}_1^\mu \times \bar{a}_1^\nu + w\partial^\mu \bar{\pi} \times w\partial^\nu \bar{\pi}) \\
& \quad + g_1^2(\bar{\rho}^\mu \times \bar{\rho}^\nu + \bar{a}_1^\mu \times \bar{a}_1^\nu + w\partial^\mu \bar{\pi} \times w\partial^\nu \bar{\pi})^2] \\
& - \frac{1}{4} \{ [\partial^\mu(\bar{a}_1^\nu + w\partial^\nu \bar{\pi}) - \partial^\nu(\bar{a}_1^\mu + w\partial^\mu \bar{\pi})]^2 \\
& \quad + 2g_1[\partial^\mu(\bar{a}_1^\nu + w\partial^\nu \bar{\pi}) - \partial^\nu(\bar{a}_1^\mu + w\partial^\mu \bar{\pi})] \cdot \\
& \quad [\bar{\rho}^\mu \times \bar{a}_1^\nu + \bar{\rho}^\mu \times w\partial^\nu \bar{\pi} + \bar{a}_1^\mu \times \bar{\rho}^\nu + w\partial^\mu \bar{\pi} \times \bar{\rho}^\nu] \\
& \quad + g_1^2[\bar{\rho}^\mu \times \bar{a}_1^\nu + \bar{\rho}^\mu \times w\partial^\nu \bar{\pi} + \bar{a}_1^\mu \times \bar{\rho}^\nu + w\partial^\mu \bar{\pi} \times \bar{\rho}^\nu]^2\} \\
& + \frac{m_1^2}{2} [\omega^{\mu 2} + \bar{\rho}^{\mu 2} + (f_1^\mu)^2 + 2w f_1^\mu \partial^\mu \eta + w^2(\partial^\mu \eta)^2 + (\bar{a}_1^\mu)^2 \\
& \quad + 2w \bar{a}_1^\mu \cdot \partial^\mu \bar{\pi} + w^2(\partial^\mu \bar{\pi})^2] . \tag{2.51}
\end{aligned}$$

After redefining the axial vectors the additional terms in  $\mathcal{L}_\Phi$  that arise from SSB and contain the unwanted bilinear terms are

$$\begin{aligned}
\mathcal{L}_{\phi_0} = & \frac{1}{2} \{ -2g_1\phi_0\partial^\mu \eta f_1^\mu + 2g_1^2\phi_0^2 w f_1^\mu \partial^\mu \eta + 2g_1\phi_0 w(\partial^\mu \eta)^2 + g_1^2\phi_0^2 f_1^{\mu 2} \\
& \quad + g_1^2\phi_0^2 w^2(\partial^\mu \eta)^2 + 2\phi_0 g_1^2[\sigma(f_1^\mu + w\partial^\mu \eta)]^2 \\
& \quad + (f_1^\mu + w\partial^\mu \eta)\bar{a}_0 \cdot (\bar{a}_1^\mu + w\partial^\mu \bar{\pi})\} \\
& + \frac{1}{2} \{ -2g_1\phi_0\partial^\mu \bar{\pi} \cdot \bar{a}_1^\mu + 2g_1^2\phi_0^2 w \bar{a}_1^\mu \cdot \partial^\mu \bar{\pi} + 2g_1\phi_0 w(\partial^\mu \bar{\pi})^2 + g_1^2\phi_0^2 \bar{a}_1^{\mu 2} \\
& \quad + g_1^2\phi_0^2 w^2(\partial^\mu \bar{\pi})^2 + 2\phi_0 g_1^2[\sigma(\bar{a}_1^\mu + w\partial^\mu \bar{\pi})]^2 \\
& \quad + (f_1^\mu + w\partial^\mu \eta)\bar{a}_0 \cdot (\bar{a}_1^\mu + w\partial^\mu \bar{\pi}) + (\bar{\pi} \times \bar{\rho}^\mu) \cdot (\bar{a}_1^\mu + w\partial^\mu \bar{\pi})\} \\
& + \dots \tag{2.52}
\end{aligned}$$

where the ellipsis hides the terms that are unaffected by the redefinition.

Together with the shifted axial-vector fields the terms in  $\mathcal{L}_5$  that are also affected by the spontaneous symmetry breaking read

$$\begin{aligned}
& \frac{h_1}{2} \phi_0 \sigma [(f_{1\mu} + w \partial_\mu \eta)^2 + \omega_\mu^2 + (\vec{a}_{1\mu} + w \partial_\mu \vec{\pi})^2 + \vec{\rho}_{1\mu}^2] \\
& + \frac{h_1}{4} \phi_0^2 [f_{1\mu}^2 + 2w f_{1\mu} \partial_\mu \eta + w^2 (\partial_\mu \eta)^2 + \omega_\mu^2 \\
& \quad + \vec{a}_{1\mu}^2 + 2w \vec{a}_{1\mu} \cdot \partial_\mu \vec{\pi} + w^2 (\partial_\mu \vec{\pi})^2 + \vec{\rho}_{1\mu}^2] \\
& + \frac{h_2}{2} \phi_0 \sigma [(f_{1\mu} + w \partial_\mu \eta)^2 + \omega_\mu^2 + (\vec{a}_{1\mu} + w \partial_\mu \vec{\pi})^2 + \vec{\rho}_{1\mu}^2] \\
& + \frac{h_2}{4} \phi_0^2 [f_{1\mu}^2 + 2w f_{1\mu} \partial_\mu \eta + w^2 (\partial_\mu \eta)^2 + \omega_\mu^2 \\
& \quad + \vec{a}_{1\mu}^2 + 2w \vec{a}_{1\mu} \cdot \partial_\mu \vec{\pi} + w^2 (\partial_\mu \vec{\pi})^2 + \vec{\rho}_{1\mu}^2] \\
& + h_2 \phi_0 [(f_{1\mu} + w \partial_\mu \eta) \vec{a}_0 \cdot (\vec{a}_{1\mu} + w \partial_\mu \vec{\pi}) + \omega_\mu \vec{a}_0 \cdot \vec{\rho}] \\
& + \frac{h_3}{2} \phi_0 \sigma [-(f_{1\mu} + w \partial_\mu \eta)^2 + \omega_\mu^2 - (\vec{a}_{1\mu} + w \partial_\mu \vec{\pi})^2 + \vec{\rho}_{1\mu}^2] \\
& + \frac{h_3}{4} \phi_0^2 [-f_{1\mu}^2 - 2w f_{1\mu} \partial_\mu \eta - w^2 (\partial_\mu \eta)^2 + \omega_\mu^2 \\
& \quad - \vec{a}_{1\mu}^2 - 2w \vec{a}_{1\mu} \cdot \partial_\mu \vec{\pi} - w^2 (\partial_\mu \vec{\pi})^2 + \vec{\rho}_{1\mu}^2] \\
& + h_3 \phi_0 \{ \omega_\mu \vec{a}_0 \cdot \vec{\rho} - (f_{1\mu} + w \partial_\mu \eta) \vec{a}_0 \cdot (\vec{a}_{1\mu} + w \partial_\mu \vec{\pi}) + \vec{\pi} \cdot [(\vec{a}_{1\mu} + w \partial_\mu \vec{\pi}) \times \vec{\rho}] \} .
\end{aligned} \tag{2.53}$$

Adding together the red terms in (2.51), (2.52), and (2.53) yields

$$[-g_1 \phi_0 + g_1^2 \phi_0^2 w + m_1^2 w + \frac{1}{2} \phi_0^2 w (h_1 + h_2 - h_3)] f_1^\mu w \partial^\mu \eta , \tag{2.54}$$

$$[-g_1 \phi_0 + g_1^2 \phi_0^2 w + m_1^2 w + \frac{1}{2} \phi_0^2 w (h_1 + h_2 - h_3)] \vec{a}_1^\mu \cdot w \partial^\mu \vec{\pi} . \tag{2.55}$$

With  $w$  as defined in (2.48) and  $m_{a_1}^2 = m_1^2 + g_1^2 \phi_0^2 + \frac{1}{2} \phi_0^2 (h_1 + h_2 - h_3)$  the prefactors of the bilinear terms cancel each other

$$\begin{aligned}
& -g_1 \phi_0 + g_1^2 \phi_0^2 w + m_1^2 w + \frac{1}{2} \phi_0^2 w (h_1 + h_2 - h_3) \\
& = \frac{-2g_1 \phi_0 m_{a_1}^2 + 2g_1^2 \phi_0^2 g_1 \phi_0 + 2m_1^2 g_1 \phi_0 + \phi_0^2 g_1 \phi_0 (h_1 + h_2 - h_3)}{2m_{a_1}^2} \\
& = \frac{g_1 \phi_0 [(-m_{a_1}^2 + g_1^2 \phi_0^2 + m_1^2 + \frac{1}{2} \phi_0^2 (h_1 + h_2 - h_3))]}{m_{a_1}^2} \\
& = 0 .
\end{aligned} \tag{2.56}$$

Now, the kinetic terms of  $\eta$  and  $\pi$  obtained additional prefactors. They are seen in the blue-marked terms in (2.51), (2.52), and (2.53) that, after being

added to the kinetic term in (2.50), reduce to

$$\begin{aligned} \frac{1}{2} - g_1 \phi_0 w + \frac{1}{2} g_1^2 \phi_0^2 w^2 + \frac{1}{2} m_1^2 w^2 + \frac{1}{2} \phi_0^2 w^2 (h_1 + h_2 - h_3) \\ = \frac{1}{2} \frac{m_{a_1}^2 - (g_1 \phi_0)^2}{m_{a_1}^2} . \end{aligned} \quad (2.57)$$

In order to obtain the canonically normalised kinetic terms, the pseudoscalar fields must additionally be renormalised by a constant  $Z$

$$\eta \longrightarrow Z\eta, \quad \vec{\pi} \longrightarrow Z\vec{\pi} , \quad (2.58)$$

where  $Z^2$  is defined as

$$Z^2 = \frac{g_1 \phi_0}{m_1^2 w} = \frac{m_1^2 + (g_1 \phi_0)^2}{m_1^2} . \quad (2.59)$$

Thus, the ‘‘unsolicited’’ prefactor is absorbed by a renormalisation of the pseudoscalars fields.

This is the renormalisation  $Z$  that was mentioned in the equations of the pseudoscalar masses in (2.42) and (2.43).

To determine  $\phi_0$  the relations for the vacuum expectation value (2.36) and the pion mass (2.43) are recalled

$$\begin{aligned} \left[ m_0^2 + \left( \lambda_1 + \frac{\lambda_2}{2} \right) \phi_0^2 - c \right] Z^2 = m_\pi^2 , \\ \left[ m_0^2 + \left( \lambda_1 + \frac{\lambda_2}{2} \right) \phi_0^2 - c \right] \phi_0 - h_0 = 0 . \end{aligned}$$

From here the parameter  $h_0$  that generates the explicit breaking of chiral symmetry is calculated to be

$$h_0 = \frac{m_\pi^2 \phi_0}{Z^2} . \quad (2.60)$$

The assumption that the pions are the quasi-Goldstone bosons of an approximately conserved chiral symmetry as it is expressed in the PCAC relation  $\partial_\mu A_i^\mu = m_\pi^2 f_\pi \pi_i$  yields

$$\frac{\phi_0}{Z} m_\pi^2 \pi_i = m_\pi^2 f_\pi \pi_i ,$$

such that finally  $\phi_0$  can be expressed as

$$\phi_0 = Z f_\pi = \sqrt{\frac{m_1^2 + (g_1 \phi_0)^2}{m_1^2}} f_\pi . \quad (2.61)$$

The chiral condensate is thus determined to be proportional to the pion vacuum decay constant  $f_\pi$  and the pion renormalisation constant  $Z$ .

## 2.2 $SU(2)_L \times U(1)_Y$ and Weak Interaction

In Section 1.4 the Gell-Mann-Nishijima relation was introduced as

$$Q = I_3 + \frac{Y}{2},$$

with  $Q$  being the electromagnetic charge of a Dirac field,  $I_3$  its weak isospin and  $Y$  its hypercharge. In the GWS model of electroweak interactions the the physical photon field that couples to the charge  $Q$  is a linear combination of the bare  $SU(2)_L \times U(1)_Y$  gauge fields  $W_3^\mu$  and  $B^\mu$ . The photon couples with same strength  $Q$  to fermions and their antifermions, while  $W_3^\mu$  only couples to fields with weak isospin  $I_3$ . Thus,  $B^\mu$  couples to both left- and right-handed fields but with different strength. In order to answer the question how the group  $SU(2)_L \times U(1)_Y$  acts on the mesonic field  $\Phi$  so that the characteristics of the GWS model are reproduced, the constituent quark fields in  $\Phi$  will undergo a transformation according to the one discussed in Section 1.4.

### 2.2.1 $U(1)_Y$ Transformation

Under local  $U(1)_Y$  the left-handed doublet  $q_1 = (u_L, d_L)^T$  and the right-handed singlets  $q_2 = u_R$ ,  $q_3 = d_R$ , according to (1.81), transform as

$$q_i \longrightarrow q'_i = U_{Y_i} q_i, \quad (2.62)$$

with the unitary transformation matrix

$$U_{Y_i} = e^{iy_i \theta_Y(x^\mu)}, \quad i = 1, 2, 3,$$

and assigned hypercharges

$$y_1 = 2 \left( Q_u - \frac{1}{2} \right) = Q_d + \frac{1}{2} = \frac{1}{3}, \quad (2.63)$$

$$y_2 = 2Q_u = \frac{4}{3}, \quad y_3 = 2Q_d = -\frac{2}{3}. \quad (2.64)$$

The scalar and pseudoscalar fields were defined as

$$\Phi_{kl} \simeq \frac{1}{\sqrt{2}} (\bar{q}_l q_k - \bar{q}_l \gamma^5 q_k) \simeq \sqrt{2} \bar{q}_{l,R} q_{k,L}, \quad i, j = u, d. \quad (2.65)$$

The matrix for scalar and pseudoscalars is defined as

$$\Phi \simeq \begin{pmatrix} \bar{u}_R u_L & \bar{d}_R u_L \\ \bar{u}_R d_L & \bar{d}_R d_L \end{pmatrix}. \quad (2.66)$$



Since  $\Phi$  obeys the same transformation laws as the external product of the left- and right-handed quark vectors, the transformation of  $\Phi$  under  $U(1)_Y$  can be found by transforming the constituent fields. Their transformation properties are well-known from the Standard Model of Electroweak Interactions. Therefore the  $U(1)_Y$  transformation acts on  $\Phi$  according to

$$\begin{aligned}
\Phi \xrightarrow{U(1)} \Phi' &\simeq \begin{pmatrix} \bar{u}_R e^{-iy_2\theta_Y} u_L e^{iy_1\theta_Y} & \bar{d}_R e^{-iy_3\theta_Y} u_L e^{iy_1\theta_Y} \\ \bar{u}_R e^{-iy_2\theta_Y} d_L e^{iy_1\theta_Y} & \bar{d}_R e^{-iy_3\theta_Y} d_L e^{iy_1\theta_Y} \end{pmatrix} \\
&= \begin{pmatrix} \bar{u}_R u_L e^{i(-\frac{4}{3}+\frac{1}{3})\theta_Y} & \bar{d}_R u_L e^{i(\frac{2}{3}+\frac{1}{3})\theta_Y} \\ \bar{u}_R d_L e^{i(-\frac{4}{3}+\frac{1}{3})\theta_Y} & \bar{d}_R d_L e^{i(\frac{2}{3}+\frac{1}{3})\theta_Y} \end{pmatrix} \\
&= \begin{pmatrix} \bar{u}_R u_L e^{-i\frac{1}{2}\theta_Y} & \bar{d}_R u_L e^{i\frac{1}{2}\theta_Y} \\ \bar{u}_R d_L e^{-i\frac{1}{2}\theta_Y} & \bar{d}_R d_L e^{i\frac{1}{2}\theta_Y} \end{pmatrix} \\
&= \begin{pmatrix} \bar{u}_R u_L & \bar{d}_R u_L \\ \bar{u}_R d_L & \bar{d}_R d_L \end{pmatrix} \begin{pmatrix} e^{-i\frac{1}{2}\theta_Y} & 0 \\ 0 & e^{i\frac{1}{2}\theta_Y} \end{pmatrix}.
\end{aligned}$$

Since  $\theta_Y$  is infinitesimal the transformation can also be written down as an expansion in  $\theta_Y$ , such that

$$\begin{aligned}
\Phi' &\simeq \begin{pmatrix} \bar{u}_R u_L & \bar{d}_R u_L \\ \bar{u}_R d_L & \bar{d}_R d_L \end{pmatrix} \begin{pmatrix} 1 - i\frac{1}{2}\theta_Y + O[\theta_Y]^2 & 0 \\ 0 & 1 + i\frac{1}{2}\theta_Y + O[\theta_Y]^2 \end{pmatrix} \\
&= \begin{pmatrix} \bar{u}_R u_L & \bar{d}_R u_L \\ \bar{u}_R d_L & \bar{d}_R d_L \end{pmatrix} + \begin{pmatrix} \bar{u}_R u_L & \bar{d}_R u_L \\ \bar{u}_R d_L & \bar{d}_R d_L \end{pmatrix} \begin{pmatrix} -i\frac{1}{2}\theta_Y & 0 \\ 0 & +i\frac{1}{2}\theta_Y \end{pmatrix} \\
&\quad + \begin{pmatrix} \bar{u}_R u_L & \bar{d}_R u_L \\ \bar{u}_R d_L & \bar{d}_R d_L \end{pmatrix} \begin{pmatrix} O[\theta_Y]^2 & 0 \\ 0 & O[\theta_Y]^2 \end{pmatrix} \\
&\simeq \begin{pmatrix} \bar{u}_R u_L & \bar{d}_R u_L \\ \bar{u}_R d_L & \bar{d}_R d_L \end{pmatrix} - i\frac{\theta_Y}{2} \begin{pmatrix} \bar{u}_R u_L & \bar{d}_R u_L \\ \bar{u}_R d_L & \bar{d}_R d_L \end{pmatrix} \begin{pmatrix} +1 & 0 \\ 0 & -1 \end{pmatrix}.
\end{aligned}$$

The transformation of  $\Phi$  can now be expressed in terms of the already given strong isospin algebra spanned by  $\{t_i\} = \{\frac{\sigma_i}{2}\}$

$$\Phi \xrightarrow{U(1)_Y} \Phi' = \Phi U_Y^\dagger \simeq \Phi - i\theta_Y \Phi t_3, \quad (2.67)$$

with

$$U_Y = e^{i\theta_Y (x^\mu) t_3}.$$

The Lagrangian without the explicit symmetry breaking terms  $\mathcal{L}_A$  and  $\mathcal{L}_{eSB}$

$$\begin{aligned}
\mathcal{L} &= \text{Tr}[(D^\mu \Phi^\dagger)(D^\mu \Phi)] - m_0^2 \text{Tr}[\Phi^\dagger \Phi] - \lambda_1 \text{Tr}[(\Phi^\dagger \Phi)^2] - \lambda_2 (\text{Tr}[\Phi^\dagger \Phi])^2 \\
&\quad - \frac{1}{4} \text{Tr}[(L^{\mu\nu})^2 - (R^{\mu\nu})^2] + \frac{m_1}{2} \text{Tr}[(L^\mu)^2 + (R^\mu)^2]
\end{aligned}$$

$$+ \mathcal{L}_3 + \mathcal{L}_4 + \mathcal{L}_5 \quad (2.68)$$

is invariant under local  $U(1)_Y$  transformations if a vector field  $B^\mu t_3$  is introduced in the covariant derivative

$$D^\mu \Phi = \partial_\mu \Phi - ig_1(L^\mu \Phi - \Phi R^\mu) + ig' \Phi B_\mu t_3 . \quad (2.69)$$

Then  $B^\mu t_3$  transforms under adjoint representation as

$$B^\mu t_3 \longrightarrow (B^\mu t_3)' = U_Y B^\mu t_3 U_Y^\dagger + \frac{i}{g'} U_Y \partial^\mu U_Y^\dagger . \quad (2.70)$$

The invariance of  $\mathcal{L}$  is preserved if the covariant derivative transforms under  $U(1)_Y$  as the field itself. The covariant derivative also contains the interaction terms between the scalar, pseudoscalar, vector, and axial-vector fields. Since  $U(1)_Y$  is a subgroup of  $SU(2)_R \times U(1)_V$  and the vector fields are treated as massive Yang-Mills bosons their transformation leaves the Lagrangian invariant if they transform as the adjoint representation<sup>2</sup> as well:

$$\begin{aligned} L^\mu &\longrightarrow L^{\mu'} = U_Y L^\mu U_Y^\dagger = L^\mu , \\ R^\mu &\longrightarrow R^{\mu'} = U_Y R^\mu U_Y^\dagger . \end{aligned} \quad (2.71)$$

For the covariant derivative one obtains

$$\begin{aligned} (D^\mu \Phi)' &= \partial^\mu \Phi' - ig_1(L^{\mu'} \Phi' - \Phi' R^{\mu'}) + ig' \Phi' (B^\mu t_3)' \\ &= \partial^\mu (\Phi U_Y^\dagger) - ig_1(L^\mu \Phi U_Y^\dagger - \Phi U_Y^\dagger U_Y R^\mu U_Y^\dagger) \\ &\quad + ig' (\Phi U_Y^\dagger) (U_Y B^\mu t_3 U_Y^\dagger + \frac{i}{g'} U_Y \partial^\mu U_Y^\dagger) \\ &= (\partial^\mu \Phi) U_Y^\dagger + \Phi \partial^\mu U_Y^\dagger - ig_1(L^\mu \Phi U_Y^\dagger - \Phi R^\mu U_Y^\dagger) \\ &\quad + ig' \Phi U_Y^\dagger U_Y B^\mu t_3 U_Y^\dagger - \Phi U_Y^\dagger U_Y \partial^\mu U_Y^\dagger \\ &= (\partial^\mu \Phi) U_Y^\dagger - ig_1(L^\mu \Phi U_Y^\dagger - \Phi R^\mu U_Y^\dagger) + ig' \Phi B^\mu t_3 U_Y^\dagger \\ &\quad + \Phi \partial^\mu U_Y^\dagger - \Phi \partial^\mu U_Y^\dagger \\ &= (D^\mu \Phi) U_Y^\dagger . \end{aligned} \quad (2.72)$$

---

<sup>2</sup>This can also be seen by applying the transformation explicitly to left- and right-handed fields. The left-handed doublet only transforms with an overall phase factor, while the transformation of the right-handed "doublet" becomes dependent on the same overall phase and  $t_2$ , which turns out to be equivalent to the transformation under the  $U(1)_Y$  adjoint representation:

$$\begin{aligned} R^\mu &\longrightarrow R^{\mu'} = U_Y R^\mu U_Y^\dagger = e^{i\theta_Y t_3} R^\mu e^{-i\theta_Y t_3} \\ &\simeq (1 + i\theta_Y t_3) R^\mu (1 - i\theta_Y t_3) \\ &= R^\mu + 2i\theta_Y R^\mu t_2 + O[\theta_Y]^2 . \end{aligned}$$

Thus

$$\begin{aligned}
\text{Tr}[(D^\mu\Phi)'^\dagger (D^\mu\Phi)'] &= \text{Tr}[U_Y(D_\mu\Phi)^\dagger(D^\mu\Phi)U_Y^\dagger] \\
&= \text{Tr}[(D^\mu\Phi)U_Y^\dagger U_Y(D^\mu\Phi)^\dagger] \\
&= \text{Tr}[(D^\mu\Phi)^\dagger(D^\mu\Phi)].
\end{aligned}
\tag{2.73}$$

Now, one could also introduce the other weak gauge bosons into the model. However, the group  $SU(2)_L$  is non-Abelian - the relation  $e^{A+B} = e^A e^B$  only holds for commuting matrices  $A$  and  $B$  - so one cannot simply repeat the steps above and transform each composite field in order to find the transformation law for  $\Phi$  under  $SU(2)_L$ .

## 2.2.2 Vector Meson Dominance

Another possibility to construct gauge-invariant interaction vertices between the weak bosons and  $\Phi$  is Vector Meson Dominance (VMD). The following résumé about VMD is based on the introduction given in [24].

Sakurai developed VMD to answer the question of how the photon couples to hadronic matter (here pions). The higher-order self-energy contributions of the photon propagator do not only consist of virtual  $e^+e^-$  pairs but also of virtual quark-antiquark pairs. As the photon is a vector field, these hadronic ( $\bar{q}q$ ) vacuum polarisations should be vector-like, too. VMD is now based on the assumption that the hadronic contributions to the photon self-energy consist only of the known vector mesons. The field-current identity states that the hadronic electromagnetic current is proportional to a vector meson, the neutral  $\rho$  meson

$$j_{EM}^\mu = \frac{m_\rho^2}{g_\rho} \rho_0^\mu. \tag{2.74}$$

Equation (2.74) was later generalised to the  $\rho$  triplet, where the neutral  $\rho_0$  is the third component of an isospin triplet.

Different attempts were made by Sakurai, Lurie, Kroll, Lee, and Zumino to generate interactions between the vector mesons and hadronic matter. There was the idea from Sakurai to treat the vector mesons as the gauge fields of a local  $SU(2)$  strong isospin symmetry, but it had the problem of a vector-meson mass term which destroyed gauge invariance. Lurie coupled the vector mesons within a global  $SU(2)_V$  symmetry to conserved hadronic currents. Later, Kroll, Lee, and Zumino introduced the interactions between the vector mesons and hadronic matter in terms of the field-current identity in Equation (2.74).

Today there exist basically two representations of vector meson dominance, VMD1 and VMD2. In both representations Sakurai coupled the vector mesons to hadrons (pions) by the covariant derivative

$$D_\mu \vec{\pi} = \partial_\mu \vec{\pi} - g_{\rho\pi\pi} \vec{\rho} \times \vec{\pi} \quad (2.75)$$

Based on the assumption that the  $\rho$  self-interactions are negligible, the current  $J_\pi^\mu$  is defined as

$$J_\pi^\mu = (\vec{\pi} \times \partial^\mu \vec{\pi})_0 = i(\pi^- \partial^\mu \pi^+ - \pi^+ \partial^\mu \pi^-) \quad (2.76)$$

and accounts only for the terms that correspond to the neutral component  $\rho_\mu^0$  interacting with two charged pions<sup>3</sup>. Thus, from now on,  $\rho_\mu$  is understood to refer only to the neutral  $\rho$  meson component  $\rho_\mu^0$ . Both representations, VMD1 and VMD2, are based on the Lagrangian

$$\mathcal{L}_{VMD} = -\frac{1}{4} F_{\mu\nu} F^{\mu\nu} - \frac{1}{4} \rho_{\mu\nu} \cdot \rho^{\mu\nu} + \frac{1}{2} m_\rho^2 \rho_\mu \cdot \rho^\mu - g_{\rho\pi\pi} \rho_\mu \cdot J_\pi^\mu . \quad (2.77)$$

The dynamics of the photon field and of the vector field are described by  $F_{\mu\nu}$  and  $\rho_{\mu\nu}$  respectively, with both of them being ordinary field strength tensors. Now, VMD1 and VMD2 differ in the way they couple the photon field to the  $\rho$  meson

- VMD1 generates the  $\gamma\rho$  interaction by

$$-e A_\mu J_\pi^\mu - \frac{2}{2g_\rho} F_{\mu\nu} \rho^{\mu\nu} . \quad (2.78)$$

Because of the derivatives in the field strength tensors the coupling of the photon to  $\rho$  depends on the exchanged momenta  $q^2$  and vanishes for  $q^2 \rightarrow 0$ . Then the contribution of the direct photon-hadron coupling in  $e A_\mu J_\pi^\mu$  becomes dominant and describes the energy region below the  $\rho$  meson's mass.

- VMD2 generates the interaction by

$$-e \frac{m_\rho^2}{g_\rho} \rho_\mu{}' A^{\mu'} + \frac{1}{2} \left( \frac{e}{g_\rho} \right)^2 m_\rho^2 A_\mu{}' A^{\mu'} . \quad (2.79)$$

Despite the photon mass term in VMD2 the photon propagator turns out to be of the correct form, if one assumes that its self-energy contributions consist only of vector mesons.

---

<sup>3</sup>This accounts for the fact that the neutral  $\rho$  meson decays almost entirely via the two pion channel.

If the coupling of  $\rho$  is the same for all interactions  $g_\rho = g_{\rho\pi\pi}$ , the above representations are equivalent to each other. The transition from VMD2 to VMD1 is made by a transformation of the fields. The field  $\rho^{\mu'}$  in VMD2 is a mixed state of  $\rho^\mu$  and  $A^\mu$  of VMD1

$$\rho'_\mu = \rho_\mu + \frac{e}{g_\rho} A_\mu, \quad (2.80)$$

$$A^{\mu'} = A_\mu \sqrt{1 - \frac{e^2}{g_\rho^2}}, \quad (2.81)$$

$$e' = e \sqrt{1 - \frac{e^2}{g_\rho^2}}. \quad (2.82)$$

### 2.2.3 Electroweak Interactions

Now, how can VMD be of use for introducing the weak bosons by minimal coupling into the Linear Sigma Model? In the  $U(2)_L \times U(2)_R$  model the scalar and pseudoscalar fields are obtained from the direct product of a left-handed quark doublet and a right-handed anti-doublet. The covariant derivative in (2.68) generates interactions between left- and right-handed fields with  $\Phi$ . While the bare weak bosons  $W^\mu$  couple only to fields that carry weak isospin (left-handed fields), the  $U(1)_Y$  gauge field  $B^\mu$  couples to both, left- and right-handed fields. Moreover,  $B^\mu$  is a mixed field of the physical fields  $A^\mu$  and  $Z^\mu$ .

One can now assume that the vacuum polarisation of the bare gauge field  $B^\mu$  consists only of hypercharged quark-antiquark pairs. Similarly the self-energy contributions of the weak bosons  $W^\mu$  would only consist of left-handed quark-antiquark pairs. Therefore  $W^\mu$  can be regarded as being “proportional” to the left-handed fields in  $L^\mu$ , while the hypercharge gauge field  $B^\mu$  should contain contributions from  $L^\mu$  and  $R^\mu$  since left- and right-handed fields carry hypercharge.

That way one can ensure that  $W^\mu$  couples only to the left-handed content in  $\Phi$ , while  $B^\mu$  couples to both. Together they should also yield the Weinberg mixing of the physical fields and thus allow for describing the interactions of the charged and neutral electroweak currents.

The  $U(1)_Y$  gauge boson  $B^\mu$  couples to the hypercharge with  $y_i$  as given by (2.64). Since the hypercharge values differ for right-handed up and down quark the analogue to the field-current identity reads

$$J_Y^\mu \equiv \frac{g'}{2} \begin{pmatrix} y_1 & 0 \\ 0 & y_1 \end{pmatrix} L^\mu + \frac{g'}{2} \begin{pmatrix} y_2 & 0 \\ 0 & y_3 \end{pmatrix} R^\mu$$

$$\simeq \frac{g'}{2} \begin{pmatrix} y_1 \bar{u}_L \gamma^\mu u_L & 0 \\ 0 & y_1 \bar{d}_L \gamma^\mu d_L \end{pmatrix} + \frac{g'}{2} \begin{pmatrix} y_2 \bar{u}_R \gamma^\mu u_R & 0 \\ 0 & y_3 \bar{d}_R \gamma^\mu d_R \end{pmatrix}. \quad (2.83)$$

Based on the assumption that, as depicted<sup>4</sup> in Figure 2.1, the left-handed vacuum polarisation of  $B^\mu$  couples to the left-handed quark fields in  $L^\mu$  and the right-handed vacuum polarisation of  $B^\mu$  couples to the right-handed fields in  $R_\mu$  one can now express  $L^\mu$  and  $R^\mu$  in terms of the  $U(1)_Y$  gauge field  $B^\mu$ .

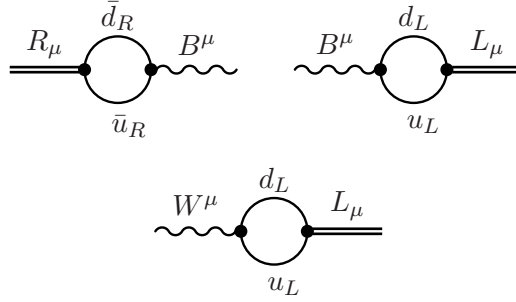


Figure 2.1: The bare  $U(1)_Y$  gauge field  $B^\mu$  couples to the left- and right-handed fields  $L_\mu$  and  $R_\mu$ , while the  $SU(2)_L$  gauge field  $W^\mu$  only couples to the left-handed fields  $L_\mu$ .

This basically means that the vector and axial-vector fields obtain an additional contribution from  $B^\mu$

$$L^\mu \rightarrow L^\mu + \frac{g'}{2g_1} \begin{pmatrix} y_1 & 0 \\ 0 & y_1 \end{pmatrix} B^\mu, \quad (2.84)$$

$$R^\mu \rightarrow R^\mu + \frac{g'}{2g_1} \begin{pmatrix} y_2 & 0 \\ 0 & y_3 \end{pmatrix} B^\mu \quad (2.85)$$

and the covariant derivative becomes

$$\begin{aligned} D^\mu \Phi &= \partial^\mu \Phi - ig_1 \left\{ \left[ L^\mu + \frac{g'}{2g_1} \begin{pmatrix} y_1 & 0 \\ 0 & y_1 \end{pmatrix} B^\mu \right] \Phi - \Phi \left[ R^\mu + \frac{g'}{2g_1} \begin{pmatrix} y_2 & 0 \\ 0 & y_3 \end{pmatrix} B^\mu \right] \right\} \\ &= \partial^\mu \Phi - ig_1 (L^\mu \Phi - \Phi R^\mu) - i \frac{g'}{2} \left[ \begin{pmatrix} y_1 & 0 \\ 0 & y_1 \end{pmatrix} B^\mu \Phi - \Phi \begin{pmatrix} y_2 & 0 \\ 0 & y_3 \end{pmatrix} B^\mu \right] \\ &= \partial^\mu \Phi - ig_1 (L^\mu \Phi - \Phi R^\mu) - i \frac{g'}{2} \Phi \begin{pmatrix} y_1 - y_2 & 0 \\ 0 & y_1 - y_3 \end{pmatrix} B^\mu. \end{aligned}$$

<sup>4</sup>The graph in Figure 2.1 is only used as an visualisation of the idea. It is not a Feynman diagram! It also has to be remembered that  $u_R$  and  $d_R$  couple with different strengths to the hypercharge gauge field.

Together with the hypercharge values  $y_1 = 1/3$ ,  $y_2 = 4/3$  and  $y_3 = -2/3$  this reduces to

$$D^\mu \Phi = \partial^\mu \Phi - ig_1(L^\mu \Phi - \Phi R^\mu) + ig' \Phi B^\mu t_3 \quad (2.86)$$

and reproduces the result (2.69) that was previously obtained from directly transforming the quark components.

This is equivalent to defining  $R^\mu$  as

$$R^\mu \longrightarrow R^\mu + \frac{g'}{g_1} B^\mu t_3 \quad (2.87)$$

and can now be generalised to describe  $SU(2)_L$  interactions.

The gauge field of  $U(1)_Y$  lies in the direction of  $t_3$  as a consequence of the fact that, in order to obtain QED from  $SU(2)_L \times U(1)_Y$ , the  $U(1)_Y$  gauge field couples with different strength to the different flavours of the right-handed fermions. Since the weak bosons couple universally to the left-handed flavours, one can immediately see that

$$L^\mu \longrightarrow L^\mu + \frac{g}{g_1} W^\mu, \quad W^\mu = W_a^\mu t_a, \quad (2.88)$$

after  $\Phi$  has been transformed under local  $SU(2)_L$  according to<sup>5</sup>

$$\Phi \longrightarrow U_L \Phi, \quad U_L = e^{-i\theta_L^a(x^\mu) t_a}. \quad (2.89)$$

With (2.87) and (2.88) the covariant derivative finally reads

$$\begin{aligned} D^\mu \Phi &= \partial^\mu \Phi - ig_1 \left[ (L^\mu + \frac{g}{g_1} W^\mu) \Phi - \Phi (R^\mu + \frac{g'}{g_1} B^\mu) \right] \\ &= \partial^\mu \Phi - ig_1 (L^\mu \Phi - \Phi R^\mu) + ig' \Phi B^\mu - ig W^\mu \Phi. \end{aligned} \quad (2.90)$$

The Lagrangian

$$\begin{aligned} \mathcal{L} = & \text{Tr}[(D^\mu \Phi^\dagger)^2 D^\mu \Phi] - \frac{1}{4} \text{Tr}[W_{\mu\nu} W^{\mu\nu} + B_{\mu\nu} B^{\mu\nu}] \\ & - m_0^2 \text{Tr}[\Phi^\dagger \Phi] - \lambda_1 \text{Tr}[(\Phi^\dagger \Phi)^2] - \lambda_2 (\text{Tr}[\Phi^\dagger \Phi])^2 \\ & - \frac{1}{4} \text{Tr}[(L^{\mu\nu})^2 - (R^{\mu\nu})^2] + \frac{m^2}{2} \text{Tr}[(L^\mu)^2 + (R^\mu)^2] \\ & + \mathcal{L}_3 + \mathcal{L}_4 + \mathcal{L}_5 \end{aligned} \quad (2.91)$$

<sup>5</sup>The signs in the exponent of the definitions of the transformations are conventional. Although the convention used here might be confusing since it results in different signs for the gauge-field terms in the covariant derivative it was chosen because it allows to write the  $SU(2)_L \times U(1)_Y$  transformation acting on the fields  $\phi, L^\mu, R^\mu$  analogously to the chiral transformation under  $SU(2)_L \times SU(2)_R$ .

is invariant under local  $SU(2)_L \times U(1)_Y$  transformations

$$\begin{array}{lcl}
\Phi & \longrightarrow & \Phi' = U_L \Phi U_Y^\dagger \\
L^\mu & \longrightarrow & L^{\mu'} = U_L L^\mu U_L^\dagger, \\
R^\mu & \longrightarrow & R^{\mu'} = U_Y R^\mu U_Y^\dagger, \\
B^\mu & \longrightarrow & B^{\mu'} = U_Y B^\mu U_Y^\dagger + \frac{i}{g'} U_Y \partial^\mu U_Y^\dagger, \\
W^\mu & \longrightarrow & W^{\mu'} = U_L W^\mu U_L^\dagger + \frac{i}{g} U_L \partial^\mu U_L^\dagger.
\end{array} \tag{2.92}$$

The covariant derivative term transforms as

$$\begin{aligned}
(D^\mu \Phi)' &= \partial^\mu \Phi' + ig' \Phi' B^{\mu'} - ig W^{\mu'} \Phi' - ig_1 (L^{\mu'} \Phi' - \Phi' R^{\mu'}) \\
&= \partial^\mu (U_L \Phi U_Y^\dagger) - ig_1 (U_L L^\mu U_L^\dagger U_L \Phi U_Y^\dagger - U_L \Phi U_Y^\dagger U_Y R^\mu U_Y^\dagger) \\
&\quad + ig' (U_L \Phi U_Y^\dagger) (U_Y B^\mu U_Y^\dagger + \frac{i}{g'} U_Y \partial^\mu U_Y^\dagger) \\
&\quad - ig (U_L W^\mu U_L^\dagger - \frac{i}{g} (\partial^\mu U_L) U_L^\dagger) (U_L \Phi U_Y^\dagger) \\
&= (\partial^\mu U_L) \Phi U_Y^\dagger + U_L (\partial^\mu \Phi) U_Y^\dagger + U_L \Phi \partial^\mu U_Y^\dagger + ig' U_L \Phi B^\mu U_Y^\dagger \\
&\quad - U_L \Phi \partial^\mu U_Y^\dagger - ig U_L W^\mu \Phi U_Y^\dagger - (\partial^\mu U_L) \Phi U_Y^\dagger \\
&\quad - ig_1 (U_L L^\mu \Phi U_Y^\dagger - U_L \Phi R^\mu U_Y^\dagger) \\
&= U_L (\partial^\mu \Phi) U_Y^\dagger + ig' U_L \Phi B^\mu U_Y^\dagger - ig U_L W^\mu \Phi U_Y^\dagger \\
&\quad - ig_1 (U_L L^\mu \Phi U_Y^\dagger - U_L \Phi R^\mu U_Y^\dagger) \\
&= U_L (D^\mu \Phi) U_Y^\dagger.
\end{aligned} \tag{2.93}$$

where  $\partial^\mu (UU^\dagger) = (\partial^\mu U)U^\dagger + U\partial^\mu U^\dagger = 0$  has been used. Therefore, the kinetic term is invariant under the combined  $SU(2)_L \times U(1)_Y$  transformation. The invariance of all other terms is seen by the analogue procedure.

#### 2.2.4 Weinberg Mixing, Field Strength Tensors $L^{\mu\nu}$ , $R^{\mu\nu}$

In order to express the bare gauge fields  $W_3^\mu$  and  $B^\mu$  in terms of their physical counterparts  $A^\mu$  and  $Z^\mu$  the Weinberg rotation is applied to the bare gauge fields in (2.90)

$$\begin{pmatrix} W_3^\mu \\ B^\mu \end{pmatrix} = \begin{pmatrix} \cos\theta_W & \sin\theta_W \\ -\sin\theta_W & \cos\theta_W \end{pmatrix} \begin{pmatrix} Z^\mu \\ A^\mu \end{pmatrix} \tag{2.94}$$

and leads to

$$ig' \Phi B^\mu t_3 - ig W_3^\mu t_3 \Phi = i\Phi g' (-\sin\theta_W Z^\mu + \cos\theta_W A^\mu) t_3$$



$$\begin{aligned}
& -ig(\cos\theta_W Z^\mu + \sin\theta_W A^\mu)t_3\Phi \\
& = iA^\mu(g'\cos\theta_W\Phi t_3 - g\sin\theta_W t_3\Phi) \\
& \quad - iZ^\mu(g\cos\theta_W t_3\Phi + g'\sin\theta_W\Phi t_3). \\
& = ieA^\mu[\Phi, t_3] - iZ^\mu(g\cos\theta_W t_3\Phi + g'\sin\theta_W\Phi t_3). \tag{2.95}
\end{aligned}$$

Using  $e = g\sin\theta_W = g'\cos\theta_W$  and redefining  $A^\mu t_3 \rightarrow A^\mu$ ,  $Z^\mu t_3 \rightarrow Z^\mu$  yields the result

$$ig'\Phi B^\mu t_3 - igW_3^\mu t_3 = -ie[A^\mu, \Phi] - ig\cos\theta_W (Z^\mu\Phi + \tan^2\theta_W\Phi Z^\mu). \tag{2.96}$$

Hence the final covariant derivative in terms of the physical, charged and neutral, interaction fields together with left- and right-handed fields reads

$$\boxed{
\begin{aligned}
D^\mu\Phi &= \partial^\mu\Phi - ig_1(L^\mu\Phi - \Phi R^\mu) - ig(W_1^\mu t_1 + W_2^\mu t_2)\Phi \\
&\quad - ie[A^\mu, \Phi] - ig\cos\theta_W (Z^\mu\Phi + \tan^2\theta_W\Phi Z^\mu). \tag{2.97}
\end{aligned}
}$$

Finally the field-strength tensors  $L^{\mu\nu}$  and  $R^{\mu\nu}$  undergo a redefinition, too. The derivative terms in the definition (2.22) of the original field strength tensors  $L^{\mu\nu}$  and  $R^{\mu\nu}$  contribute terms that would destroy the invariance of the Lagrangian under local  $SU(2)_L \times U(1)_Y$  transformations. Therefore the partial derivative in (2.22) is also promoted to a covariant one by inserting the gauge fields. From the local  $SU(2)_L$  transformation arise the following terms in the field strength tensors

$$\partial^\mu L^{\nu'} = U_L(\partial^\mu L^\nu)U_L^\dagger + (\partial^\mu U_L)L^\nu U_L^\dagger + U_L L^\nu (\partial^\mu U_L^\dagger). \tag{2.98}$$

The second two terms have to be removed by the contributions from the gauge field transformation (2.92). If the covariant derivative is defined to be

$$D_L^\mu L^\nu = \partial^\mu L^\nu - ig[W^\mu, L^\nu], \tag{2.99}$$

then the commutator reads after the transformation

$$\begin{aligned}
ig[W^{\mu'}, L^{\nu'}] &= ig\left[U_L W^\mu U_L^\dagger + \frac{i}{g}U_L\partial^\mu U_L^\dagger, U_L L^\nu U_L^\dagger\right] \\
&= ig(U_L W^\mu L^\nu U_L^\dagger - \frac{i}{g}(\partial^\mu U_L)L^\nu U_L^\dagger - U_L L^\nu W^\mu U_L^\dagger - \frac{i}{g}U_L L^\nu \partial^\mu U_L^\dagger) \\
&= igU_L[W^\mu, L^\nu]U_L^\dagger + (\partial^\mu U_L)L^\nu U_L^\dagger + U_L L^\nu (\partial^\mu U_L^\dagger). \tag{2.100}
\end{aligned}$$

The terms arising from the local transformation in (2.98) are now cancelled by the additional terms arising from the transformation of the gauge field and thus

$$(D_L^\mu L^\nu)' = U_L(\partial^\mu L^\nu - ig[W^\mu, L^\nu])U_L^\dagger = U_L(D_L^\mu L^\nu)U_L^\dagger. \tag{2.101}$$

Applying the analogous procedure to the derivatives acting on the right-handed fields shows that the covariant derivative for  $R^\mu$  has to be

$$D_R^\mu R^\nu = \partial^\mu R^\nu - ig'[B^\mu, R^\nu] . \quad (2.102)$$

In terms of the physical fields generating the electroweak phenomenology the field strength tensors for left- and right-handed fields then read

$$\begin{aligned} L^{\mu\nu} &= D_L^\mu L^\nu - D_L^\nu L^\mu \\ &= \partial^\mu L^\nu - ig[W_1^\mu t_1 + W_2^\mu t_2, L^\nu] \\ &\quad - ie[A^\mu, L^\nu] - ig \cos \theta_W [Z^\mu, L^\nu] \\ &\quad - \{\partial^\nu L^\mu - ig[W_1^\nu t_1 + W_2^\nu t_2, L^\mu] \\ &\quad - ie[A^\nu, L^\mu] - ig \cos \theta_W [Z^\nu, L^\mu]\} \\ R^{\mu\nu} &= D_R^\mu R^\nu - D_R^\nu R^\mu \\ &= \partial^\mu R^\nu - ie[A^\mu, R^\nu] + ig \sin \theta_W [Z^\mu, R^\nu] \\ &\quad - (\partial^\nu R^\mu - ie[A^\nu, R^\mu] + ig \sin \theta_W [Z^\nu, R^\mu]) . \end{aligned} \quad (2.103)$$

The field strength tensors can also be derived from the commutator of the covariant derivative according to

$$[D^\mu, D^\nu] = -ig_1 F^{\mu\nu} . \quad (2.104)$$

Since this needs a careful treatment of indices of the “left” and “right” product spaces, this calculation was delegated to Appendix A.

### 2.2.5 The $W\rho$ Vertex

Because of the spontaneously broken axial symmetry, the Lagrangian that has been developed so far does not contain any mixing terms between the charged weak gauge bosons and the vector mesons. After  $\sigma$  is shifted by its constant VEV

$$\Phi = \phi_0 t_0 + (\sigma_a + i\pi_a) t_a , \quad (2.105)$$

mixing terms between the left- and right-handed fields and the charged electroweak bosons arise. Both, left- and right-handed fields contain contributions from the vector mesons. But the mixing terms turn out to contain only a mixing between the charged weak bosons and the axial-vector mesons. For the term which contains the dynamics between the vector and axial-vector hadronic states and the scalars and pseudoscalars  $g_1(L^\mu \Phi - \Phi R^\mu)$  in (2.97) one obtains

$$g_1(L^\mu \Phi - \Phi R^\mu)$$

$$\begin{aligned}
&= g_1 [(V_a^\mu + A_a^\mu)t_a\phi_0t_0 - \phi_0t_0(V_a^\mu - A_a^\mu)t_a] \\
&\quad + g_1 \sum_{a,b=0}^3 [(V_a^\mu + A_a^\mu)(\sigma_b - i\pi_b)t_at_b - (\sigma_a - i\pi_a)(V_b^\mu + A_b^\mu)t_at_b] \\
&= \frac{1}{2}g_1\phi_0A_a^\mu t_a \\
&\quad + g_1 \sum_{a,b=0}^3 [(V_a^\mu + A_a^\mu)(\sigma_b - i\pi_b)t_at_b - (\sigma_a - i\pi_a)(V_b^\mu + A_b^\mu)t_at_b] . \quad (2.106)
\end{aligned}$$

From  $(D^\mu\Phi)^\dagger D^\mu\Phi$  one then can only obtain mixing terms between  $W^\mu$  and  $f_1^\mu, \vec{a}_1^\mu$

$$\begin{aligned}
&\text{Tr}[(ig_1(\Phi^\dagger L_\mu - R_\mu\Phi^\dagger) + ig\Phi^\dagger W_\mu)(-ig_1(L^\mu\Phi - \Phi R^\mu) - igW^\mu\Phi)] \\
&= \text{Tr}[(2ig_1\phi_0t_0A_{\mu a}t_a + ig\phi_0t_0W_{\mu a}t_a + \dots)(-2ig_1\phi_0t_0A_a^\mu t_a - igW_a^\mu t_a\phi_0t_0 + \dots)] \\
&= 2gg_1\phi_0^2A_{\mu a}W_b^\mu\text{Tr}[t_0t_0t_at_b] + 2gg_1\phi_0^2W_{\mu a}A_b^\mu\text{Tr}[t_0t_0t_at_b] + \dots \\
&= \frac{1}{2}gg_1\phi_0^2W_{\mu a}A_b^\mu\delta_{ab} + \dots . \quad (2.107)
\end{aligned}$$

The mixing terms are proportional to the chiral condensate in  $t_0$  direction, thus the contributions from the vector mesons cancel and only the  $W_\mu A^\mu$  mixing term survives in (2.107). The ellipses denote those terms that already lead to three-point interaction vertices and are not needed at the moment.

However, the main contributions in the vector channel of the  $\tau$  decay come from the intermediate  $\rho$  resonance. These contributions could not be accounted for with the Lagrangian that has been defined so far. Thus it is necessary to “manually” introduce a chirally invariant term of the form

$$\mathcal{L}_{W\rho} = \frac{\delta g}{2}\text{Tr}[W_{\mu\nu}L^{\mu\nu}] . \quad (2.108)$$

This is the only way how it is possible to introduce a  $W_\mu V^\nu$  term which is allowed by symmetry. It has exactly the same structure as the term Sakurai used to generate the electromagnetic interaction between the photon and the  $\rho$  meson in VMD1 and as a product of two covariantly transforming field strength tensors, it is of course gauge invariant, too. The newly introduced parameter  $\delta$  will be fixed later in the  $\rho$ - $2\pi$  channel.

## 2.2.6 The Lagrange Density with Electroweak Interactions

So far, all considerations were based on the chiral eigenstates. Because of Cabibbo mixing the weak coupling constant  $g$  has to be multiplied by the factor  $\cos\theta_C$ . Even though here weak interactions are only acting on two

flavours, up and down, the down quark has to be rotated into its weak counterpart  $d'$ .

For this reason the prefactor that accounts for the Cabibbo mixing is needed in all terms that generate interactions between the charged weak bosons and the mesonic bound quark-antiquark states. Then the covariant derivative acting on  $\Phi$  in its final form reads

$$D^\mu \Phi = \partial^\mu \Phi - ig_1(L^\mu \Phi - \Phi R^\mu) - ig \cos \theta_C (W_1^\mu t_1 + W_2^\mu t_2) \Phi - ie[A^\mu, \Phi] - ig \cos \theta_W (Z^\mu \Phi + \tan^2 \theta_W \Phi Z^\mu)$$

(2.109)

and the Lagrangian with all terms reads

$$\begin{aligned} \mathcal{L}_\Phi = & \text{Tr}[(D^\mu \Phi)^\dagger (D^\mu \Phi)] + \frac{\delta g \cos \theta_C}{2} \text{Tr}[W_{\mu\nu} L^{\mu\nu}] \\ & - m_0^2 \text{Tr}[\Phi^\dagger \Phi] - \lambda_1 \text{Tr}[(\Phi^\dagger \Phi)^2] - \lambda_2 (\text{Tr}[\Phi^\dagger \Phi])^2 \\ & - \frac{1}{4} \text{Tr}[(L^{\mu\nu})^2 - (R^{\mu\nu})^2] + \frac{m_1}{2} \text{Tr}[(L^\mu)^2 - (R^\mu)^2] \\ & + \frac{1}{4} \text{Tr}[(W^{\mu\nu})^2 + (B^{\mu\nu})^2] + \text{Tr}[H(\Phi + \Phi^\dagger)] \\ & + c(\det \Phi + \det \Phi^\dagger) + \mathcal{L}_3 + \mathcal{L}_4 + \mathcal{L}_5 . \end{aligned}$$

(2.110)

The partial derivatives in  $\mathcal{L}_3$  have also been replaced by the  $SU(2)_L \times U(1)_Y$  covariant derivatives  $D_L^\mu$  and  $D_R^\mu$  for the left- and right-handed fields as they were defined in (2.99) and (2.102).

## Chapter 3

# Tree-Level Vertices

In this chapter the vertex factors for calculating the spectral functions of the vector and axial-vector  $\tau$  decay channels will be derived from the Lagrangian (2.110). That way the necessary coupling constants for calculating the  $\tau$  vector and axial-vector spectral functions are obtained.

Because of its big mass of 1.777 GeV the  $\tau$  lepton does not only participate in leptonic decays, but also in semileptonic (hadronic) decays. Because it is a flavour changing process, it can only be mediated by the charged weak bosons. The  $\tau$  lepton decays into  $W$  and  $\nu_\tau$ . The  $W$  boson then in turn decays itself into either a lepton pair (leptonic decays) or into hadrons (semi-leptonic decays). Since hadrons are built up from strongly interacting matter, the  $\tau$  decay is a good object to study the interplay of electroweak and strong interactions within an effective field theory that describes the QCD hadronic degrees of freedom. The semi-leptonic decays of the  $\tau$  contribute with about 55% to its total decay width and can generally be divided into the vector channel with G-parity 1, reflected in an even number of hadronic decay products, and into the axial-vector channel with G-parity  $-1$ , reflected in an odd number of final hadrons. As the current work is based on a two-flavour Linear Sigma Model, only the decays resulting in final pion states will be studied.

After the spontaneous breaking of chiral symmetry the fields in the Lagrangian  $\Phi$ ,  $L^\mu$ , and  $R^\mu$  read

$$\begin{aligned}\Phi &= (\sigma_a + iZ\pi_a)t_a + \phi_0 t_0 \\ &= (\sigma + \phi_0 + iZ\eta)t_0 + (\vec{a}_0 + iZ\vec{\pi}) \cdot \vec{t}\end{aligned}\tag{3.1}$$

$$\begin{aligned}L^\mu &= V^\mu + A^\mu, \quad R^\mu = V^\mu - A^\mu \\ A^\mu &= (f_1^\mu + wZ\partial^\mu\eta)t_0 + (\vec{a}_1^\mu + wZ\partial^\mu\vec{\pi}) \cdot \vec{t}, \quad V^\mu = \omega^\mu t_0 + \vec{\rho}^\mu \cdot \vec{t}.\end{aligned}\tag{3.2}$$

The relevant interaction vertices with the charged weak bosons are obtained from

$$\mathcal{L}_{\text{int}} = \text{Tr} \left[ (D^\mu \Phi^\dagger) D^\mu \Phi \right] + \frac{g \cos \theta_C \delta}{2} \text{Tr} [W_{\mu\nu} L^{\mu\nu}] + \frac{1}{4} \text{Tr} [(L^{\mu\nu})^2] + \mathcal{L}_3 . \quad (3.3)$$

The neutral currents do not contribute to the examined decays, thus, from now on,  $W^\mu$  is defined to be

$$W^\mu = W_1^\mu t_1 + W_2^\mu t_2 , \quad (3.4)$$

and for the following calculations the covariant derivative in (3.3) is redefined to

$$\begin{aligned} D^\mu \Phi &= \partial^\mu \Phi - ig_1 (L^\mu \Phi - \Phi R^\mu) - ig \cos \theta_C W^\mu \Phi , \\ (D^\mu \Phi)^\dagger &= \partial_\mu \Phi^\dagger + ig_1 (\Phi^\dagger L_\mu - R_\mu \Phi^\dagger) + ig \cos \theta_C \Phi^\dagger W_\mu . \end{aligned} \quad (3.5)$$

The field strength tensor for the left-handed fields then reads

$$L^{\mu\nu} = \partial^\mu L^\nu - ig \cos \theta_C [W^\mu, L^\nu] - (\partial^\nu L^\mu - ig \cos \theta_C [W^\nu, L^\mu]) , \quad (3.6)$$

and for the right-handed fields

$$R^{\mu\nu} = \partial^\mu R^\nu - \partial^\nu L^\mu . \quad (3.7)$$

### 3.1 $\tau \rightarrow W \nu_\tau$ Vertex

The process  $\tau \rightarrow W \nu_\tau$  can be calculated from the electroweak interaction Lagrangian as it was derived in Section 1.4, Equation (1.87). As already given by (1.74), the weak isospin doublet for the third lepton family is

$$\psi = \begin{pmatrix} \tau \\ \nu_\tau \end{pmatrix}$$

and the charged weak interaction Lagrangian for  $\tau$  reads

$$\mathcal{L}_{\tau \rightarrow W \nu_\tau} = \frac{g}{2\sqrt{2}} \bar{\nu}_\tau W_\mu^- \gamma^\mu (1 - \gamma^5) \tau + h.c. . \quad (3.8)$$

From here the decay rate of  $\tau$  into an asymptotic off-shell  $W$  boson is worked out to be

$$\Gamma_{(\tau \rightarrow W \nu_\tau)}(x^2) = \frac{1}{8\pi} \left( \frac{-g}{2\sqrt{2}} \right)^2 \frac{m_\tau^3}{M_W^2} \left( 1 - \frac{x^2}{m_\tau^2} \right)^2 \left( 1 + \frac{2M_W^2}{m_\tau^2} \right) . \quad (3.9)$$

The detailed calculation of the decay width is found in Appendix D. Further, the above result can also be used to calculate the momentum-dependent tree-level decay width of the  $\tau$  lepton into a  $\tau$  neutrino and an off-shell vector or axial-vector resonance. Therefore, the  $W$  propagator is replaced by an effective coupling that can be constructed from the Standard Model of Electroweak Interactions and the Lagrangian of the Linear Sigma Model. In the following sections, the tree-level vertices of the weak  $W$  bosons in the vector and axial-vector channel will be determined. The obtained tree-level couplings can then be used to calculate the decay rates for  $\tau^- \rightarrow \rho^- \nu_\tau$  and  $\tau^- \rightarrow a_1^- \nu_\tau$ .

## 3.2 Vector Channel

The non-strange contributions to the  $\tau$  spectral functions in the vector channel come from processes that result in either two- or four-pion final states (Figure 3.1). The total branching fraction of the non-strange vector channel is given by  $B_V = (31.82 \pm 0.18 \pm 0.12)\%$ . The vector channel is clearly dominated by the two-pion channel which contributes with 25.471%, while the four-pion vector channel contributes only with 5.567%.

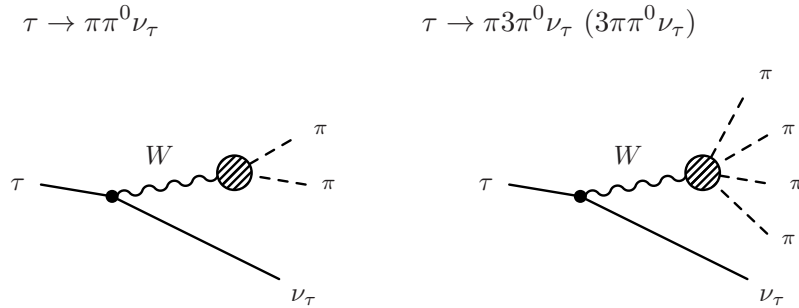


Figure 3.1: Vector channel contributions  $\pi\pi^0$  and  $\pi 3\pi^0, 3\pi\pi^0$ .

### 3.2.1 $2\pi$ Vector Channel

The processes that yield two-pion final states are depicted in Figure 3.2. There is one process in which the  $W$  boson decays directly in two pions and another process in which  $W$  transforms into a  $\rho$  meson which then disintegrates in two final pions.

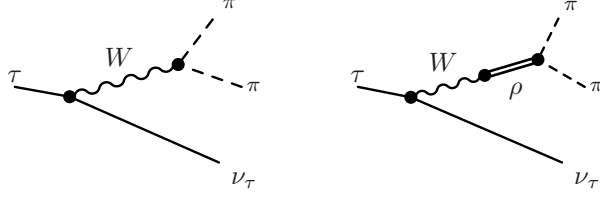


Figure 3.2: Intermediate states for the  $\pi\pi^0$  vector channel.

$W \rightarrow \pi\pi^0$ :

The tree-level three-vertices that account for  $W^- \rightarrow \pi^- \pi^0$  arise only from the square of the covariant derivative<sup>1</sup> which contains products from the partial derivative term for scalars and pseudoscalars with the  $W$  interaction term

$$\begin{aligned}
& ig \cos \theta_C \text{Tr} \left[ -\partial_\mu \Phi^\dagger W^\mu \Phi + \Phi^\dagger W_\mu \partial^\mu \Phi \right] \\
&= ig \cos \theta_C \times \\
& \quad \text{Tr} \left\{ -\partial^\mu [(\sigma_a - iZ\pi_a)t_a + \phi_0 t_0] (W_1^\mu t_1 + W_2^\mu t_2) [(\sigma_b + iZ\pi_b)t_b + \phi_0 t_0] \right. \\
& \quad \left. + [(\sigma_a + iZ\pi_a)t_a + \phi_0 t_0] (W_1^\mu t_1 + W_2^\mu t_2) \partial^\mu [(\sigma_b - iZ\pi_b)t_b + \phi_0 t_0] \right\}.
\end{aligned}$$

All terms proportional to  $\phi_0$  and  $\phi_0^2$  will be omitted since they either generate mixing terms between  $W$  and the (pseudo-) scalar fields, or they are proportional to simple propagators of the weak bosons. Terms proportional to  $\sigma_a$  and  $\eta$  also do not contribute to the direct  $W\pi\pi^0$  vertex as well and are omitted, too.

With indices  $k = 1, 2$  and  $i, j = 1, 2, 3$  the above equation simplifies to

$$-ig \cos \theta_C Z^2 (\pi_j W_{\mu k} \partial^\mu \pi_i - \pi_i W_{\mu k} \partial^\mu \pi_j) \text{Tr}[t_i t_k t_j], \quad (3.10)$$

where, according to Einstein's sum convention, summation over repeated indices is implied. Using the identity for the trace over a product of the three  $SU(2)$  generators

$$\text{Tr}[t_i t_j t_k] = \frac{i}{4} \varepsilon_{ijk} \quad (3.11)$$

yields

$$\frac{g \cos \theta_C Z^2}{2} [W_1^\mu (\pi_2 \partial^\mu \pi_3 - \pi_3 \partial^\mu \pi_2) + W_2^\mu (\pi_3 \partial^\mu \pi_1 - \pi_1 \partial^\mu \pi_3)] . \quad (3.12)$$

<sup>1</sup>There are no contributions from  $\frac{1}{4} \text{Tr}[L_{\mu\nu} L^{\mu\nu}]$ . This term does only seem to contain momentum-dependent tree-level three-vertices with one weak boson and two pionic states. But these contributions cancel each other, since they are proportional to  $(\partial_\mu \partial^\nu - \partial_\nu \partial^\mu) \pi_3$ .



Now one can change to the physical charged representation and the tree-level vertices for  $W^\pm \rightarrow \pi^\pm \pi^0$  read

$$\frac{ig \cos \theta_C Z^2}{2} [W^- (\pi^+ \partial^\mu \pi^0 - \pi^0 \partial^\mu \pi^+) + W^+ (\pi^0 \partial^\mu \pi^- - \pi^- \partial^\mu \pi^0)] . \quad (3.13)$$

The  $W^\pm \pi^\pm \pi^0$  vertex receives another contribution from the covariant derivative, the product terms of  $W$  and  $\Phi$  and the vector and axial-vector fields with  $\Phi$ . The calculation to obtain that vertex will be shown in detail for once, for the other vertices in the vector channel as well as in the axial-vector channel an analogous procedure was applied. From the covariant derivative one obtains another contribution to the coupling between

$$\begin{aligned} & g \cos \theta_C g_1 \text{Tr} \left[ \Phi^\dagger W_\mu (L^\mu \Phi - \Phi R^\mu) + (\Phi^\dagger L_\mu - R_\mu \Phi^\dagger) W^\mu \Phi \right] \\ &= g \cos \theta_C g_1 \times \\ & \quad \text{Tr} \left\{ [(\sigma_a - iZ\pi_a)t_a + \phi_0 t_0] W_{\mu k} t_k (V_b^\mu + A_b^\mu) t_b [(\sigma_c + iZ\pi_c)t_c + \phi_0 t_0] \right. \\ & \quad - [(\sigma_a - iZ\pi_a)t_a + \phi_0 t_0] W_{\mu k} t_k [(\sigma_b + iZ\pi_b)t_b + \phi_0 t_0] (V_c^\mu - A_c^\mu) t_c \\ & \quad + [(\sigma_a - iZ\pi_a)t_a + \phi_0 t_0] (V_{\mu b} + A_{\mu b}) t_b W_{\mu k} t_k [(\sigma_c + iZ\pi_c)t_c + \phi_0 t_0] \\ & \quad \left. - (V_{\mu a} - A_{\mu a}) t_a [(\sigma_b - iZ\pi_b)t_b + \phi_0 t_0] W_{\mu k} t_k [(\sigma_c + iZ\pi_c)t_c + \phi_0 t_0] \right\} \\ &= g \cos \theta_C g_1 \text{Tr} \left[ (-iZ\pi_a t_a + \phi_0 t_0) W_{\mu k} t_k A_b^\mu t_b (iZ\pi_c t_c + \phi_0 t_0) \right. \\ & \quad + (-iZ\pi_a t_a + \phi_0 t_0) W_{\mu k} t_k (iZ\pi_b t_b + \phi_0 t_0) A_c^\mu t_c \\ & \quad + (-iZ\pi_a t_a + \phi_0 t_0) A_{\mu b} t_b W_{\mu k} t_k (iZ\pi_c t_c + \phi_0 t_0) \\ & \quad + A_{\mu a} t_a (-iZ\pi_b t_b + \phi_0 t_0) W_{\mu k} t_k (iZ\pi_c t_c + \phi_0 t_0) \\ & \quad \left. + \dots (\text{terms} \propto V_\mu) \right] \\ &= g \cos \theta_C g_1 \left( -iZ\pi_a W_{\mu k} A_b^\mu \phi_0 \text{Tr}[t_a t_k t_b t_0] + \phi_0 W_{\mu k} A_a^\mu iZ\pi_b \text{Tr}[t_0 t_k t_a t_b] \right. \\ & \quad - iZ\pi_a W_{\mu k} \phi_0 A_b^\mu \text{Tr}[t_a t_k t_0 t_b] + \phi_0 W_{\mu k} iZ\pi_a A_b^\mu \text{Tr}[t_0 t_k t_a t_b] \\ & \quad - iZ\pi_a A_{\mu b} W_k^\mu \phi_0 \text{Tr}[t_a t_b t_k t_0] + \phi_0 A_{\mu a} W_k^\mu iZ\pi_b \text{Tr}[t_0 t_a t_k t_b] \\ & \quad - A_{\mu a} iZ\pi_b W_k^\mu \phi_0 \text{Tr}[t_a t_b t_k t_0] + A_{\mu a} \phi_0 W_k^\mu iZ\pi_b \text{Tr}[t_a t_0 t_k t_b] \\ & \quad \left. + \dots \right) \\ &= \frac{iZg \cos \theta_C g_1 \phi_0}{2} \left( \pi_a W_{\mu k} A_b^\mu \text{Tr}[t_k t_a t_b] + \pi_a W_{\mu k} A_b^\mu \text{Tr}[t_k t_a t_b] \right. \\ & \quad + W_{\mu k} \pi_a A_b^\mu \text{Tr}[t_k t_a t_b] - \pi_a A_{\mu b} W_k^\mu \text{Tr}[t_k t_a t_b] \\ & \quad - A_{\mu a} W_k^\mu \pi_b \text{Tr}[t_k t_a t_b] + W_{\mu k} A_a^\mu iZ\pi_b \text{Tr}[t_k t_a t_b] \\ & \quad - A_{\mu a} \pi_b W_k^\mu \text{Tr}[t_k t_a t_b] - A_{\mu a} W_k^\mu \pi_b \text{Tr}[t_k t_a t_b] \\ & \quad \left. + \dots \right) \\ &= \frac{iZg \cos \theta_C g_1 \phi_0}{2} \left( \pi_a W_{\mu k} A_b^\mu \text{Tr}[t_k t_a t_b] + \pi_a W_{\mu k} A_b^\mu \text{Tr}[t_k t_a t_b] \right. \\ & \quad \left. - A_{\mu b} \pi_a W_k^\mu \text{Tr}[t_k t_b t_a] - A_{\mu b} W_k^\mu \pi_a \text{Tr}[t_k t_b t_a] \right) \end{aligned}$$

$$\begin{aligned}
& + \dots) \\
= & \frac{iZg \cos \theta_C g_1 \phi_0}{2} (4W_{\mu k} \pi_a A_b^\mu \text{Tr}[t_k t_a t_b] + \dots) .
\end{aligned} \tag{3.14}$$

Again, the index  $k = 1, 2$  describes the isospin index of the two charged weak bosons. The three-point vertices of  $W$  and two pions in the above equation arise now as consequence of the spontaneously broken axial symmetry. Because of the  $a_1\pi$  mixing, the axial-vector bare fields have been redefined in terms of their physical fields (see Equation (3.2)) and also contain normalised pseudoscalar fields  $wZ\partial^\mu\eta$  and  $wZ\partial^\mu\vec{\pi}$ . With  $A^\mu = (f_1^\mu + wZ\partial^\mu\eta)t_0 + (\vec{a}_1^\mu + wZ\partial^\mu\vec{\pi}) \cdot \vec{t}$ , the coupling between  $W$  and the pseudoscalar pions is obtained as

$$2iwZ^2g \cos \theta_C g_1 \phi_0 W_{\mu k} \pi_a (\partial^\mu \pi_b) \text{Tr}[t_k t_a t_b] . \tag{3.15}$$

After the trace has been performed this reads

$$\frac{iwZ^2g \cos \theta_C g_1 \phi_0}{2} (W_{\mu 1} \pi_2 \partial^\mu \pi_3 - W_{\mu 1} \pi_3 \partial^\mu \pi_2 + W_{\mu 2} \pi_3 \partial^\mu \pi_1 - W_{\mu 2} \pi_1 \partial^\mu \pi_3) . \tag{3.16}$$

Changing to the physical charged representation yields the following result for the contribution to the  $W^\pm \rightarrow \pi^\pm \pi^0$  vertex from (3.14)

$$\frac{ig \cos \theta_C g_1 \phi_0 w Z^2}{2} [W_\mu^- (\pi^0 \partial^\mu \pi^+ - \pi^+ \partial^\mu \pi^0) + W_\mu^+ (\pi^- \partial^\mu \pi^0 - \pi^0 \partial^\mu \pi^-)] . \tag{3.17}$$

Together with (3.13) the vertex prefactor of the decay channel where  $W$  decays directly into two pions as depicted in Figure 3.2 is then

$$\left( \frac{ig \cos \theta_C Z^2}{2} - \frac{ig \cos \theta_C g_1 \phi_0 w Z^2}{2} \right) . \tag{3.18}$$

After the explicit expressions for the parameters

$$w = \frac{g_1 \phi_0}{m_{a_1}^2} , \quad \phi_0 = Z f_\pi , \quad g_1 = \frac{m_{a_1}}{Z f_\pi} \sqrt{1 - \frac{1}{Z^2}} \tag{3.19}$$

are inserted, (3.18) simplifies to

$$-\frac{ig \cos \theta_C}{2} . \tag{3.20}$$

As it could already be expected, the coupling in the process  $W \rightarrow \pi\pi^0$  is only influenced by the weak interaction coupling constant  $g$  and the Cabibbo mixing angle.

$W \rightarrow \rho$ :

The  $2\pi$  vector-channel decay takes place over the intermediate  $\rho$  resonance which yields the dominant contribution to the vector channel. It is accounted for by the  $W\rho$  mixing term that is manually incorporated into the Lagrangian in (2.108) by  $\frac{g \cos \theta_C \delta}{2} \text{Tr}[W_{\mu\nu} L^{\mu\nu}]$ . With the indices  $k = 1, 2$  and  $i = 1, 2, 3$  this yields

$$\begin{aligned} & \frac{g \cos \theta_C \delta}{2} \text{Tr}[(\partial_\mu W_\nu - \partial_\nu W_\mu)(\partial^\mu L^\nu - \partial^\nu L^\mu)] \\ &= \frac{g \cos \theta_C \delta}{2} [\partial_\mu W_{\nu k}(\partial^\mu V_i^\nu + \partial^\mu A_i^\nu) - \partial_\mu W_{\nu k}(\partial^\nu V_i^\mu + \partial^\nu A_i^\mu) \\ & \quad - \partial_\nu W_{\mu k}(\partial^\mu V_i^\nu + \partial^\mu A_i^\nu) + \partial_\nu W_{\mu k}(\partial^\nu V_i^\mu + \partial^\nu A_i^\mu)] \text{Tr}[t_k t_i] . \end{aligned} \quad (3.21)$$

Since here only those vertices are considered that yield contributions to the process  $\tau \rightarrow \pi\pi^0$  on tree-level, the terms accounting for the gauge field self-interactions have been left out. Using the identity

$$\text{Tr}[t_i t_j] = \frac{1}{2} \delta_{ij} \quad (3.22)$$

then leads to

$$\begin{aligned} & \frac{g \cos \theta_C \delta}{4} [(\partial_\mu W_{\nu 1} - \partial_\nu W_{\mu 1})(\partial^\mu \rho_1^\nu - \partial^\nu \rho_1^\mu + \partial^\mu a_{11}^\nu - \partial^\nu a_{11}^\mu) \\ & \quad + (\partial_\mu W_{\nu 2} - \partial_\nu W_{\mu 2})(\partial^\mu \rho_2^\nu - \partial^\nu \rho_2^\mu + \partial^\mu a_{12}^\nu - \partial^\nu a_{12}^\mu)] . \end{aligned} \quad (3.23)$$

Transforming the bare fields in (3.23) into their physical, charged representation then yields the following contributions to the two  $\pi$  vector channel with intermediate  $\rho$  resonance

$$\frac{g \cos \theta_C \delta}{2} \partial_\mu W_\nu^- (\partial^\mu \rho^{\nu+} - \partial^\nu \rho^{\mu+}) + h.c. . \quad (3.24)$$

After performing integration by parts, using the Proca condition  $\partial_\mu \rho^\mu = 0$  and  $\partial^\mu \rightarrow iq^\mu$  one obtains the momentum dependent  $W\rho$  mixing term<sup>2</sup>

$$\frac{g \cos \theta_C \delta q^2}{2} (W_\mu^- \rho^{\mu+} + W_\mu^+ \rho^{\mu-}) . \quad (3.25)$$

From (3.23) an additional  $W a_1$  mixing contribution was obtained that also influences the axial-vector channel, which is subject of the next chapter. The contributions to the  $W a_1$  mixing read

$$\frac{g \cos \theta_C \delta q^2}{2} (W_\mu^- a_1^{\mu+} + W_\mu^+ a_1^{\mu-}) . \quad (3.26)$$

---

<sup>2</sup>The full calculation for this mixing term is found in Appendix B.

### 3.2.2 $4\pi$ Vector Channel

The four-pion vector channel  $\tau^- \rightarrow \nu_\tau 3\pi\pi^0$  ( $\pi 3\pi^0$ ) in Figure 3.1 consists of the intermediate processes in Figure 3.3

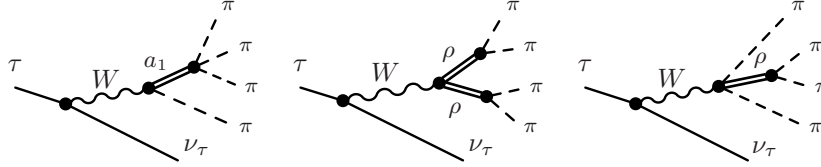


Figure 3.3: Intermediate processes of the four pion vector channel.

$W \rightarrow a_1\pi$ :

The contributions to the  $W a_1\pi$  vertex are obtained from the squared covariant derivative  $\text{Tr}[(D^\mu\Phi^\dagger)D^\mu\Phi]$  by

$$\begin{aligned} & \text{Tr} \left[ (D^\mu\Phi)^\dagger D^\mu\Phi \right] \\ &= \text{Tr} \left[ (\partial_\mu\Phi^\dagger + ig_1(\Phi^\dagger L_\mu - R_\mu\Phi^\dagger) + ig\Phi^\dagger W_\mu) \times \right. \\ & \quad \left. (\partial^\mu\Phi - ig_1(L^\mu\Phi - \Phi R^\mu) - igW^\mu\Phi) \right] \\ &= g_1g\text{Tr} \left[ (\Phi^\dagger L_\mu - R_\mu\Phi^\dagger)W^\mu\Phi + \Phi^\dagger W_\mu(L^\mu\Phi - \Phi R^\mu) \right] + \dots \quad (3.27) \end{aligned}$$

and from the square of the field strength tensor  $L^{\mu\nu}$  by

$$\begin{aligned} \frac{1}{4}\text{Tr}[L_{\mu\nu}L^{\mu\nu}] &= -\frac{1}{4}\text{Tr} \left\{ [\partial^\mu L^\nu - ig[W^\mu, L^\nu] - (\partial^\nu L^\mu - ig[W^\nu, L^\mu])]^2 \right\} \\ &= -\frac{1}{4}ig\text{Tr} \left( (\partial_\mu L_\nu - \partial_\nu L_\mu) \{ [W^\mu, L^\nu] - [W^\nu, L^\mu] \} \right. \\ & \quad \left. + \{ [W^\mu, L^\nu] - [W^\nu, L^\mu] \} (\partial_\mu L_\nu - \partial_\nu L_\mu) \right) + \dots \quad (3.28) \end{aligned}$$

From (3.27) the amplitude for the vertex  $W^- \rightarrow a_1^-\pi^0$  ( $a_1^0\pi^-$ ) is then determined to be

$$\frac{1}{2}igg_1Z\phi_0W_\mu^-(a_1^{\mu+}\pi^0 - a_1^{\mu 0}\pi^+) + h.c. , \quad (3.29)$$

and the contribution from (3.28) reads

$$\begin{aligned} & \frac{1}{4}igwZ \left[ (W_\mu^-\partial_\nu\pi^+ - W_\nu^-\partial_\mu\pi^+)(\partial^\mu a_1^{\nu 0} - \partial^\nu a_1^{\mu 0}) \right. \\ & \quad \left. - (W_\mu^-\partial_\nu\pi^0 - W_\nu^-\partial_\mu\pi^0)(\partial^\mu a_1^{\nu+} - \partial^\nu a_1^{\mu+}) \right] + h.c. \quad (3.30) \end{aligned}$$

$W \rightarrow \rho\rho^0$ :

The  $W^- \rho^- \rho^0$  vertex is also obtained from the square of the left-handed field strength tensor (3.28). It is given by

$$\begin{aligned} & \frac{1}{4}ig [(W_\mu^- \rho_\nu^+ - W_\nu^- \rho_\mu^+)(\partial^\mu \rho_1^{\nu 0} - \partial^\nu \rho_1^{\mu 0}) \\ & \quad - (W_\mu^- \rho_\nu^0 - W_\nu^- \rho_\mu^0)(\partial^\mu \rho_1^{\nu +} - \partial^\nu \rho_1^{\mu +})] \\ & + h.c. \quad . \end{aligned} \quad (3.31)$$

$W \rightarrow \rho\pi\pi$ :

The four-leg vertex of the decay  $W^- \rightarrow \rho^0\pi^-\pi^0(\rho^-2\pi^0, \rho^-2\pi)$  is not only influenced by the covariant derivative

$$\frac{1}{2}gg_1Z^2W_\mu^- [\pi^0(\pi^0\rho^{\mu+} - \pi^+\rho^{\mu 0}) + \pi^+(\pi^-\rho^{\mu+} - \pi^+\rho^{\mu-})] + h.c. \quad . \quad (3.32)$$

but also by the interaction terms in  $\mathcal{L}_3$

$$-2ig_2\text{Tr}\{L_{\mu\nu}[L_\mu, L_\nu]\} = 2ig_2\text{Tr}\{(ig[W^\mu, L^\nu] - ig[W^\nu, L^\mu])\}[L_\mu, L_\nu] \quad . \quad (3.33)$$

Together with the normalised identity for the trace of the product over four Pauli matrices

$$\text{Tr}[t_it_jt_kt_l] = \frac{1}{8}\delta_{ij}\delta_{kl} + \frac{1}{8}\delta_{il}\delta_{jk} - \frac{1}{8}\delta_{ik}\delta_{jl} \quad , \quad (3.34)$$

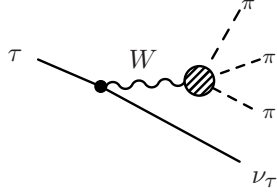
the  $W\rho^02\pi^0$  and  $W\rho^02\pi$  vertex is obtained as

$$\begin{aligned} & -gg_2w^2Z^2\times \\ & \left\{ W_\mu^- [\rho^{\mu-}(\partial_\nu\pi^+)^2 - \partial_\nu\pi^0(\partial^\nu\pi^0\rho^{\mu+} - \partial^\mu\pi^0\rho^{\nu+}) \right. \\ & \quad + \partial_\nu\pi^+(\partial^\nu\pi^0\rho^{\mu 0} + \partial^\mu\pi^0\rho^{\nu 0} - \partial^\nu\pi^-\rho^{\mu+} + 2\partial^\mu\pi^-\rho^{\nu+}) \\ & \quad \left. - \partial^\mu\pi^+(2\partial_\nu\pi^0\rho^{\nu 0} + \partial_\nu\pi^+\rho^{\nu-} + \partial_\nu\pi^-\rho^{\nu+}) \right] \\ & + W_\nu^- [\rho^{\nu-}(\partial_\mu\pi^+)^2 + \partial_\mu\pi^0(\partial^\nu\pi^0\rho^{\mu+} - \partial^\mu\pi^0\rho^{\nu+}) \\ & \quad + \partial_\mu\pi^+(\partial^\nu\pi^0\rho^{\mu 0} + \partial^\mu\pi^0\rho^{\nu 0} + 2\partial^\nu\pi^-\rho^{\mu+} - \partial^\mu\pi^-\rho^{\nu+}) \\ & \quad \left. - \partial^\nu\pi^+(2\partial_\mu\pi^0\rho^{\mu 0} + \partial_\mu\pi^-\rho^{\mu+} + \partial_\mu\pi^+\rho^{\mu-}) \right\} \quad . \quad (3.35) \end{aligned}$$

### 3.3 Axial-Vector Channel

The axial-vector channel contains those processes with odd G-parity. The non-strange contributions in the decay of  $\tau$  into the axial-vector channel consist of three- or five-pion final states (Figure 3.4) and their total branching fraction is  $B_A = (30.19 \pm 0.18 \pm 0.12)\%$ .

$$\tau \rightarrow \nu_\tau \pi 2\pi^0 \quad (3\pi)$$



$$\tau \rightarrow \nu_\tau \pi 4\pi^0 \quad (3\pi 2\pi^0, 5\pi)$$

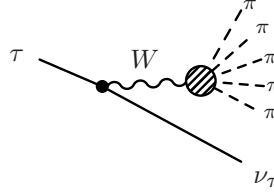


Figure 3.4: The three- and five-pion channels of the axial-vector channel in the  $\tau$  decay.

### 3.3.1 $3\pi$ Axial-Vector Channel

The amplitudes for the intermediate states of the decay into the  $3\pi$  axial-vector channel are depicted in Figure 3.5. In the three-pion decay channel there are two contributions from  $\tau \rightarrow 3\pi\nu_\tau$  and  $\tau \rightarrow \pi 2\pi^0\nu_\tau$ . They have the branching fractions  $B_{3\pi} = 9.041\%$  and  $B_{\pi 2\pi^0} = 9.239\%$ . The three-pion decay channel is dominated by the  $a_1$  resonance and the small difference in the two branching fractions is due to a small breaking of strong isospin symmetry because of the mass difference between the charged and neutral pions [25]. The blob in the diagram with the  $a_1$  intermediate state contains the decay channels of  $a_1 \rightarrow 3\pi$  ( $\pi 2\pi^0$ ),  $a_1 \rightarrow \rho\pi^0$  ( $\rho^0\pi$ ),  $a_1 \rightarrow f_0\pi$  and  $a_1 \rightarrow \sigma\pi$ .

$$\underline{W \rightarrow 3\pi(\pi 2\pi^0):}$$

The decay  $W \rightarrow 3\pi(\pi 2\pi^0)$  receives contributions from the covariant derivative  $\text{Tr}[(D^\mu\Phi)^\dagger D^\mu\Phi]$ , as well as from  $\mathcal{L}_3$  by  $-2ig_2\text{Tr}\{L_{\mu\nu}[L^\mu, L^\nu]\}$ . The contributions from the covariant derivative read

$$\frac{1}{2}g \cos\theta_C g_1 Z^3 w W_\mu^- (\pi^+\pi^0\partial^\mu\pi^0 + \pi^+\pi^-\partial^\mu\pi^+ + \pi^+\pi^+\partial^\mu\pi^-) + h.c. \quad (3.36)$$

and the contributions from  $\mathcal{L}_3$  are

$$\begin{aligned} & gg_2 \cos\theta_C w^3 Z^3 \times \\ & \left( W_\mu^- \{ \partial^\mu\pi^+ [(\partial_\nu\pi^0)^2 + \partial_\nu\pi^-\partial^\nu\pi^+] - \partial_\nu\pi^+ [\partial^\mu\pi^0\partial^\nu\pi^0 + \partial^\mu\pi^-\partial^\nu\pi^+] \} \right. \\ & \quad \left. + W_\nu^- \{ \partial^\nu\pi^+ [(\partial_\mu\pi^0)^2 + \partial_\mu\pi^-\partial^\mu\pi^+] - \partial_\mu\pi^+ [\partial^\mu\pi^0\partial^\nu\pi^0 + \partial_\mu\pi^+\partial^\nu\pi^-] \} \right) \\ & + h.c. . \end{aligned} \quad (3.37)$$

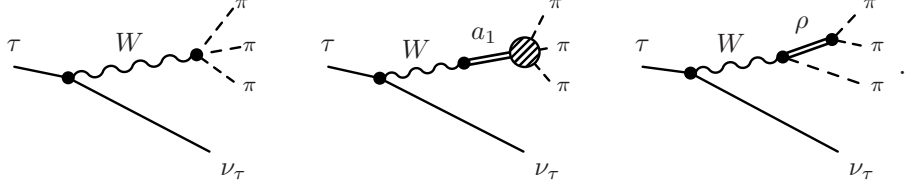


Figure 3.5: Intermediate states of the three-pion axial-vector channel.

$W \rightarrow a_1$ :

The dominant  $a_1$  intermediate state in the three pion axial-vector channel arises from the covariant-derivative term. Because of spontaneous breaking of the axial symmetry there arise terms between the axial-vector fields and the charged weak bosons that are proportional to the chiral condensate  $\phi_0^2$ . They read

$$\frac{1}{2}g \cos \theta_C g_1 \phi_0^2 W_\mu^- a_1^{\mu+} + h.c. \quad . \quad (3.38)$$

The  $W a_1$  mixing term is affected by the extra term (2.108) that was incorporated into the model in order to generate the amplitudes for the  $W \rho$  mixing. The modification of the  $W a_1$  mixing amplitude is given by (3.26). It reads

$$\frac{g \cos \theta_C \delta q^2}{2} W_\mu^- a_1^{\mu+} + h.c. \quad . \quad (3.39)$$

Thus the probability of the  $W a_1$  mixing contribution in the axial-vector channel can be calculated from

$$\frac{g \cos \theta_C}{2} (\delta q^2 + g_1 \phi_0^2) W_\mu^- a_1^{\mu+} + h.c. \quad . \quad (3.40)$$

$W \rightarrow \rho\pi$ :

The vertex of the third and last contribution to the  $3\pi$  axial-vector channel from the intermediate process of  $W$  coupling directly to a  $\rho$  meson and a pion is obtained from the covariant derivative but also from the field strength tensors squared. The amplitudes can be calculated from

$$\frac{1}{2}ig \cos \theta_C g_1 Z \phi_0 W_\mu^- (\rho^{\mu 0} \pi^+ - \rho^{\mu+} \pi^0) + h.c. \quad (3.41)$$

and

$$\begin{aligned} \frac{1}{2}ig \cos \theta_C Z w [(W_\mu^- \partial_\nu \pi^+ - W_\nu^- \partial_\mu \pi^+) (\partial^\mu \rho^{\nu 0} - \partial^\nu \rho^{\mu 0}) \\ - (W_\mu^- \partial_\nu \pi^0 - W_\nu^- \partial_\mu \pi^0) (\partial^\mu \rho^{\nu+} - \partial^\nu \rho^{\mu+})] + h.c. \quad . \quad (3.42) \end{aligned}$$

### 3.3.2 $5\pi$ Axial-Vector Channel

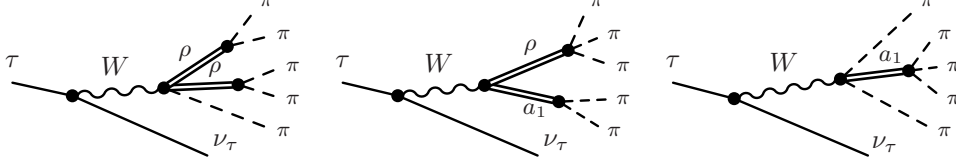


Figure 3.6: Intermediate processes of the five-pion axial-vector channel.

The five-pion axial-vector channel contributes less than 1% to the axial-vector branching fraction. The vertices for its intermediate states (Figure 3.6) are extracted analogously to the previous ones and are now only listed:

$W \rightarrow 2\rho\pi$ :

$$\begin{aligned} & Zgg_2w \left\{ W_\mu^- \left[ \rho^{\mu+} (2\partial_\nu \pi^0 \rho^{\nu 0} + \partial_\nu \pi^- \rho^{\nu+} + \partial_\nu \pi^+ \rho^{\nu-}) \right. \right. \\ & \quad + \rho_\nu^0 (\rho^{\nu 0} \partial^\mu \pi^+ - \rho^{\mu 0} \partial^\nu \pi^+ - \rho^{\nu+} \partial^\mu \pi^0) \\ & \quad \left. \left. - \rho_\nu^+ (\partial^\nu \pi^0 \rho^{\mu 0} + \partial^\mu \pi^- \rho^{\nu+} - \partial^\mu \pi^+ \rho^{\nu-} + 2\rho^{\mu-} \partial^\nu \pi^+) \right] \right. \\ & \quad + W_\nu^- \left[ \rho^{\nu+} (\partial_\mu \pi^+ \rho^{\mu-} + \partial_\mu \pi^- \rho^{\mu+} + 2\partial_\mu \pi^0 \rho^{\mu 0}) \right. \\ & \quad + \rho_\mu^0 (\partial^\nu \pi^+ \rho^{\mu 0} - \partial^\mu \pi^+ \rho^{\nu 0} - \rho^{\mu+} \partial^\nu \pi^0) \\ & \quad \left. \left. - \rho_\mu^+ (\partial^\mu \pi^0 \rho^{\nu 0} + \partial^\nu \pi^- \rho^{\mu+} - \partial^\nu \pi^+ \rho^{\mu-} + 2\partial^\mu \pi^+ \rho^{\nu-}) \right] \right\}, \end{aligned}$$

$W \rightarrow \rho a_1$ :

$$\begin{aligned} & -\frac{1}{4}ig \left\{ W_\mu^- \left[ a_\nu^0 (\partial^\mu \rho^{\nu+} - \partial^\nu \rho^{\nu+}) - a_\nu^+ (\partial^\mu \rho^{\nu 0} - \partial^\nu \rho^{\nu 0}) \right. \right. \\ & \quad \left. \left. - \rho_\nu^0 (\partial^\mu a^{\nu+} - \partial^\nu a^{\nu+}) - \rho_\nu^+ (\partial^\mu a^{\nu 0} - \partial^\nu a^{\nu 0}) \right] \right. \\ & \quad W_\nu^- \left[ a_\mu^0 (\partial^\nu \rho^{\mu+} - \partial^\mu \rho^{\mu+}) - a_\mu^+ (\partial^\nu \rho^{\mu 0} - \partial^\mu \rho^{\mu 0}) \right. \\ & \quad \left. \left. - \rho_\mu^0 (\partial^\nu a^{\mu+} - \partial^\mu a^{\mu+}) - \rho_\mu^+ (\partial^\nu a^{\mu 0} - \partial^\mu a^{\mu 0}) \right] \right\}, \end{aligned}$$

$W \rightarrow a_1 \pi \pi$ :

$$\begin{aligned} & -\frac{1}{2}gg_1Z^2W_\mu^- (\pi^+ \pi^0 a_\mu^0 + (\pi^+)^2 a_\mu^- + \pi^+ \pi^- a_\mu^+ + h.c.) \\ & + gg_2w^2Z^2 \left\{ W_\nu^- \left[ \partial_\mu \pi^+ (\partial^\mu \pi^- a^{\nu+} - a^{\nu-} \partial^\mu \pi^+ - a^{\mu 0} \partial^\nu \pi^0 - 2\partial^\nu \pi^- a^{\mu+}) \right. \right. \\ & \quad + \partial_\mu \pi^0 (\partial^\mu \pi^0 a^{\nu+} - a^{\nu 0} \partial^\mu \pi^+ - \partial^\nu \pi^0 a^{\mu+}) \\ & \quad \left. \left. + \partial_\nu \pi^+ (\partial^\mu \pi^+ a^{\mu-} + \partial^\mu \pi^- a^{\mu+} + 2a^{\mu 0} \partial^\mu \pi^0) \right] \right. \\ & \quad + W_\mu^- \left[ \partial_\nu \pi^+ (\partial^\nu \pi^- a^{\mu+} - a^{\mu-} \partial^\nu \pi^+ - a^{\nu 0} \partial^\mu \pi^0 - 2\partial^\mu \pi^- a^{\nu+}) \right. \\ & \quad + \partial_\nu \pi^0 (\partial^\nu \pi^0 a^{\mu+} - a_{\mu+} \partial^\nu \pi^+ - \partial^\mu \pi^0 a_{\nu+}) \\ & \quad \left. \left. + \partial_\mu \pi^+ (\partial^\nu \pi^+ a^{\nu-} + \partial^\nu \pi^- a^{\nu+} + 2a^{\nu 0} \partial^\nu \pi^0) \right] \right\}. \quad (3.43) \end{aligned}$$



## Chapter 4

# Decay Widths and Spectral Functions

### 4.1 Källen-Lehmann Representation and Optical Theorem

In general the spectral density function  $\rho(s)$  is defined in the Källen-Lehmann representation of the two-point correlation function

$$\Delta(s) = \int_0^{\infty} \frac{dp^2}{2\pi} \frac{\rho(p^2)}{s - p^2 + i\varepsilon} , \quad (4.1)$$

where the spectral density contains the sum over all possible transition amplitudes between the vacuum and each outgoing state  $\lambda$

$$\rho(s) = \sum_{\lambda} (2\pi) \delta(s - m_{\lambda}^2) |\langle 0 | \phi(0) | \lambda_0 \rangle|^2 , \quad (4.2)$$

and the variable  $s$  is the running mass squared in the centre-of-mass frame.

After performing the integration in (4.1) and using the identity

$$\lim_{y \rightarrow 0^+} \frac{1}{x \pm iy} = \text{p.v.} \frac{1}{x} \mp i\pi\delta(x) ,$$

the spectral density is obtained as the imaginary part of the propagator

$$\rho(s) = |2\text{Im}[\Delta(s)]| .$$

Splitting the two-point correlation function into intervals below and above the threshold for two-particle production yields

$$\begin{aligned}\Delta(s) &= \int_0^{(2m)^2} \frac{dp^2}{2\pi} \frac{\rho(p^2)}{s - p^2 + i\varepsilon} + \int_{(2m)^2}^{\infty} \frac{dp^2}{2\pi} \frac{\rho(p^2)}{s - p^2 + i\varepsilon} \\ &= \frac{Z}{s - m^2 + i\varepsilon} + \int_{(2m)^2}^{\infty} \frac{dp^2}{2\pi} \frac{\rho(p^2)}{s - p^2 + i\varepsilon} .\end{aligned}\quad (4.3)$$

The first term is the free propagator for a particle of mass  $m$ . The constant  $Z$  accounts for the field-strength renormalisation of the transition amplitude of the incoming field to a single outgoing field. Possible bound states would occur as further poles in the region below  $(2m)^2$ .

The second term describes the multi-particle final state of the resonance after the interaction, with a branching cut of the propagator in the complex  $p^2$  plane above the threshold of  $(2m)^2$  that contains the continuous distributions of all the multi-particle final states, starting with the process with two final particles.

Consequently the spectral density may be expressed as

$$\rho(s) = 2\pi Z \delta(s - m^2) + 2\text{Im}[\tilde{\Delta}(s)] .\quad (4.4)$$

The delta distribution yields exactly the one-particle state and the second term contains the continuum contributions of the branching cut.

## 4.2 Interacting Lagrangian and Spectral Functions

Based on an interacting Lagrangian of the form

$$\mathcal{L} = \frac{1}{2} (\partial_\mu S)^2 - \frac{1}{2} m_0^2 S^2 + \frac{1}{2} (\partial_\mu \varphi)^2 - \frac{1}{2} m^2 \varphi^2 + g S \varphi^2 ,\quad (4.5)$$

one can find another possibility to parametrise the spectral density of the scalar field  $S$  and describe, e.g., the process  $S \rightarrow 2\varphi$  [26].

The propagator of the interacting theory then reads

$$\Delta(s) = \frac{1}{s - m_0^2 + g^2 \text{Re}[\Sigma(s)] + g^2 i \text{Im}[\Sigma(s)] + i\varepsilon} ,\quad (4.6)$$

For a non-interacting theory ( $g \rightarrow 0$ ) this is the free propagator of a scalar field

$$\Delta_S(s) = \frac{1}{s - m_0 + i\varepsilon} .\quad (4.7)$$

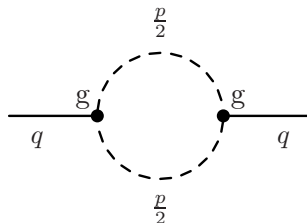


Figure 4.1: Vacuum polarisations of a resonance

In the interacting case, for cubic point interactions, the self-energy  $\Sigma$  contains the sum<sup>1</sup> of the loop diagrams depicted in Fig. 4.1

$$\Sigma(s) = -i \int \frac{d^4 q}{(2\pi)^4} \frac{1}{[(q + \frac{p}{2})^2 - m^2 + i\varepsilon][(q - \frac{p}{2})^2 - m^2 + i\varepsilon]} . \quad (4.8)$$

This approach is discussed for a scalar resonance in [26]. If  $g$  goes to zero, the propagator of the free field with mass  $m_0$  is obtained. For  $g \neq 0$  the mass of the intermediate resonance fulfils the equation

$$m_r - m_0^2 + g^2 \text{Re} [\Sigma(m_r)] = 0 .$$

The spectral density can thus be defined as

$$\rho(s) = Z\delta(s - m_r)\Theta(2m - s) + \frac{1}{\pi} \text{Im} [\tilde{\Delta}(s)] .$$

The generalised optical theorem relates the imaginary part of the self-interaction to the decay width

$$g^2 \text{Im} [\Sigma(s)] = \sqrt{s} \Gamma(s)$$

and with  $m_r = m_0 + g^2 \text{Re} [\Sigma(s)]$  the spectral density above threshold reads

$$\rho(s) = \frac{1}{\pi} \frac{\sqrt{s} \Gamma(s)}{(s - m_r^2)^2 + (\sqrt{s} \Gamma(s))^2} . \quad (4.9)$$

For a momentum-independent decay width  $\Gamma_{\text{full}}$  and mass  $m_r$  the Breit-Wigner distribution is obtained and reads

$$\rho_{\text{BW}}(s) = \frac{1}{\pi} \frac{m_r \Gamma_{\text{full}}}{(s - m_r^2)^2 + (m_r \Gamma_{\text{full}})^2} . \quad (4.10)$$

Now one can also consider coupled decay processes of an initial state via a resonance into a final state. As it was shown in [26] the mass distribution

---

<sup>1</sup>Because of the logarithmic divergence in the definition of the self-energy in (4.8) it is necessary to use a regularisation function  $f_\Lambda(s)$  to implement a cut-off  $\Lambda$  which will modify the decay width by a multiplicative  $s$ -dependent factor. The appropriate cut-off function  $f_\Lambda(s)$  will be introduced when it is needed for the further analysis.

of the decay width of a process  $i \rightarrow r + f' \rightarrow f' + f$  can be expressed as convolution of the decay  $\Gamma_{i \rightarrow r f'}(s)$  of the initial state  $i$  into an intermediate resonance-like state  $r$  and a final state  $f'$  and the spectral density function  $\rho(s)$  of the resonance with final states  $f$

$$\Gamma_{i \rightarrow f f'} = \int_0^\infty ds \rho_{r \rightarrow f}(s) \Gamma_{i \rightarrow r f'}(s) , \quad (4.11)$$

where  $f$  describes a final state, that may consist of  $1, 2, \dots, n$  particles.

For example; the decay of the  $\tau$  lepton via its vector  $\rho$  or axial-vector  $a_1$  decay channels can be calculated from the decay rate of  $\tau \rightarrow \nu_\tau r$ , with  $r = \rho, a_1$ , and the vector or axial-vector spectral density of the resonances  $\rho_V(s)$  and  $\rho_A(s)$  as follows

$$\Gamma_{\tau \rightarrow \nu_\tau 2\pi(4\pi)} = \int_0^\infty ds \rho_{\rho \rightarrow 2\pi(4\pi)}(s) \Gamma_{\tau \rightarrow \rho \nu_\tau}(s) , \quad (4.12)$$

$$\Gamma_{\tau \rightarrow \nu_\tau 3\pi(5\pi)} = \int_0^\infty ds \rho_{a_1 \rightarrow 3\pi(5\pi)}(s) \Gamma_{\tau \rightarrow a_1 \nu_\tau}(s) . \quad (4.13)$$

### 4.3 ALEPH Spectral Functions and their Parametrisation within the Linear Sigma Model

The ALEPH collaboration has measured the  $\tau$  spectral function in great detail [25]. The spectral functions  $v_1(s)$  and  $a_1(s)$  in the vector and axial-vector channel are given by

$$v_1(s) = \frac{m_\tau^2}{6 \cos^2 \theta_C S_{EW}} \frac{B(\tau^- \rightarrow V^- \nu_\tau)}{B(\tau^- \rightarrow e^- \bar{\nu}_e \nu_\tau)} \times \frac{dN_V}{N_V ds} \left[ \left(1 - \frac{s}{m_\tau^2}\right)^2 \left(1 + \frac{2s}{m_\tau^2}\right) \right]^{-1} , \quad (4.14)$$

$$a_1(s) = \frac{m_\tau^2}{6 \cos^2 \theta_C S_{EW}} \frac{B(\tau^- \rightarrow A^- \nu_\tau)}{B(\tau^- \rightarrow e^- \bar{\nu}_e \nu_\tau)} \times \frac{dN_A}{N_A ds} \left[ \left(1 - \frac{s}{m_\tau^2}\right)^2 \left(1 + \frac{2s}{m_\tau^2}\right) \right]^{-1} . \quad (4.15)$$

They are related to the imaginary part of the two-point correlation functions as

$$\text{Im}[\Delta_V(s)] = \frac{1}{2\pi} v_1(s) , \quad (4.16)$$

$$\text{Im}[\Delta_A(s)] = \frac{1}{2\pi} a_1(s) . \quad (4.17)$$

The factor  $dN/Nds$  describes the normalised invariant mass-squared distribution. As shown in Appendix C, it is related to the spectral density  $\rho(s)$  and the decay width  $\Gamma_{\tau \rightarrow V^-/A^- \nu_\tau}(s)$  by

$$\frac{dN_V}{N_V ds} = \frac{\rho_V(s) \Gamma_{\tau \rightarrow V^- \nu_\tau}(s)}{\Gamma_{\tau \rightarrow V^- \nu_\tau}}, \quad \frac{dN_A}{N_A ds} = \frac{\rho_A(s) \Gamma_{\tau \rightarrow A^- \nu_\tau}(s)}{\Gamma_{\tau \rightarrow A^- \nu_\tau}} \quad (4.18)$$

where  $\Gamma_{\tau \rightarrow V^- \nu_\tau}$  and  $\Gamma_{\tau \rightarrow A^- \nu_\tau}$  are the partial widths in the corresponding channel. They are related to the branching fraction by

$$\Gamma_{\tau \rightarrow V^-(A^-) \nu_\tau} = B(\tau^- \rightarrow V^-(A^-) \nu_\tau) \cdot \Gamma_\tau^{\text{full}}.$$

The partial decay widths are also related to  $\rho(s)$  by the mass distribution of the decay width in Equation (4.11).

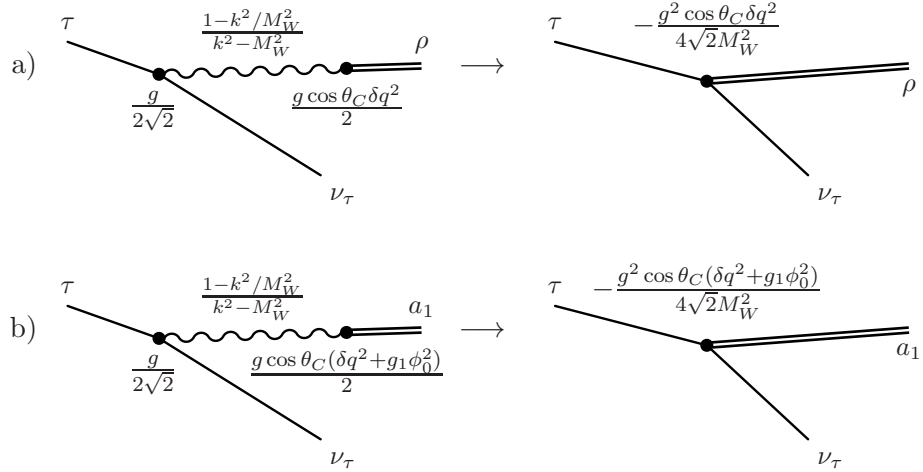


Figure 4.2: Effective couplings of a)  $\tau \rightarrow \rho \nu_\tau$  and b)  $\tau \rightarrow a_1 \nu_\tau$ .

The decay width  $\Gamma_{\tau \rightarrow W \nu_\tau}(s)$  was calculated in Appendix D based on the assumption of  $\tau$  decaying into an asymptotic off-shell  $W$  boson. The result for the decay width will now be used to further calculate the momentum-dependent decay width of the  $\tau$  lepton into a  $\tau$  neutrino and the  $\rho$  and  $a_1$  mesons. Vectors and axial vectors are both spin-1 particles just as the  $W$  boson and the result (D.12) can directly be generalised to the width for the  $\tau$  lepton decaying into a neutrino and any asymptotic spin-1 particle. Then the momentum-dependent decay widths in the centre-of-mass frame of  $\tau$  read

$$\Gamma_{\tau \rightarrow \rho \nu_\tau}(s) = \frac{g_\rho^2 m_\tau^3}{8\pi} \frac{1}{s} \left(1 - \frac{s}{m_\tau^2}\right)^2 \left(1 + \frac{2s}{m_\tau^2}\right), \quad (4.19)$$

$$\Gamma_{\tau \rightarrow a_1 \nu_\tau}(s) = \frac{g_{a_1}^2 m_\tau^3}{8\pi} \frac{1}{s} \left(1 - \frac{s}{m_\tau^2}\right)^2 \left(1 + \frac{2s}{m_\tau^2}\right) \quad (4.20)$$

and only the couplings  $g_\rho$  and  $g_{a_1}$  remain to be identified. Compared to the energy scale of 1 GeV of the investigated processes the mass  $M_W = 80,399 \pm 0.023$  GeV is large and the  $W$  propagator can be reduced to

$$-\frac{g_{\mu\nu}}{M_W^2} . \quad (4.21)$$

Thus, the couplings  $g_\rho$  and  $g_{a_1}$  are obtained from representing the exchange of the weak  $W$  boson by a point-like interaction vertex, as shown in the diagrams in Figure 4.3. Together with the couplings that were derived from the Lagrangian in Chapter 3 in (3.24) and (3.40), and with  $q^2 \rightarrow s$ , the effective vector coupling  $g_\rho$  and the effective axial-vector coupling  $g_{a_1}$  are defined as

$$g_\rho = \frac{g^2 \cos \theta_C}{4\sqrt{2}M_W^2} \delta \cdot s , \quad (4.22)$$

$$g_{a_1} = \frac{g^2 \cos \theta_C}{4\sqrt{2}M_W^2} (g_1 \phi_0^2 + \delta \cdot s) . \quad (4.23)$$

Finally, since each spectral density has to fulfil the sum rule

$$\int_0^\infty \rho(s) ds = 1 , \quad (4.24)$$

a normalisation factor

$$\frac{1}{N}, \quad N = \int_0^\infty \rho(s) ds \quad (4.25)$$

is added to the definitions of  $v_1(s)$  and  $a_1(s)$ .

Now, the relations between the ALEPH spectral functions  $v_1(s), a_1(s)$  and the spectral densities  $\rho_V(s), \rho_A(s)$  within the framework of the Linear Sigma Model read

$$v_1(s) = \frac{(2\pi)^2}{S_{EW}} (\delta \cdot s)^2 \frac{1}{s} \frac{\rho_V(s)}{N} , \quad (4.26)$$

$$a_1(s) = \frac{(2\pi)^2}{S_{EW}} (\delta \cdot s + g_1 \phi_0^2)^2 \frac{1}{s} \frac{\rho_A(s)}{N} . \quad (4.27)$$

The influence of the model is seen at two points. At first by means of the two couplings  $g_\rho$  and  $g_{a_1}$ . They have been directly derived from the Lagrangian  $\mathcal{L}_{\text{int}}$ , which itself is based on gauge invariance and the assumption that  $\rho$  and  $a_1$  are chiral partners. Second, the  $s$ -dependent decay widths in (4.9) can also be calculated directly from  $\mathcal{L}_{\text{int}}$ .

## Chapter 5

# Vector Channel Spectral Function

In this chapter the vector-channel spectral density of the  $\tau$  decay is calculated and used to determine the value for the vector channel coupling  $\delta$ . Since several different approaches to parametrise the spectral density are used, this chapter is now shortly summarised.

1. The vector-channel coupling  $\delta$  is estimated to  $\delta \simeq 0.20662$  on the basis of the convolution (5.2) from the previous section.
2. The Breit-Wigner spectral density which is based on the  $s$ -independent full width at half maximum is used as a first approximation and yields  $\delta \simeq 0.19946$ .
3. The fully  $s$ -dependent spectral function is calculated on the basis of the  $s$ -dependent decay width  $\Gamma_{\rho^- \rightarrow \pi^- \pi^0}(s)$  obtained from the Linear Sigma Model. Within that section it will be found that it is necessary to shift the  $\rho$  meson mass to improve the agreement between the data and the spectral function. The spectral function will be fitted with respect to three parameters; the  $\rho$  mass  $m_\rho$ , the full width  $\Gamma_\rho(m_\rho^2)$  and the free parameter  $\delta$ . The results of this fit will then be inserted into the Breit-Wigner spectral density to compare the two parametrisations.
4. Implementing the  $W\rho$  mixing in a different way on the basis of a new Lagrangian avoids the shift of the  $\rho$  mass. The Breit-Wigner spectral density and the fully  $s$ -dependent spectral density will be applied to calculate the vector spectral function. The result is compared to the one from the previous section.

5. Two other  $s$ -dependent  $\rho$  decay widths (Gounaris-Sakurai, Vojik-Lichard) for the decay  $\rho^- \rightarrow \pi^- \pi^0$  will be used to parametrise the spectral function. The result is again compared to the result from the  $s$ -dependent decay width  $\Gamma_{\rho^- \rightarrow \pi^- \pi^0}(s)$  of the Linear Sigma Model.

Section (5.3) contains the approximation in 3. It will be seen, that the fully  $s$ -dependent spectral function  $v_1(s)$ , based on the decay width  $\Gamma_{\rho^- \rightarrow \pi^- \pi^0}(s)$  from the Linear Sigma Model and a derivative  $W\rho$  coupling  $\sim \delta s$ , yields the best dynamical description of the vector channel.

## 5.1 First Estimate of the Parameter $\delta$

The main contribution to the inclusive<sup>1</sup> vector spectral function of the  $\tau$  lepton in [25] comes from the  $\pi^- \pi^0$  channel. It has a clearly defined peak with  $v_1(s = 0.5875 \text{ GeV}^2) = 2.7654$ . The data of the inclusive and exclusive invariant mass squared distributions from the ALEPH collaboration are found in [27].

The decay of  $\tau$  into two-pion final states is the result of the direct decay of  $W$  into two pions together with the process where  $W$  mixes with the  $\rho$  meson which then itself decays into two pions. This would yield to a probability for the total decay of  $\tau$  into two pions where the amplitudes of the two processes interfere with each other. Based on the assumption that the direct contributions from  $W^- \rightarrow \pi^- \pi^0$  are small, the decay rate for  $\tau^- \rightarrow \pi^- \pi^0 \nu_\tau$  will only depend on the free parameter  $\delta$ . This is the  $W\rho$  coupling constant that was introduced in Chapter 2.2 by

$$\mathcal{L}_{W\rho} = \frac{g \cos \theta_C \delta}{2} \text{Tr}[W_{\mu\nu} \rho^{\mu\nu}]. \quad (5.1)$$

The exclusive spectral density of the process  $\tau^- \rightarrow \rho^- \nu_\tau \rightarrow \pi^- \pi^0 \nu_\tau$  then makes it possible to determine the numerical value of  $\delta$ .

The following gedankenexperiment only leads an estimate of the range of  $\delta$  and is not used in further calculations. Following the purely hypothetical assumption that the  $\rho$  meson is “stable”<sup>2</sup>, the spectral density in the

---

<sup>1</sup>The inclusive spectral function describes the sum of all spectral functions in the respective channel, e.g., in the case of the non-strange vector channel the inclusive spectral function contains the spectral functions of the processes  $\tau^- \rightarrow \pi^- \pi^0 \nu_\tau$  and  $\tau^- \rightarrow \pi^+ 2\pi^- \nu_\tau (\pi^- 2\pi^0 \nu_\tau)$ , while the exclusive spectral function only contains one or some of the partial spectral functions.

<sup>2</sup>If the  $\rho$  resonance were stable, the final state of the  $\tau$  decay in the  $\pi^- \pi^0$  vector channel would of course not contain any pions. But still, since  $\rho$  can only decay into two



convolution (4.11) would reduce to a delta distribution  $\delta(s - m_\rho^2)$ . After performing the integration in (4.11) the following relation

$$\begin{aligned}\Gamma_{\tau^- \rightarrow \pi^- \pi^0 \nu_\tau} &= \int_0^\infty ds \delta(s - m_\rho^2) \Gamma_{\tau^- \rightarrow \rho^- \nu_\tau}(s) \\ &= \Gamma_{\tau^- \rightarrow \rho^- \nu_\tau}(m_\rho^2) \\ &= \frac{m_\tau^3}{8\pi m_\rho^2} \left( \frac{g^2 \cos \theta_C}{4\sqrt{2} M_W^2} \delta m_\rho \right)^2 \left( 1 - \frac{m_\rho^2}{m_\tau^2} \right)^2 \left( 1 + \frac{2m_\rho^2}{m_\tau^2} \right)\end{aligned}\quad (5.2)$$

is obtained. This is also in agreement with the fact that in the process where  $\tau$  decays into two final pions via an intermediate  $\rho$ , the  $\rho$  meson itself can, because of parity conservation, only decay into two pions. From  $\Gamma_{\tau^- \rightarrow \pi^- \pi^0 \nu_\tau}^{\text{exp.}} = 5.7811 \cdot 10^{-13}$  GeV the parameter  $\delta$  is expected to be approximately  $\delta \approx 0.20662$ .

### 5.1.1 The Breit-Wigner Spectral Density and the fully $s$ -Dependent Spectral Density

In order to obtain an exact value for  $\delta$ , different parametrisations of the spectral density  $\rho_V(s)$  which enters the definition of the vector-channel spectral function

$$v_1(s) = \frac{(2\pi)^2}{S_{EW}} (\delta s)^2 \frac{1}{s} \rho_V(s), \quad (5.3)$$

are calculated and compared to the data for the  $\pi^- \pi^0$  exclusive vector channel.

The Breit-Wigner spectral density is defined as

$$\rho_V^{\text{BW}}(s) = \frac{1}{\pi} \frac{m_\rho \Gamma_\rho^{\text{full}}}{(s - m_\rho^2)^2 + (m_\rho \Gamma_\rho^{\text{full}})^2}, \quad (5.4)$$

where  $\Gamma_\rho^{\text{full}}$  is the experimentally determined full width at half maximum of the  $\rho$  resonance and  $m_\rho$  is defined as the square root of the resonance's peak position. The Breit-Wigner spectral density is only an approximation of the spectral density based on an  $s$ -dependent decay width  $\Gamma(s)$  for the resonance in question.

---

pions and since  $\rho$  is considered to be the dominating intermediate state, one can infer that all two-pion final states in the vector channel result from an intermediate  $\rho$  and thus the decay rate of  $\tau^- \rightarrow \pi^- \pi^0 \nu_\tau$  must be the same as the decay rate  $\Gamma_{\tau^- \rightarrow \rho^- \nu_\tau}(m_\rho^2)$ .

The fully  $s$ -dependent spectral density for the  $\rho$  meson reads

$$\rho_V(s) = \frac{1}{\pi} \frac{\sqrt{s} \Gamma_\rho(s)}{(s - m_\rho^2)^2 + (\sqrt{s} \Gamma_\rho(s))^2}. \quad (5.5)$$

From the  $s$ -dependent decay width  $\Gamma_\rho(s)$  one obtains the full width by the definition

$$\Gamma_\rho(s = m_\rho^2) \equiv \Gamma_\rho^{\text{full}}. \quad (5.6)$$

## 5.2 Breit-Wigner Spectral Density

Since the  $\rho$  resonance's full width at half maximum is small compared to its mass, it can be approximated by the Breit-Wigner spectral density given in (5.4). This allows for an estimate of the influence of the vector coupling  $\delta$  and also for a first testing of the parametrisation of the spectral density  $v_1(s)$  within the Linear Sigma Model. E.g., the convolution formula for the unstable  $\rho$  meson (4.11) enters the normalisation constant in the definition of the spectral density  $v_1(s)$  in Equation 5.3 and then also influences the numerical value for the vector coupling  $\delta$ .

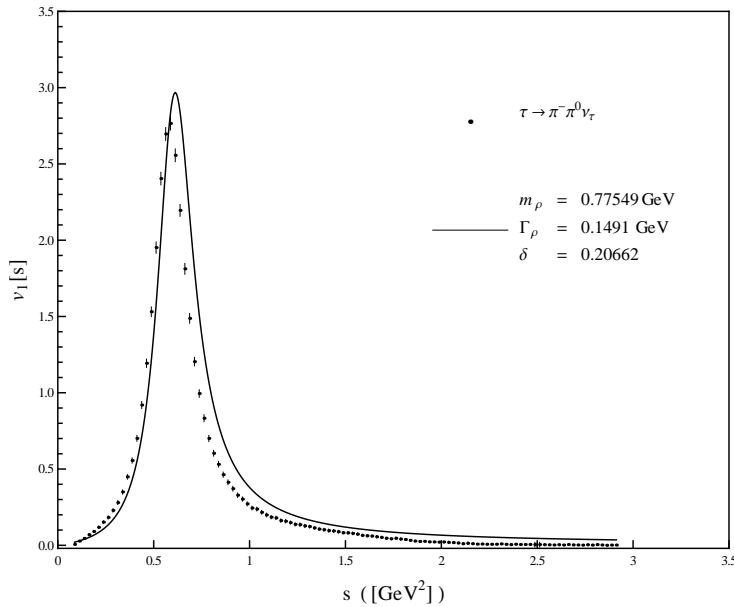


Figure 5.1: Breit-Wigner approximation of the vector channel with  $\rho$  mass and width from the PDG;  $m_\rho = 0.77549$  GeV,  $\Gamma_\rho^{\text{full}} = 0.1491$  GeV. The vector-channel coupling  $\delta = 0.20662$  is obtained from (5.2).

The result for the spectral function with Breit-Wigner spectral density  $\rho_V^{\text{BW}}(s)$  is presented in Figure 5.1 where the  $\rho$  mass and full width are the values given by the Particle Data Group (PDG):

$$\begin{aligned} m_\rho &= 0.77549 \text{ GeV} , \\ \Gamma_\rho^{\text{full}} &= 0.1491 \text{ GeV} . \end{aligned} \tag{5.7}$$

The result is already remarkably good, although the function exceeds the peak of the data about 9%. Fig. 5.1 is still based on the vector coupling constant that was obtained from the assumption of a “stable”  $\rho$  meson which is not only a strong simplification but moreover, this is not the case in nature. The too large peak value of  $v_1(s)$  can be improved by adjusting  $\delta$  so that the spectral function reproduces the height of the peak.

A fit for the vector coupling yields

$$\delta = 0.19946 . \tag{5.8}$$

The result is seen in Figure 5.2 and agrees remarkably well with the data. With the Breit-Wigner spectral density and the fitted  $W\rho$  coupling  $\delta$  the lineshape of the vector channel is reasonably well reproduced. There is however a small shift about  $25 \text{ MeV}^2$  of the entire spectral function  $v_1(s)$  to higher values of  $s$ . The free parameter  $\delta$  only influences the height of the spectral density. It can not be modified in a way that the spectral density would be shifted to smaller values of  $s$ .

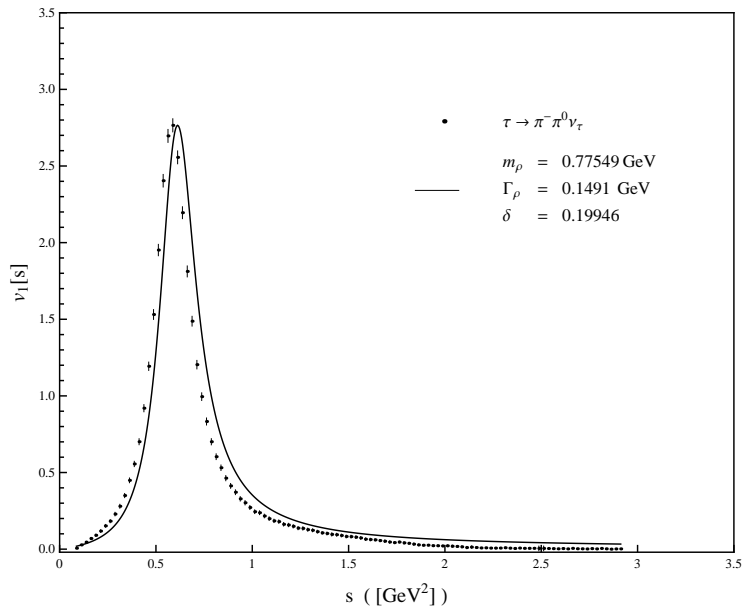


Figure 5.2: Breit-Wigner approximation of the vector channel with parameters  $m_\rho = 0.77549 \text{ GeV}$ ,  $\Gamma_\rho^{\text{full}} = 0.1491 \text{ GeV}$  from the PDG, and fitted  $\delta = 0.19946$ .

It was seen how the  $\rho$  resonance can be approximated by a spectral function that uses the Breit-Wigner parametrisation of the spectral density. Using the full width at half maximum does not account for the full dynamics of the decay  $\rho^- \rightarrow \pi^- \pi^0$  since it does not include the momentum-dependence in the  $\rho$ -meson decay width. In the next section the fully  $s$ -dependent spectral density (5.5) will be calculated.

### 5.3 Spectral Density based on the $s$ -Dependent Decay Width $\Gamma_{\rho^- \rightarrow \pi^- \pi^0}(s)$ from the Linear Sigma Model

The dynamics of the decaying  $\rho$  meson is described by the momentum-dependent decay width  $\Gamma_{\rho^- \rightarrow \pi^- \pi^0}(s)$  which has been calculated within the  $U(2)_L \times U(2)_R$  Linear Sigma Model in [28] and can now be inserted into the definition of the spectral density (5.5).

The result for the decay width is

$$\Gamma_{\rho^- \rightarrow \pi^- \pi^0}(s) = \frac{m_\rho^5}{48\pi m_{a_1}^4} \left[ 1 - \left( \frac{2m_\pi}{\sqrt{s}} \right)^2 \right]^{\frac{3}{2}} \left[ g_1 Z^2 + \frac{g_2}{2} (1 - Z^2) \right]^2. \quad (5.9)$$

The parameters  $g_1$  and  $g_2$  are given by

$$g_1 = \frac{m_{a_1}}{Z f_\pi} \sqrt{1 - \frac{1}{Z^2}}, \quad (5.10)$$

$$g_2 = \frac{2}{Z^2 - 1} \left( g_1 Z^2 - \frac{4m_{a_1}^2}{m_\rho} \sqrt{\frac{3\pi \Gamma_{\rho^- \rightarrow \pi^- \pi^0}}{(m_\rho^2 - 4m_\pi^2)^{\frac{3}{2}}}} \right). \quad (5.11)$$

They are related to each other in such a way that, independent from the choice of the parameters  $Z$  and  $m_{a_1}$ , the momentum-dependent decay width reproduces the full width if  $s = m_\rho^2$ :

$$\Gamma_{\rho^- \rightarrow \pi^- \pi^0}(m_\rho^2) = \Gamma_\rho^{\text{full}}.$$

The fully  $s$ -dependent spectral density  $v_1(s)$  based on  $\Gamma_{\rho^- \rightarrow \pi^- \pi^0}(s)$  reads

$$v_1(s) = \frac{4\pi}{S_{EW}} (\delta s)^2 \frac{1}{s} \frac{\sqrt{s} \Gamma_{\rho^- \rightarrow \pi^- \pi^0}(s)}{(s - m_\rho^2)^2 + (\sqrt{s} \Gamma_{\rho^- \rightarrow \pi^- \pi^0}(s))^2}. \quad (5.12)$$

Figure 5.3 presents the result for the spectral density with momentum dependent decay width  $\Gamma_{\rho^- \rightarrow \pi^- \pi^0}(s)$  and the  $\rho$  mass and width as they are given by the PDG. The vector-channel coupling  $\delta = 0.20625$  was again fitted to the value of the peak. It is surprisingly close to the value that was obtained by the convolution formula in (5.2) which was based on the assumption that  $\rho$  was stable, but here the full dynamical process of the  $\rho$  meson decay is described. With one free parameter and the momentum-dependent  $\rho$  decay width in (5.5), the vector-channel spectral density is well described.

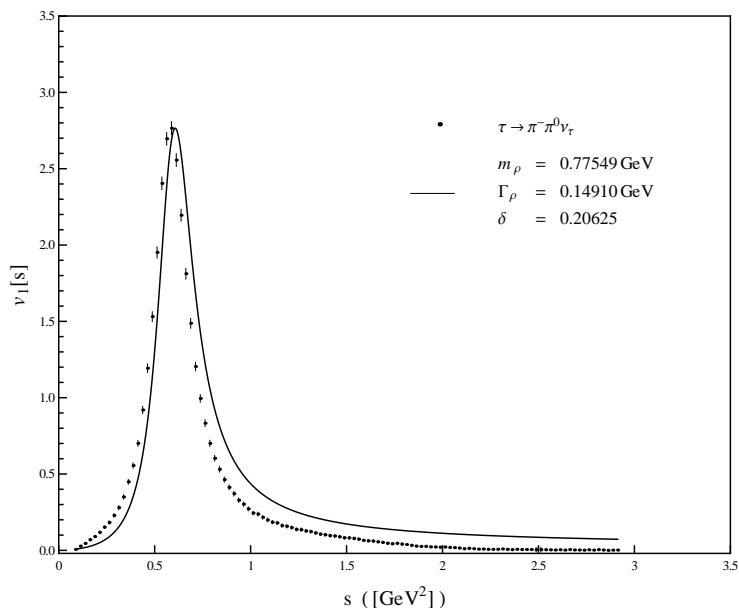


Figure 5.3: The vector spectral density  $v_1(s)$  based on the  $s$ -dependent decay width  $\Gamma_{\rho^- \rightarrow \pi^- \pi^0}(s)$  from the Linear Sigma Model with mass  $m_\rho = 0.77549$  GeV, full width  $\Gamma_{\rho^- \rightarrow \pi^- \pi^0}(m_\rho^2) = 0.14910$  GeV from the PDG, and fitted  $\delta = 0.20625$ .

### 5.3.1 Fitted Spectral Function based on $\Gamma_{\rho^- \rightarrow \pi^- \pi^0}(s)$

However, there is still the small shift towards the higher  $s$ -range, that was already seen in the previous section for the Breit-Wigner spectral density. As it was, e.g., shown in [29] the values for the obtained masses for the  $\rho$  meson depend strongly on the underlying parametrisation of the momentum-dependent decay width.

Thus, the spectral density with momentum-dependent decay width (5.12) is subjected to a fit with respect to the  $\rho$  mass and width, and the vector-coupling  $\delta$ . The fitting method is the so-called  $\chi^2$ -fit, that is based on the method of the least squares.

The result is shown in Figure 5.4. The vector channel coupling  $\delta$  obtains a small downward scaling to

$$\delta = 0.20397 \quad (5.13)$$

but is of almost the same size as the previous results from the convolution formula,  $\delta = 0.20662$ , and the simply to the peak-value fitted coupling  $\delta = 0.20625$ .

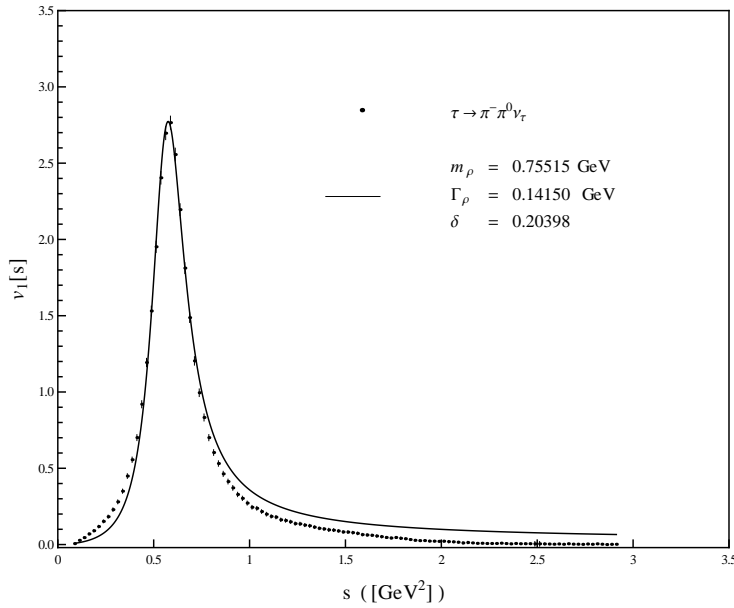


Figure 5.4: The vector-channel spectral density  $v_1(s)$  based on the  $s$ -dependent decay width  $\Gamma_{\rho^- \rightarrow \pi^- \pi^0}(s)$  from the Linear Sigma Model and fitted parameters:  $m_\rho = 0.75515$  GeV,  $\Gamma_{\rho^- \rightarrow \pi^- \pi^0}(m_\rho^2) = 0.14150$  GeV, and  $\delta = 0.20397$ .

For  $\rho$  mass and width the values

$$m_\rho = 0.75515 \text{ GeV} , \quad (5.14)$$

$$\Gamma_{\rho^- \rightarrow \pi^- \pi^0}(m_\rho^2) = 0.14150 \text{ GeV} \quad (5.15)$$

were obtained. With these fitted values the spectral function is shifted about  $30 \text{ MeV}^2$  to the lower  $s$ -range. The shifted  $\rho$  mass  $m_\rho = 0.75515$  GeV is only about 2.6% smaller than the value for the  $\rho$  mass given by the PDG,  $m_\rho = 0.77549$  GeV.

For  $s$ -values above  $\approx 0.7$  GeV the spectral density lies slightly above the data. This deviation results from the diverging contributions in the self-energy of the  $\rho$  meson. They correspond to the loop diagram that was discussed in (4.8). The result for the vector-channel spectral density can

then be even further improved by multiplying the momentum-dependent decay width with a regularisation function which is defined by

$$f_{\Lambda}(s) = \exp\left[\frac{4m_{\pi}^2 - s}{\Lambda^2}\right]. \quad (5.16)$$

The regularisation function  $f_{\Lambda}(s)$  is based on the exchanged momentum in the decay process and a cut-off parameter  $\Lambda$  which is of dimension GeV.

The  $s$ -dependent width of the resonance is then modified to

$$\Gamma_{\rho^{-} \rightarrow \pi^{-} \pi^0}(s) \xrightarrow{f_{\Lambda}(s)} \Gamma_{\rho^{-} \rightarrow \pi^{-} \pi^0}(s) e^{\frac{4m_{\pi}^2 - s}{\Lambda^2}}. \quad (5.17)$$

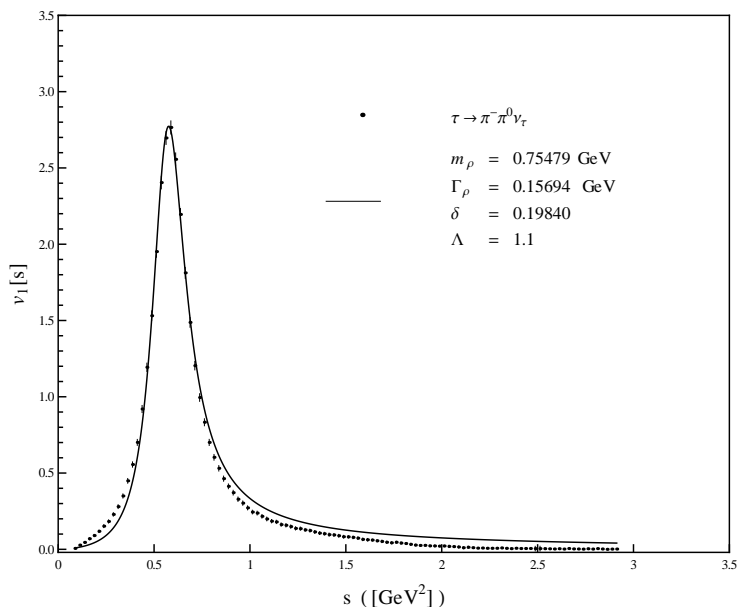


Figure 5.5: Fit to  $v_1(s)$  with  $s$ -dependent  $\rho$  decay width from the Linear Sigma Model and cut-off  $\Lambda = 1.1$  GeV and fitted values  $m_{\rho} = 0.75479$  GeV,  $\Gamma_{\rho^{-} \rightarrow \pi^{-} \pi^0}(m_{\rho}^2, \Lambda) = 0.15694$  GeV, and  $\delta = 0.19840$ .

While the value of the  $\rho$  mass is almost insensitive to value of the cut-off parameter, the full width depends strongly on the choice of the cut-off parameter  $\Lambda$ . With decreasing  $\Lambda$  the “full” width  $\Gamma_{\rho}^{\text{full}} = \Gamma_{\rho^{-} \rightarrow \pi^{-} \pi^0}(s = m_{\rho}^2)$  becomes unphysically large. This is, of course, no surprise as the regularisation function is a multiplicative factor in the decay width. Thus, the lower bound of the cut-off parameter was chosen to be 1.1 GeV. Then the result for the decay width  $\Gamma_{\rho}^{\text{full}}$  was stable and did not run to unphysically large values anymore.

The results for the fit with cut-off parameter  $\Lambda = 1.1$  GeV are

$$\delta = 0.19840 , \quad (5.18)$$

$$m_\rho(\Lambda) = 0.75479 \text{ GeV} , \quad (5.19)$$

$$\Gamma_{\rho^- \rightarrow \pi^- \pi^0}(m_\rho^2, \Lambda) = 0.15694 \text{ GeV} . \quad (5.20)$$

The fit to the spectral density with cut-off yields a decreasing  $\rho$  mass and an increasing  $\rho$  full width.

The fitted spectral density with momentum-dependent  $\rho$  decay width and cut-off is shown in Figure 5.5. The diverging contributions from the  $\rho$ -meson self-energy are almost entirely removed by the cut-off and the function smoothly follows the lineshape of the data. The spectral density  $v_1(s)$  together with the momentum-dependent decay width derived from the Lagrangian of the  $U(2)_L \times U(2)_R$  Linear Sigma Model reproduces the exclusive two-pion vector-channel spectral density in very good agreement with the data, if the  $\rho$  mass and width are slightly modified. The result can be even more improved if a cut-off is applied.

### 5.3.2 Comparison to Breit-Wigner with fitted Parameters $\delta$ and $m_\rho$

If the fitted parameters are inserted into the Breit-Wigner spectral density the result in Figure 5.6 is obtained. By the fitted mass the Breit-Wigner spectral density is shifted to a lower  $s$ -range and its peak position coincides now with the peak position of the data. However, it obtains a peak value that is too large and exceeds the data.

Compared to the spectral density with momentum dependent decay width the Breit-Wigner approximation yields underestimated values for the vector-channel coupling  $\delta$  and also underestimated values for the full width of the  $\rho$  resonance.

It will now be examined how other parametrisations for the  $s$ -dependent  $\rho$  decay width can be applied to calculate the spectral density for the vector channel.



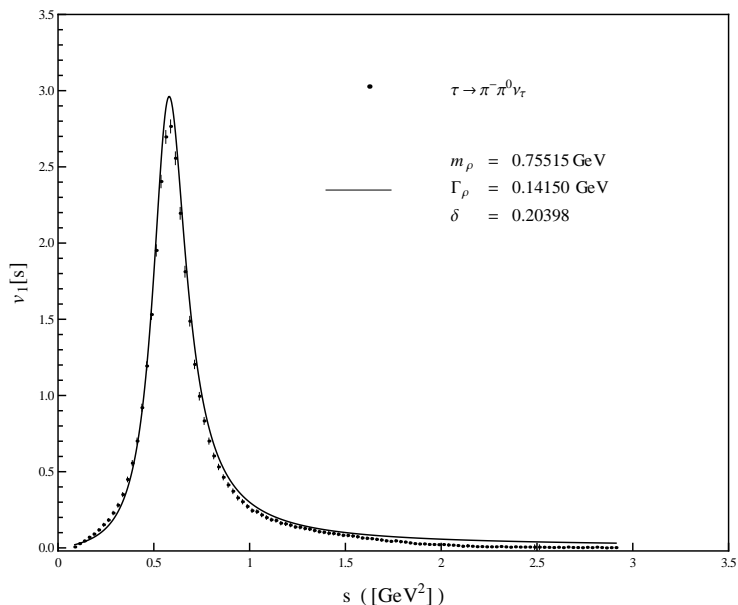


Figure 5.6: Result for  $v_1(s)$  with the Breit-Wigner spectral density and the fitted parameters from (5.15):  $m_\rho = 0.75515$  GeV,  $\Gamma_\rho^{\text{full}} = 0.1415$  GeV, and  $\delta = 0.20398$ .

## 5.4 Comparison to other Parametrisations for the $W\rho$ Vertex and the $s$ -Dependent $\rho$ Decay Width

### 5.4.1 Momentum-Independent $W\rho$ Mixing

One possibility to avoid the shift of the  $\rho$  mass and keep the values given by the PDG is to generate the  $W\rho$  vertex within the Linear Sigma model by a non-derivative coupling.

Therefore, the additional term that was introduced to the Lagrangian at the end of Section 2.2 in (2.108) is replaced by

$$\mathcal{L}_{mi} = \frac{g \cos \theta_C \delta m_\rho}{2} \text{Tr}[W_\mu \rho^\mu] . \quad (5.21)$$

The additional constant factor  $m_\rho$  could, in principle, be absorbed in the coupling constant  $\delta$ . Writing it down explicitly in the above Lagrangian helps to obtain the vector-channel coupling with a numerical value that can be compared to the results of the previous sections.

The “new” spectral function, with the non-derivative coupling for the  $W\rho$  mixing term reads now

$$v_1^{\text{nd}}(s) = \frac{(2\pi)^2}{S_{EW}} (\delta m_\rho^2)^2 \frac{1}{s} \rho_V(s) , \quad (5.22)$$

where for  $\rho_V(s)$  one can again insert either the Breit-Wigner approximation (5.4) based on the full width  $\Gamma_\rho^{\text{full}}$  or the fully  $s$ -dependent spectral density (5.5) based on the momentum-dependent decay width. The result for this approximation with PDG values for  $m_\rho$  and  $\Gamma_\rho^{\text{full}}$  is shown in Fig. 5.7. Again the vector-coupling  $\delta$  was fitted so that the spectral density obtains the peak value of the data.

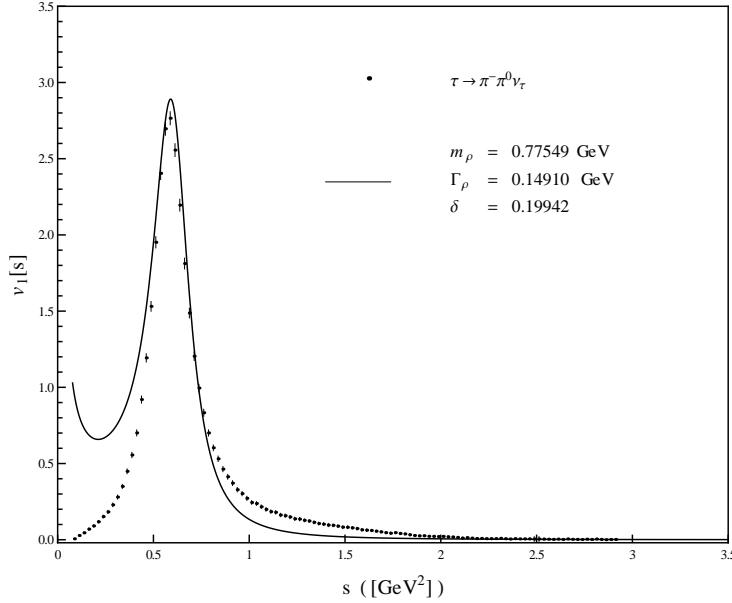


Figure 5.7: Breit-Wigner approximation of the vector channel spectral density  $v_1^{\text{nd}}(s)$  with non-derivative coupling in the  $W\rho$  mixing Lagrangian. Mass  $m_\rho = 0.77549$  GeV and full width  $\Gamma_\rho^{\text{full}} = 0.1491$  GeV are the values from the PDG and the vector coupling is fitted to  $\delta = 0.19942$ .

The peak of  $v_1^{\text{nd}}(s)$  is moved to the correct position. But the spectral density now only reproduces the data around the position of the peak. For small  $s$  and above the  $2\pi$ -production threshold the spectral density based on the non-derivative coupling yields a too large result for the two-pion decay and for  $s \gtrsim 0.7$  GeV<sup>2</sup> the calculated spectral density goes much faster to zero than the data. Moreover, in the low  $s$  region the spectral density  $v_1(s)$  based on full width  $\Gamma_\rho^{\text{full}}$  already starts to diverge above the threshold for two-pion production. Because of the constant vector-channel coupling  $\sim \delta m_\rho$  the  $1/s$ -dependence in the definition of the spectral function  $v_1(s)$  becomes dominant for small  $s$ . With a non-derivative vector-channel coupling  $\sim \delta m_\rho$  only the data in the range  $0.4$  GeV<sup>2</sup>  $< s < 0.7$  GeV<sup>2</sup> can be described.

Figure 5.8 presents the result for the fully momentum-dependent spectral density based on the decay width  $\Gamma_{\rho^- \rightarrow \pi^- \pi^0}(s)$  and with non-derivative coupling. Although, the peak is again shifted to the right position the result is, compared to the previous case of Breit-Wigner, not improved. The fully

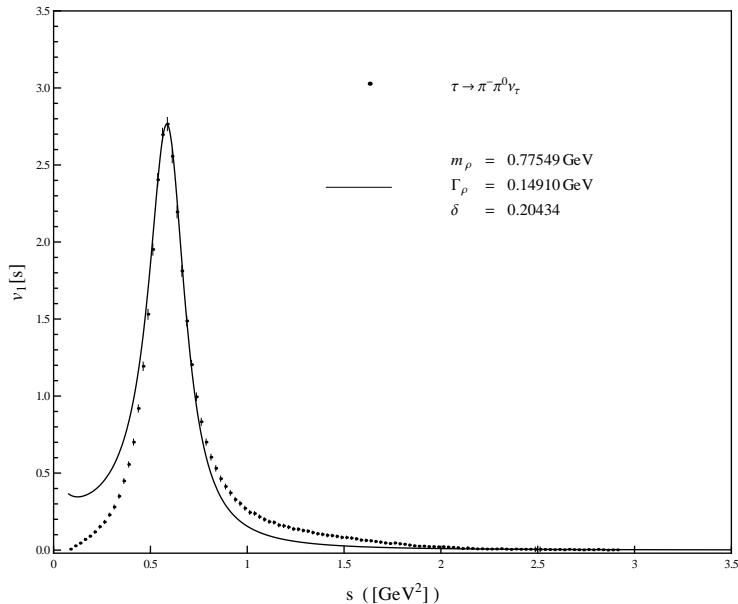


Figure 5.8: Spectral density based on the momentum-dependent decay width  $\Gamma_{\rho^- \rightarrow \pi^- \pi^0}(s)$  with non-derivative coupling in the  $W\rho$  mixing term;  $m_\rho = 0.77549$  GeV and  $\Gamma_{\rho^- \rightarrow \pi^- \pi^0}(m_\rho^2) = 0.1491$  GeV are the values from the PDG, and the vector coupling is fitted to  $\delta = 0.20434$ .

$s$ -dependent spectral density also shows a divergence above the two-pion threshold and lies below the data for  $s \gtrsim 0.7$  GeV<sup>2</sup>.

The spectral density based on a non-derivative coupling in the  $W\rho$  mixing term, cannot reproduce the data as well, as it was done with the spectral density based on the derivative coupling from

$$\mathcal{L}_{W\rho} = \frac{\delta g \cos \theta_C}{2} \text{Tr}[W_{\mu\nu} L^{\mu\nu}]. \quad (5.23)$$

Moreover, apart from the divergence in the low  $s$  region which is caused by the constant coupling, implementing the  $W\rho$  mixing by (5.21) would destroy the gauge invariance of the Lagrangian, while its only advantage lies in the fact that one could keep the  $\rho$  mass and width fixed to the values that are given by the Particle Data Group.

These values are, however, strongly dependent on the momentum-dependent  $\rho$  decay width which enters, e.g., the spectral density. Therefore the results for two other  $s$ -dependent decay widths are examined in the next subsection. One is the decay width of Gounaris and Sakurai and the other one is a decay width Vojik and Lichard have used in order to fit the  $\rho$  form factors, for the experiments CMD-2, SND, and KLOE.

### 5.4.2 Two other Parametrisations of the $\rho$ Decay Width

In [29] Vojik and Lichard have shown that the obtained values for the  $\rho$  mass and width depend strongly on the underlying parametrisation of the  $\rho$  decay width. Based on two parametrisations of the  $\rho$  resonance's contribution to the pion electromagnetic form factor they fitted the experimental data of different collaborations (CMD-2, SND, KLOE) and compared the obtained masses and widths.

They used two different formulas for the  $\rho^- \rightarrow \pi^- \pi^0$  decay width. On average, the values based on the parametrisation

$$\Gamma_{\text{VL}}(s) = \Gamma_\rho \frac{m_\rho^2}{s} \left( \frac{s - 4m_\pi^2}{m_\rho^2 - 4m_\pi^2} \right)^{\frac{3}{2}}, \quad (5.24)$$

are about 10 MeV smaller than the ones obtained from the generally used Gounaris-Sakurai parametrisation

$$\Gamma_{\text{GS}}(s) = \Gamma_\rho \frac{m_\rho}{\sqrt{s}} \left( \frac{s - 4m_\pi^2}{m_\rho^2 - 4m_\pi^2} \right)^{\frac{3}{2}}, \quad (5.25)$$

which is also the parametrisation underlying the Particle-Data-Group's data for the  $\rho$  mass and width.

The decay width in (5.24) is additionally modified by a regularisation function

$$\exp \left\{ \frac{m_\rho^2 - s}{24\beta^2} \right\}, \quad (5.26)$$

with cut-off

$$\beta = 0.4 \text{ GeV}. \quad (5.27)$$

Table 5.1 shows the results for  $\rho$  mass and width which they obtained by using the two decay widths in (5.25) and (5.24) to calculate the electromagnetic form factors of the  $\rho$  decay.

Both momentum-dependent decay widths  $\Gamma_{\text{VL}}(s)$  and  $\Gamma_{\text{GS}}(s)$  are now inserted into the definition of the vector-channel spectral density (5.5). It was then examined how the mass and width that were obtained from fitting the KLOE data are, when applied to the ALEPH data, can describe the two-pion vector channel.

Figure 5.9 shows the result for the spectral density based on  $\Gamma_{\text{VL}}(s)$ , the cut-off  $\beta = 0.4 \text{ GeV}$ ,  $m_\rho = 0.76139 \text{ GeV}$ ,  $\Gamma_\rho = 0.14007 \text{ GeV}$ , and  $\delta = 0.20085$ .

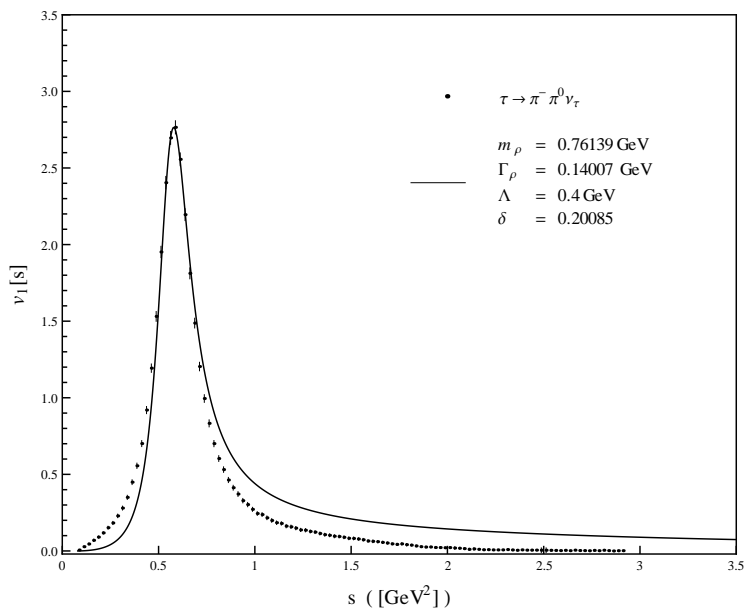


Figure 5.9: Spectral density  $v_1(s)$  for the Vojik and Lichard parametrisation of the  $s$ -dependent decay width,  $\Gamma_{\text{VL}}(s)$  with cut-off  $\beta = 0.4$  GeV applied to the ALEPH data with mass  $m_\rho = 0.76139$  GeV and width  $\Gamma_{\text{VL}}(m_\rho^2) = 0.14007$  GeV obtained from KLOE data, and with fitted  $\delta = 0.20085$ .

With a  $\rho$  mass that is shifted about 2.9% the spectral density based on  $\Gamma_{\text{VL}}(s)$  describes the peak and full width at half maximum reasonably well. The value for the vector coupling  $\delta = 0.20085$  was again fitted so that the spectral density describes the peak. However, although a cut-off of the form (5.27) is already included, the spectral density clearly gives too high values for the two-pion production in the higher  $s$ -range.

The result for the spectral density based on the Gounaris-Sakurai decay width  $\Gamma_{\text{GS}}(s)$  is presented in Fig. 5.10. The values for the  $\rho$  mass and the  $\rho$  full width are the results for the KLOE data and given in Table 5.1. It does

	$m_\rho$ [GeV]	$\Gamma_{\text{VL}}(m_\rho^2)$ [GeV]	$m_\rho$ [GeV]	$\Gamma_{\text{GS}}(m_\rho^2)$ [GeV]
CMD-2	0.76708	0.1361	0.7753	0.1423
SND	0.77460	0.1461	0.7746	0.1473
KLOE	0.76139	0.14007	0.76922	0.14471

Table 5.1: Results for the  $\rho$  mass and width obtained on the basis of the  $s$ -dependent parametrisation for the decay widths  $\Gamma_{\text{VL}}(s)$  and  $\Gamma_{\text{GS}}(s)$  as given in (5.24) and (5.25).

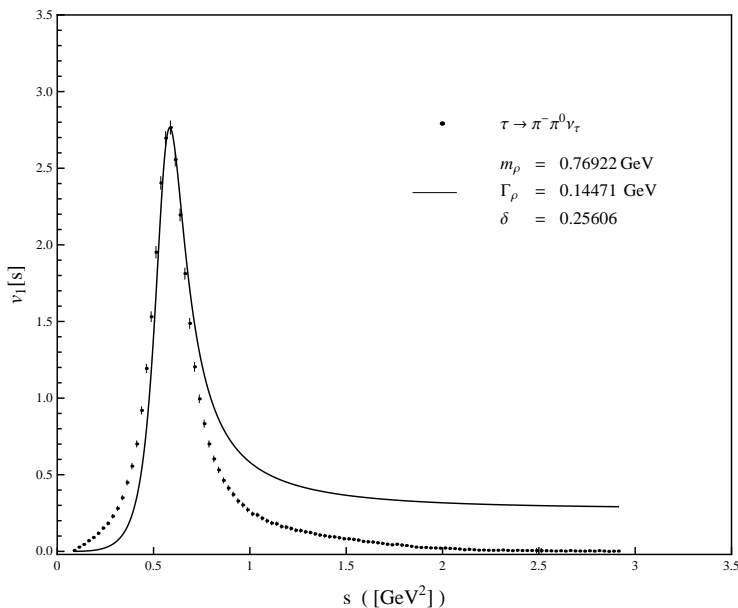


Figure 5.10: Spectral density  $v_1(s)$  for the Gounaris-Sakurai parametrisation of the  $s$ -dependent  $\rho$  decay width  $\Gamma_{\text{GS}}(s)$  applied to ALEPH data but with mass and width extracted from KLOE data:  $m_\rho = 0.76922$  GeV,  $\Gamma_{\text{GS}}(m_\rho^2) = 0.14471$  GeV, and fitted  $\delta = 0.25606$ .

not match the data as well as Vojik and Lichard's decay width  $\Gamma_{\text{VL}}(s)$ . The deviation from the data becomes much larger in the upper  $s$ -range.

In this parametrisation the vector coupling constant would be  $\delta = 0.25606$  which is about 25% higher than the values extracted from the other parametrisations. Taking  $\delta$  with a value about 0.25 would give much better results for the axial-vector channel<sup>3</sup> than with  $\delta \approx 0.2$ . Then it would not be necessary to change  $Z$  to a value that is not only outside the range  $1.47 \leq Z \leq 1.87$  as it was obtained by previous calculations of the  $\sigma \rightarrow \pi\pi$  decay width, but also predicts unphysically high values for the  $s$ -dependent width  $\Gamma_{a_1 \rightarrow \rho\pi}(s)$ .

However, as it can be clearly seen in Fig. 5.10 the full width at half maximum is not reproduced. Even with an additional regularisation function based on the momentum in (5.25), it is impossible to obtain the same width, the position of the peak and not such a strong deviation from the data points in the region of  $s > 0.7$  GeV. Moreover, a cut-off based on the Gounaris-Sakurai parametrisation would have to be approximately  $\Lambda \approx 1.8$  GeV in order to have a significant effect on the higher  $s$ -range and to obtain an appropriate width and for  $\Lambda \approx 1.8$  GeV. But then the value of the vector coupling decreases again to  $\delta = 0.19608$  and the problem with the size of

<sup>3</sup>In Section 6 the problems with the interdependencies of the coupling constants and the result for the axial-vector spectral density will be discussed in detail.

the pion wave-function renormalisation constant  $Z$  is recreated.

In this chapter the vector-channel spectral density parametrised within the  $U(2)_L \times U(2)_R$  Linear Sigma Model as it was developed in Chapter 2.2 has been calculated. The result agrees very well with the data for the exclusive two-pion vector channel given by the ALEPH collaboration. The free parameter  $\delta$  allows to adjust the height of the spectral functions. The results for  $\delta$  that were obtained for different parametrisations of the spectral function are summarised in Table 5.2.

It was found that none of the other examined parametrisations, the different expressions for the  $s$ -dependent decay width ( $\Gamma_{\text{VL}}(s)$   $\Gamma_{\text{GS}}(s)$ ) or another  $W\rho$  mixing term in the Lagrangian (5.21), lead to a better result for the spectral function, than it is obtained with the parametrisation of  $v_1(s)$  that bases on the  $\rho$  decay width from the Linear Sigma Model and  $s$ -dependent vertex with vector-channel coupling  $\delta$ .

Spectral density	$m_\rho$ [GeV]	$\Gamma(m_\rho^2)$ [GeV]	Vertex	$\delta$	Cut-off [GeV]
$\rho$ “stable”	0.77549	0.1491	$\delta s$	0.20662	none
Breit-Wigner	0.77549	0.1491	$\delta s$	0.19946	none
Breit-Wigner	0.77549	0.1491	$\delta m_\rho^2$	0.19942	none
Linear Sigma Model	0.77549	0.14910	$\delta s$	0.20625	none
<b>Linear Sigma Model</b>	<b>0.75515</b>	<b>0.14150</b>	<b><math>\delta s</math></b>	<b>0.20398</b>	<b>none</b>
Linear Sigma Model	0.75479	0.15694	$\delta s$	0.19840	$\Lambda = 1.1$
Linear Sigma Model	0.77549	0.14910	$\delta m_\rho^2$	0.20434	none
Vojik-Lichard	0.76139	0.14007	$\delta s$	0.20085	$\beta = 0.4$
Gounaris-Sakurai	0.76922	0.14471	$\delta s$	0.25606	none

Table 5.2: Values obtained for the  $W\rho$  coupling constant  $\delta$  for the different parametrisations of the  $\rho$  decay widths that enter the spectral density  $v_1(s)$ . The values in the line marked in red are the results of the fit to the vector channel spectral density and will be used for the axial-vector spectral density in the next chapter.

## Chapter 6

# Axial-Vector Channel Spectral Function

### 6.1 Breit-Wigner Spectral Density

The vector coupling constant  $\delta$  was determined in the previous chapter. The results will now be used to calculate the axial-vector channel's spectral function. The axial-vector spectral function's peak is not as sharp as the one of the vector spectral function, which leads to difficulties in the determination of the  $a_1$  meson mass. While the  $\rho$  spectral function clearly has its peak at  $v_1(s = 0.5875 \text{ GeV}^2) = 2.7654$ , the  $a_1$  resonance's peak is a broad distribution of three-pion final states between  $1.0625 \text{ GeV}^2 \leq s \leq 1.3375 \text{ GeV}^2$  with  $0.95407 \leq a_1(s) \leq 0.98189$ . In the PDG the  $a_1$  mass is given by  $m_{a_1} = (1.23 \pm 0.04) \text{ GeV}$ . The uncertainty in the full  $a_1$  width with  $0.25 \text{ GeV} < \Gamma_{a_1} < 0.6 \text{ GeV}$  is even larger. Also, recent publications by Wagner and Leupold [30, 31] have made the argument that the observed resonance might actually not be a  $\bar{q}q$  state, but a molecule-like, coupled  $\rho\pi$  state. So far, the resonance as it is shown in [25] was interpreted as the signal of the  $J^{PC} = 1^{++}$  mesonic resonance of the  $SU(N_f = 3)$  meson octet. In the following chapter, the resonance depicted in Fig. 6.1 will be studied under the assumption that the  $a_1(1260)$  resonance is indeed the  $\bar{q}q$  state that can be associated with the  $a_1$  meson of the  $N_f = 3$  meson octet and the chiral partner of  $\rho$ .

The intermediate decay processes of the axial-vector channel are identified as

$$\begin{aligned}\tau^- &\rightarrow W^- \nu_\tau \rightarrow 2\pi^- \pi^+ \nu_\tau (\pi^- 2\pi^0 \nu_\tau), \\ \tau^- &\rightarrow W^- \nu_\tau \rightarrow a_1^- \nu_\tau \rightarrow \rho^0 \pi^- \nu_\tau (\rho^- \pi^0 \nu_\tau) \rightarrow 2\pi^- \pi^+ \nu_\tau (\pi^- 2\pi^0 \nu_\tau),\end{aligned}$$



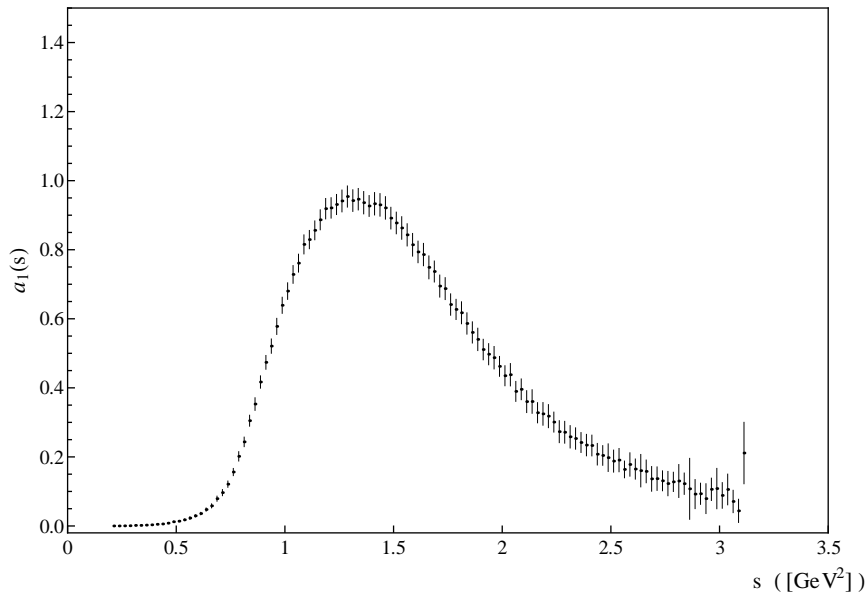


Figure 6.1: The exclusive axial-vector spectral function for the process  $\tau^- \rightarrow 3\pi^-\nu_\tau, (2\pi^-\pi^+\nu_\tau + \pi^-2\pi^0\nu_\tau)$  as it was published by the ALEPH collaboration in [25]. The raw data for the spectral function and also its errors are found in [27].

$$\begin{aligned} \tau^- &\rightarrow W^- \nu_\tau \rightarrow a_1^- \nu_\tau \rightarrow \sigma \pi^- \nu_\tau \rightarrow 2\pi^- \pi^+ \nu_\tau, \\ \tau^- &\rightarrow W^- \nu_\tau \rightarrow a_1^- \nu_\tau \rightarrow f_0 \pi^- \nu_\tau \rightarrow 2\pi^- \pi^+ \nu_\tau, \end{aligned}$$

and

$$\tau^- \rightarrow W^- \nu_\tau \rightarrow a_1 \nu_\tau \rightarrow 2\pi^- \pi^+ \nu_\tau (\pi^- 2\pi^0 \nu_\tau).$$

The branching fractions for the two different final states  $2\pi^-\pi^+\nu_\tau$  and  $\pi^-2\pi^0\nu_\tau$  are almost identical  $B(\tau^- \rightarrow 2\pi^-\pi^+) = (9.041 \pm 0.097)\%$  and  $B(\tau^- \rightarrow \pi^-2\pi^0) = (9.239 \pm 0.124)\%$ . A small breaking of strong isospin symmetry causes the mass difference between the charged and neutral pion mass and this in turn explains why these two branching fractions are not of exactly the same size. Since the two branching fractions are almost equal ( $\Gamma_{2\pi^-\pi^+}/\Gamma_{\pi^-2\pi^0} = 0.98$ ), it is valid to assume that the decay of  $a_1$  takes place predominantly via the  $\rho\pi$  intermediate state [25, 32]. If, in this decay channel, the contributions from the processes involving  $\sigma$  and  $f_0$  were not suppressed, one would see a larger difference in the two branching fractions<sup>1</sup>. There exist data on the  $a_1$  branching fractions, however, the PDG does not use the data published in [32] for further analysis. Since the dependence on the pion wave-function renormalisation constant  $Z$  is at parts very complicated, the results in [32] will nevertheless be used selectively in the course of this chapter.

<sup>1</sup>Here,  $f_0$  describes the  $f_0(1370)$  resonance.

The axial-vector spectral function in the parametrisation of the Linear Sigma Model is given by (4.27),

$$a_1(s) = \frac{(2\pi)^2}{S_{EW}} (\delta s + g_1 \phi_0^2) \frac{1}{s} \frac{\rho_A(s)}{N}. \quad (6.1)$$

The chiral condensate  $\phi_0$  is related to the pion wave-function renormalisation constant  $Z$  and the pion decay constant  $f_\pi$  by

$$\phi_0 = Z f_\pi. \quad (6.2)$$

The (axial-) vector-scalar coupling  $g_1$  depends on  $Z$  as

$$g_1 = \frac{m_{a_1}}{Z f_\pi} \sqrt{1 - \frac{1}{Z^2}}. \quad (6.3)$$

Previous calculations of the  $\sigma \rightarrow \pi\pi$  decay rate within the  $U(2)_L \times U(2)_R$  Linear Sigma Model in [28] predict  $Z$  to be in the range  $1.47 < Z < 1.87$ .

Another  $Z$  dependence is found in the process  $a_1 \rightarrow \rho\pi$  which yields the dominant contribution to the axial-vector channel. Its decay rate  $\Gamma_{a_1 \rightarrow \rho\pi}(s)$  has been calculated in [28] as

$$\Gamma_{a_1 \rightarrow \rho\pi}(s) = \frac{k(\sqrt{s}, m_\rho, m_\pi)}{12\pi m_{a_1}^2} \left[ h_{\mu\nu}^2 - \frac{(h_{\mu\nu} K_1^\nu)^2}{m_\rho^2} - \frac{(h_{\mu\nu} P^\mu)^2}{m_{a_1}^2} + \frac{(h_{\mu\nu} P^\mu K_1^\nu)^2}{m_\rho^2 m_{a_1}^2} \right]. \quad (6.4)$$

The function

$$k(m_a, m_b, m_c) = \frac{1}{2m_a} \sqrt{m_a^4 - 2m_a^2(m_b^2 + m_c^2) + (m_b^2 - m_c^2)^2} \theta(m_a - m_b - m_c) \quad (6.5)$$

describes the momentum exchange of the process  $a \rightarrow bc$ . The momentum of  $a_1$  is denoted by  $P^\mu$ , that of  $\rho$  by  $K_1^\mu$ , and that of  $\pi$  by  $K_2^\mu$ . The amplitude

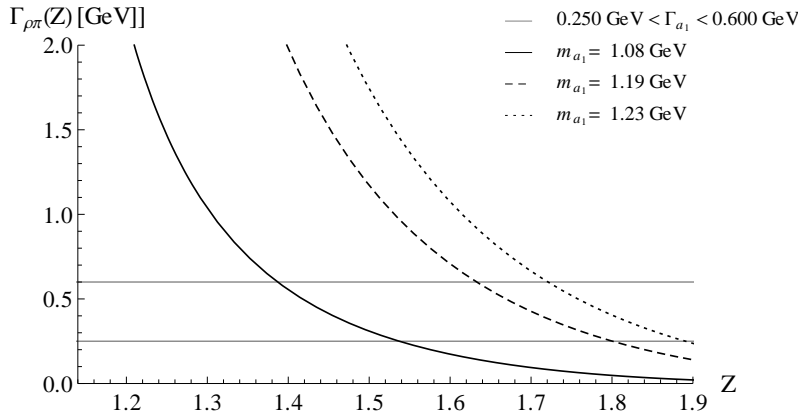


Figure 6.2: The dependence of the  $a_1 \rightarrow \rho\pi$  decay width  $\Gamma_{a_1 \rightarrow \rho\pi}(Z)$  depending on  $Z$  as calculated by [28].

is then obtained from the term in the square brackets. Its explicit form is found in [28] as well.

The decay rate in (6.4) increases with smaller values of  $Z$  and decreases when  $Z$  assumes higher values (Figure 6.2). For the mass  $m_{a_1} = 1.23$  GeV which is given by the PDG and the range of the full  $a_1$  decay width given by  $0.25 \text{ GeV} < \Gamma_{a_1} < 0.6 \text{ GeV}$  the pion renormalisation constant  $Z$  is limited to  $1.47 < Z < 1.87$ . This result agrees with the interval that has been determined from the  $\sigma \rightarrow \pi\pi$  decay width. Its range is shifted to smaller values of  $Z$  if the  $a_1$  mass is taken to be smaller than the mass given by the PDG. If  $m_{a_1} \approx 1.08$  GeV, the value of  $Z$  decreases to  $Z = 1.38$  for the upper bound of the decay rate  $\Gamma_{a_1} = 0.600$  GeV.

Before calculating the fully  $s$ -dependent spectral density  $a_1(s)$  based on  $\Gamma_{a_1 \rightarrow \rho\pi}(s)$ , the spectral function based on the Breit-Wigner approximation will be used as a consistency check for the parameters that have been obtained from the vector channel. The Breit-Wigner spectral density for the axial-vector channel reads

$$\rho_A^{\text{BW}}(s) = \frac{1}{\pi} \frac{m_{a_1} \Gamma_{a_1}^{\text{full}}}{(s - m_{a_1}^2)^2 + (m_{a_1} \Gamma_{a_1}^{\text{full}})^2}. \quad (6.6)$$

For calculating the spectral function  $a_1(s)$  with the Breit-Wigner spectral density those values of  $Z$  are used that can be associated with the  $a_1$  full width at half maximum  $\Gamma_{a_1}^{\text{full}} = \Gamma_{a_1 \rightarrow \rho\pi}(m_{a_1}^2, Z) = 0.4545$  GeV for a given mass  $m_{a_1}$ . The full width at half maximum is directly taken from the data depicted in Figure 6.1.

The results from the Breit-Wigner spectral density for three generically chosen masses  $m_{a_1} = 1.23$  (1.19, 1.08) GeV are shown in Figure 6.3. The mass  $m_{a_1} = 1.23$  GeV is the value that is usually associated with the  $a_1$  resonance,  $m_{a_1} = 1.19$  GeV is the lower bound given by the PDG and  $m_{a_1} = 1.08$  GeV lies slightly above the result of the  $a_1$  mass obtained in [20].

Although it was expected that the Breit-Wigner parametrisation is not really suitable to describe such a broad resonance as the axial-vector resonance, it is still surprising that the spectral function is not even approximately of the correct size. Naively one would expect the spectral function to deviate from the line shape of the data in form of a too narrow width. But here the calculated spectral density is about a factor 1/2 too small and describes only half of the data.

The dependence of the position of the peak on the choice of the  $a_1$  mass is also seen in Figure 6.3. As for the vector channel the peak position is shifted to smaller values of  $s$  for smaller masses  $m_{a_1}$ . Obviously  $m_{a_1} = 1.23$  GeV

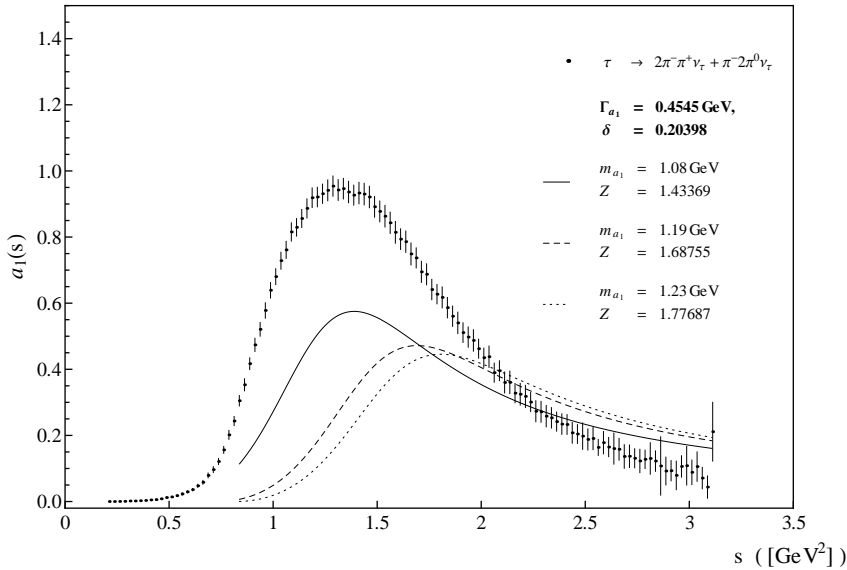


Figure 6.3: The axial-vector spectral functions in the Breit-Wigner approximation for  $m_{a_1} = 1.08$  (1.19, 1.23) GeV with  $\delta = 0.20398$ . The pion renormalisation constant  $Z$  is chosen such that  $\Gamma_{a_1 \rightarrow \rho\pi}(m_{a_1}, \Gamma_\rho, Z) = 0.4545$  GeV.

and  $m_{a_1} = 1.19$  GeV are too large to reproduce the correct peak position, while  $m_{a_1} = 1.08$  GeV yields a much better result in terms of the peak position.

## 6.2 Estimates of the Parameters $Z$ and $\delta$

The momentum-dependent spectral function  $a_1(s)$  based on  $\Gamma_{a_1 \rightarrow \rho\pi}(s)$  in Equation (6.4) could now already be calculated. But, since  $\Gamma_{a_1 \rightarrow \rho\pi}(s)$  also depends on the  $a_1$  meson's mass, it seems useful to first calculate the Breit-Wigner parametrisation and reduce the complexity of the interdependencies between the parameters. From the vector channel it is known that the Breit-Wigner spectral density works very well to approximate the fully  $s$ -dependent spectral function of this model. This enormously simplifies the investigation of the role of the  $a_1$  mass as well as the effect of different choices of the  $a_1$  full width and the influence of the parameters  $Z$  and  $\delta$ . In order to solve the problem of the too small spectral function, it was also attempted to obtain different combinations of  $Z$  and  $\delta$ .

### 6.2.1 Pion Renormalisation Constant $Z$

First,  $\delta$  remains fixed to the value obtained from the vector channel,

$$\delta = 0.20398 , \quad (6.7)$$

which is the result of the fit for the fully  $s$ -dependent vector-channel spectral function, marked in red in Table 5.2. The result is based on the assumption that the  $2\pi$  vector channel is dominated by the  $\rho$  resonance and that the contributions arising from the direct  $W^-$  into  $\pi^-\pi^0$  decay are negligibly small.

In the axial-vector channel  $W$  transforms into an  $a_1$  meson which then via its intermediate states<sup>2</sup> decays into three pions. Now, in order to estimate a new value for  $Z$  the convolution formula (4.11) was applied to the three-pion  $\tau$  decay. Here, the assumption was made that all  $3\pi$  final states can only occur via an intermediate  $a_1$  meson and then again that all intermediate  $a_1$  mesons result in three final pions:

$$\Gamma_{\tau^- \rightarrow 3\pi\nu\tau}^{exp} = \frac{m_\tau^3}{8\pi m_\rho^2} \left[ \frac{g^2 \cos \theta_C}{4\sqrt{2}M_W^2} (\delta m_{a_1}^2 - g_1 \phi_0^2) \right]^2 \left( 1 - \frac{m_\rho^2}{m_\tau^2} \right)^2 \left( 1 + \frac{2m_\rho^2}{m_\tau^2} \right) . \quad (6.8)$$

Again, this is a strong simplification, but it seems to be more reasonable than simply guessing the value of  $Z$ . The values obtained for  $Z$  based on Equation (6.8) are found in Table 6.1. They also depend on the value of  $\delta$ , the coupling constant of the  $W\rho$  vertex. In this approach the pion renormalisation constant experiences a strong downward scaling to  $Z \sim 1.2$ , which causes the spectral function to obtain a height that is approximately of the same size as the data.

$\delta_{\text{LSM}} = 0.20398$			
$m_{a_1}$	1.23 GeV	1.19 GeV	1.08 GeV
$Z$	1.27942	1.27275	1.22276
$\delta_{\text{LSMcutoff}} = 0.19840$			
$m_{a_1}$	1.23 GeV	1.19 GeV	1.08 GeV
$Z$	1.23446	1.22959	1.18643

Table 6.1:  $Z$  values, calculated from Eq. (6.8), obtained for three  $a_1$  masses and vector-channel coupling  $\delta$ . The latter is the result from the fitted fully  $s$ -dependent spectral function in the vector channel  $v_1(s)$ ; without cut-off  $\delta = 0.20398$ , with cut-off  $\delta = 0.20398$ .

Figure 6.4 shows the results for three  $a_1$  masses,  $m_{a_1} = 1.08$  (1.19, 1.23) GeV, where each graph contains three possible choices of the full width  $\Gamma_{a_1}^{\text{full}}$ .

<sup>2</sup>The dominant  $a_1 \rightarrow 3\pi$  intermediate states are  $\rho\pi$  ( $\sim 60.19\%$ ),  $\sigma\pi$  ( $\sim 18.76\%$ ), and  $f_0\pi$  ( $\sim 7.40\%$ ). Since they are taken from [32], these branching fractions need to be treated carefully, too.

Again, with decreasing mass the spectral function is entirely shifted to smaller values of  $s$ . It is important to stress that the  $Z$  value used in the calculation of the spectral functions  $a_1(s)$  in Figure 6.4 is not the one which is obtained by [28]. Using the values given in Figure 6.4 to calculate the  $a_1 \rightarrow \rho\pi$  decay width will yield unphysically large results.

With a considerably smaller  $Z$ -value it is obviously possible to parametrise the line shape of the axial-vector channel very well. However, for  $m_{a_1} = 1.08$  GeV the  $Z$ -dependent decay rate  $\Gamma_{a_1 \rightarrow \rho\pi}(m_{a_1}^2)$  calculated from Equation (6.4) is already larger than 2 GeV (see Figure 6.2). As seen in Figure 6.2 there is a strong decrease for smaller  $Z$  and the decay width  $\Gamma_{a_1 \rightarrow \rho\pi}(m_{a_1}^2)$  becomes unphysically large.

The unphysically large  $a_1$  decay rate is a serious problem since it questions the consistency of the underlying model. One thing that has not been considered yet is the fact that according to the PDG the decay  $a_1 \rightarrow \rho\pi$  might account only for about 60.19% of the  $a_1$  decay, as it has been observed at the CLEO II detector and published in [32]. The PDG states that the data is not reliable and cannot be used for averages and fits. However, it is interesting to see if the assumption that only 60.19% of the three-pion final states result from the intermediate process  $a_1 \rightarrow \rho\pi$  would resolve the problem with the too small spectral density.

The underlying assumption for the determination of  $Z$  with respect to the  $a_1 \rightarrow \rho\pi$  decay width is that  $a_1$  decays predominantly via the  $\rho\pi$  channel. Since  $Z$  depends on the value of the decay width, one would expect  $Z$  to become smaller, if the dominance of the  $\rho\pi$  intermediate state is questioned. Then  $\Gamma_{a_1 \rightarrow \rho\pi}(m_{a_1}^2)$  would only account for 60.19% of the full width. However, for a smaller  $a_1$  decay width the obtained value for  $Z(m_{a_1}, \Gamma_{a_1})$  increases, e.g.

$$\begin{aligned} Z(1.08 \text{ GeV}, 0.4545 \text{ GeV}) &= 1.43369 , \\ Z(1.08 \text{ GeV}, 0.6 \cdot 0.4545 \text{ GeV}) &= 1.52204 . \end{aligned}$$

Thus, even if, in a first guess, a smaller decay width were used to find a new estimate on the value of  $Z$  the spectral function would remain at the same size and describe only about half of the experimental data. With  $\delta \simeq 0.2$ , as it is given from the vector channel,  $Z$  would have to be in the range  $0.12 < Z < 0.14$ .

With respect to the pion renormalisation constant  $Z$  it is concluded that it is not possible to modify  $Z$  in such a way that one would not encounter inconsistency problems, if  $\delta$  remains fixed to the value from the vector channel.

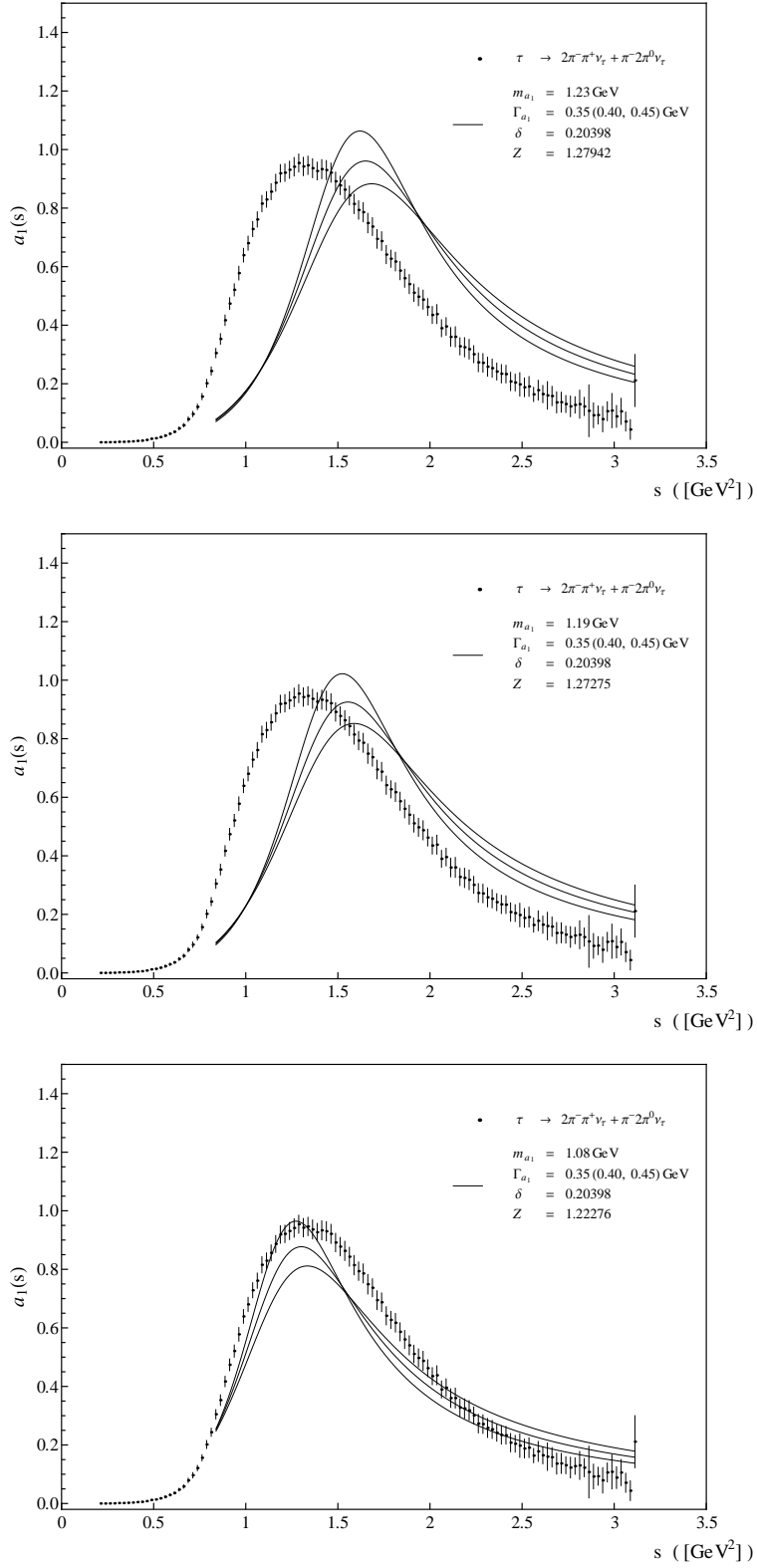


Figure 6.4: The axial-vector spectral functions in the Breit-Wigner approximation for three masses  $m_{a_1} = 1.23$  (1.19, 1.08) GeV and three full  $a_1$  decay widths  $\Gamma_{a_1}^{\text{full}} = 0.35$  (0.4, 0.45) GeV and  $m_{a_1} = 1.23$  GeV. The value  $Z = 1.27942$  is an approximation based on the partial decay width of  $\tau \rightarrow 2\pi^-\pi^+\nu_\tau$  ( $\pi^-2\pi^0\nu_\tau$ ) with  $\delta = 0.20398$  from the vector channel with Breit-Wigner approximation.

## 6.2.2 Vector Coupling $\delta$

Now it seems advisable to examine the role of the vector-channel coupling  $\delta$ . With the help of Equation (6.8)  $\delta$  is approximated with respect to the value of  $Z$  that reproduces  $\Gamma_{a_1 \rightarrow \rho\pi}(m_{a_1}^2, Z) = 0.4545 \text{ GeV}^2$ . Since  $\delta$  itself does not depend on  $m_{a_1}$  this is only done for  $m_{a_1} = 1.08 \text{ GeV}$  and the resonance's full width at half maximum  $\Gamma_{a_1}^{\text{full}} = 0.4545 \text{ GeV}$ . From (6.8) one obtains  $\delta = 0.2317$ . The result is shown in Figure 6.5. Clearly the result is

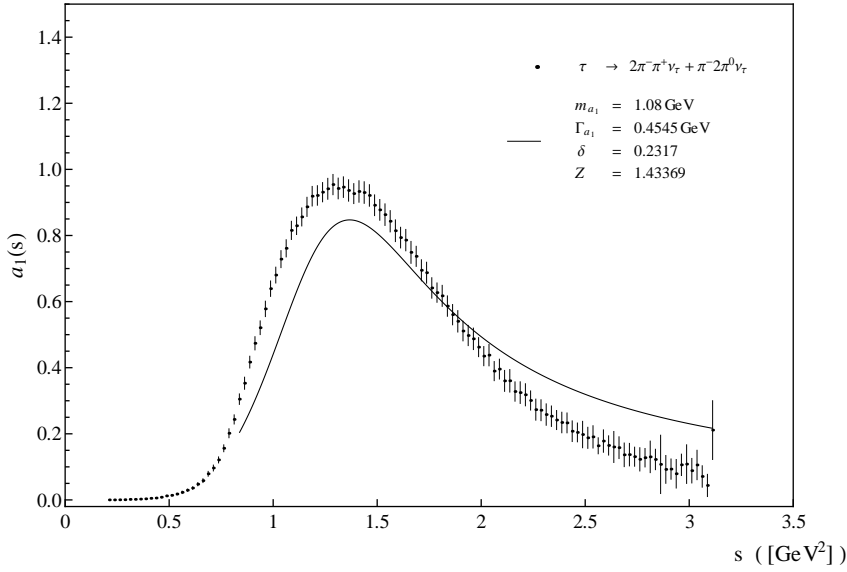


Figure 6.5: The axial-vector spectral functions in the Breit-Wigner approximation for  $m_{a_1} = 1.08 \text{ GeV}$  and full width at half maximum  $\Gamma_{a_1}^{\text{full}} = 0.4545 \text{ GeV}$ . Based on  $\Gamma_{\rho\pi}(Z = 1.43369) = 0.4545 \text{ GeV}$  the coupling  $\delta = 0.2317$  was obtained.

much better if one assumes  $\delta$  to be about 18% larger than the one that was obtained from the fit in Chapter 5.

The calculations made in Chapter 5 were based on the dominance of the  $\rho$  meson in the  $2\pi$  decay channel. The contributions from the  $W$  boson directly decaying in  $2\pi$  have been neglected. If the amplitude of the process  $W^- \rightarrow \pi^- \pi^0$  were destructively interfering with  $\rho^- \rightarrow \pi^- \pi^0$  it would lead to a bigger vector coupling  $\delta$ . That way  $Z$  would remain in the range predicted from previous calculations and it would also not enter a range where the  $\Gamma_{a_1 \rightarrow \rho\pi}(s)$  decay rate would become unphysically large.

The  $Z$  dependence of the calculated decay rate  $\Gamma_{\tau \rightarrow a_1 \nu_\tau}(Z)$  for the results of the fit to the fully  $s$ -dependent spectral function (see Table 6.1) is shown in Figure 6.6. The two constant lines describe the decay width of the process  $\tau \rightarrow 3\pi \nu_\tau$  with  $\Gamma_{\tau \rightarrow 3\pi \nu_\tau}^{\text{exp.}} = (4.1491 \pm 0.159) \cdot 10^{-13} \text{ GeV}$  given by the results



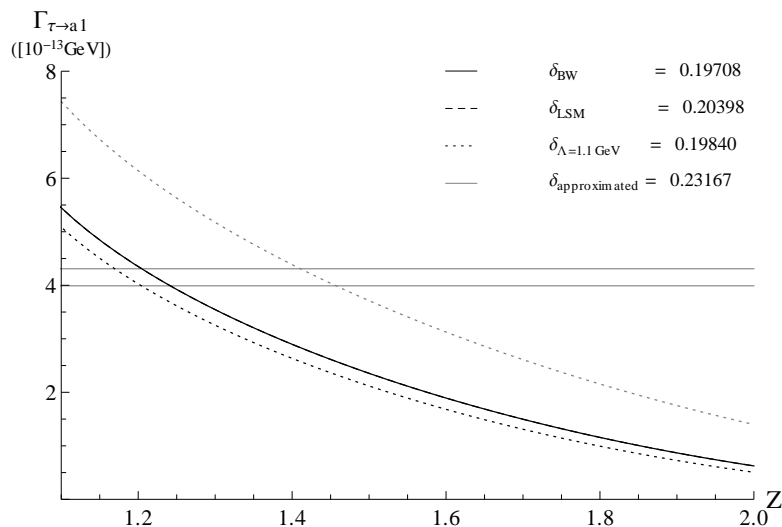


Figure 6.6: The calculated  $\Gamma_{\tau \rightarrow a_1}(Z)$  for different values of  $\delta$  compared to the  $\tau \rightarrow 2\pi^{-}\pi^{+} + \pi^{-}2\pi^{0}$  decay rate.

of the ALEPH collaboration. The decay rate  $\Gamma_{\tau \rightarrow a_1 \nu_\tau}(Z)$  for a given  $\delta$  agrees only in a small interval with the experimental data of  $\Gamma_{\tau \rightarrow 3\pi \nu_\tau}$ . But as expected, by assuming that  $\delta$  would be about 18% larger, the interval in which the calculated decay rate agrees with the experiment is shifted to higher values of  $Z$ .

The last attempt to find a possible solution for the misfit between the experimental data and the result for the spectral function based on the Breit-Wigner spectral density and the full width  $\Gamma_{a_1}^{\text{full}}$  is to investigate how the calculated spectral function is affected, if the results on the  $a_1 \rightarrow \rho\pi$  decay width from [32] are taken into account for an approximation. The convolution formula (6.8) couples the decay width  $\Gamma_{\tau \rightarrow \rho\pi}(s)$  to the spectral density distribution  $a_1(s)$ . In [32] the  $a_1$  to  $\rho\pi$  decay width is given with 60.19%. But from

$$\Gamma_{\tau \rightarrow 3\pi}^{\text{exp.}} \simeq 0.6 \cdot \Gamma_{\tau \rightarrow a_1 \nu_\tau}(m_{a_1}^2) \quad (6.9)$$

one obtains  $\delta = 0.2735$ . This is again significantly larger than the value obtained from the vector channel. Thus, in order to keep  $Z$  in the desired range, it is mandatory to examine the further contributions in the vector channel, which might result in an higher effective value of the vector coupling  $\delta$ .

### 6.3 Axial-Vector Spectral Density based on the Elastic Decay Width $a_1 \rightarrow \rho\pi$ from the Linear Sigma Model

So far, in order to examine the influence of the parameters  $m_{a_1}$ ,  $\Gamma_{a_1}$ ,  $\delta$  and  $Z$  on the the spectral function, the Breit-Wigner spectral density was used in the axial-vector spectral function  $a_1(s)$ . The results of the previous section are now applied to the study of the fully  $s$ -dependent spectral density on the basis of the  $s$ -dependent decay width  $\Gamma_{a_1 \rightarrow \rho\pi}(s)$ . The decay rate as given in [28] reads

$$\Gamma_{a_1 \rightarrow \rho\pi}(s) = \frac{k(\sqrt{s}, m_\rho, m_\pi)}{12\pi m_{a_1}^2} \left[ h_{\mu\nu}^2 - \frac{(h_{\mu\nu} K_1^\nu)^2}{m_\rho^2} - \frac{(h_{\mu\nu} P^\mu)^2}{m_{a_1}^2} + \frac{(h_{\mu\nu} P^\mu K_1^\nu)^2}{m_\rho^2 m_{a_1}^2} \right] \quad (6.10)$$

and the spectral function for the axial-vector channel is given as

$$a_1(s) = \frac{(2\pi)^2}{S_{EW}} (\delta s + g_1 \phi_0^2)^2 \frac{1}{s} \frac{\rho_A(s)}{N}. \quad (6.11)$$

With (6.10) the parametrisation of the spectral density becomes

$$\rho_A(s) = \frac{\sqrt{s} \Gamma_{a_1 \rightarrow \rho\pi}(s)}{(s - m_{a_1}^2)^2 + (\sqrt{s} \Gamma_{a_1 \rightarrow \rho\pi}(s))^2}. \quad (6.12)$$

Figure 6.7 presents the fully  $s$ -dependent spectral function for three different  $a_1$  masses, each with three different choices of  $Z$  and therefore three values for the full width  $\Gamma_{a_1 \rightarrow \rho\pi}(m_{a_1}^2, Z)$ . The width of the spectral function for a given mass is now solely modified by the choice of  $Z$ . As expected from the Breit-Wigner parametrisation with this choice of parameters  $\delta$  and  $Z$  the calculated spectral function  $a_1(s)$  does not reproduce the data's line shape. The position of the peak is again shifted to smaller  $s$  for smaller  $m_{a_1}$  and the choice of the  $a_1$  mass now also influences the height of the spectral function. With decreasing mass, the peak flattens and for the mass given by the PDG,  $m_{a_1} = 1.23$  GeV, especially for  $\Gamma_{a_1 \rightarrow \rho\pi}(m_{a_1}^2) = 0.600$  GeV, the peak of the spectral function almost disappears.

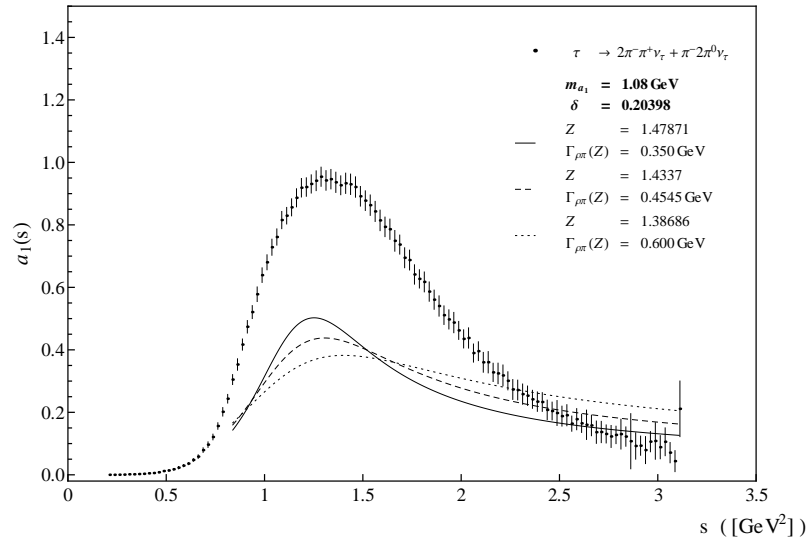
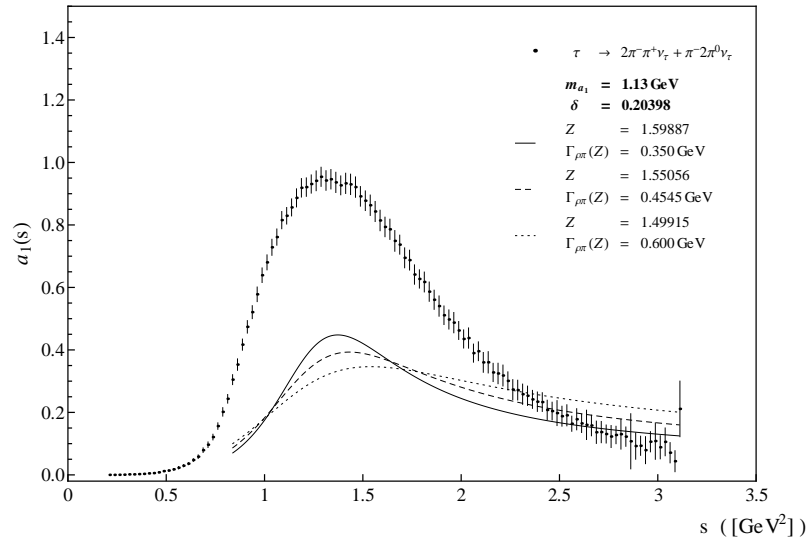
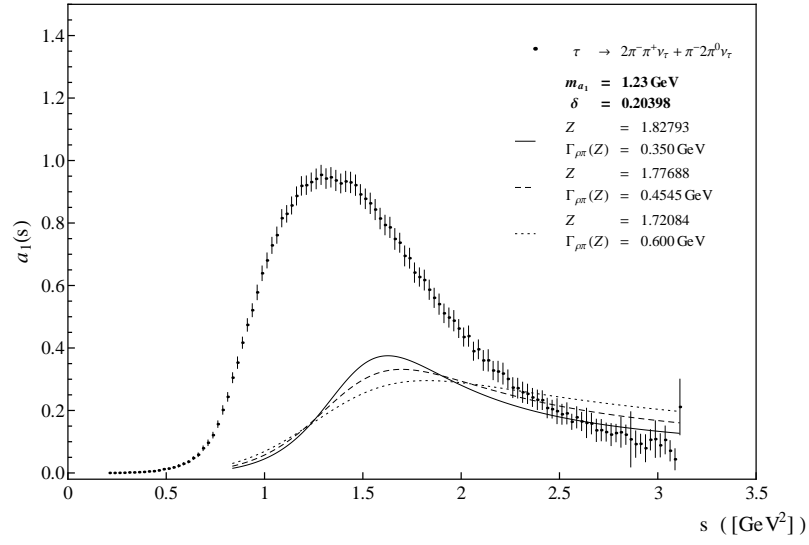


Figure 6.7: The fully  $s$ -dependent spectral function based on the momentum-dependent  $a_1$  decay width  $\Gamma_{a_1 \rightarrow \rho\pi}(s)$  and  $\delta = 0.20398$  for three masses  $m_{a_1} = 1.23$  (1.19 1.08) GeV and three full widths  $\Gamma_{a_1 \rightarrow \rho\pi}(m_{a_1}^2)$ .

## 6.4 Fitted Axial-Vector Spectral Density

Finally, a  $\chi^2$  fit was performed for the axial-vector spectral function. Apart from  $Z$ , which was restricted to  $1.38 < Z < 1.87$ , there were no restrictions imposed on the other parameters. It was attempted to fit the peak and the full width at half maximum. Therefore only a set of data points has been evaluated for the fit. The result is shown in Figure 6.8. From the fit to the fully  $s$ -dependent spectral function  $a_1(s)$  the values

$$\delta = 0.25656 , \quad (6.13)$$

$$Z = 1.48723 , \quad (6.14)$$

$$m_{a_1} = 1.0917 \text{ GeV} , \quad (6.15)$$

$$\Gamma_{\rho\pi}(Z) = 0.4051 \text{ GeV} \quad (6.16)$$

are obtained. Again, if the value for  $\delta$  is taken to be larger than the one that was obtained from assuming that the  $\rho$  resonance is the dominating decay channel in the  $\tau \rightarrow 2\pi$  vector channel one can find a set of parameters that parametrises the spectral function reasonably well within the restrictions of this model.

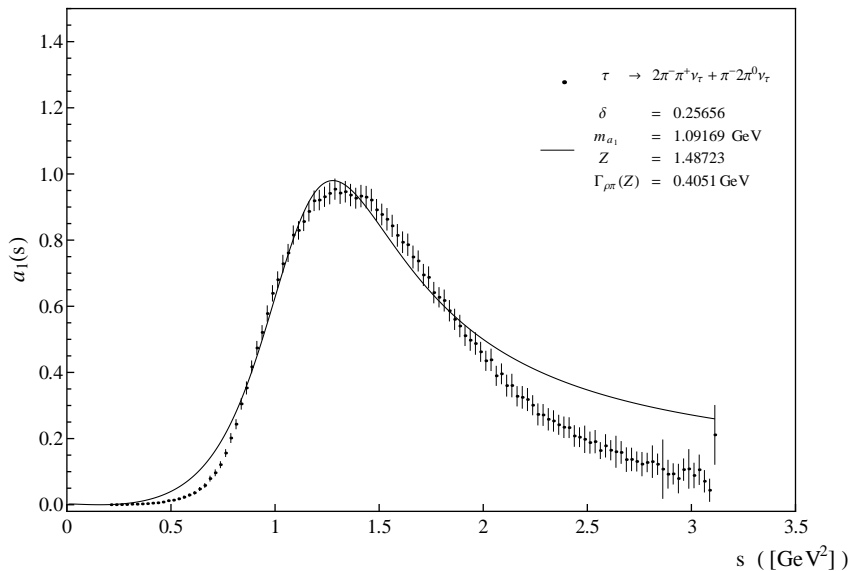


Figure 6.8: Fit for the fully  $s$ -dependent spectral function  $a_1(s)$  with momentum-dependent decay width  $\Gamma_{a_1 \rightarrow \rho\pi}(s)$ .

As in the vector channel, the divergent contributions from the self-energy result in a deviation from the data in the higher  $s$ -range. One may now also

introduce a cut-off function  $f(\Lambda)$  based on the momentum  $k(m_a, m_b, m_c)$  function in (6.10)

$$f(\Lambda) = \exp \left[ -\frac{k(m_{a_1}, m_\rho, m_\pi)^2}{\Lambda^2} \right], \quad (6.17)$$

$$\Gamma_{a_1 \rightarrow \rho\pi}(s, m_{a_1}, Z) \xrightarrow{f_\Lambda(s)} \Gamma_{a_1 \rightarrow \rho\pi}(s, m_{a_1}, Z) \cdot e^{-\frac{k(m_{a_1}, m_\rho, m_\pi)^2}{\Lambda^2}}. \quad (6.18)$$

The decay width thus depends now on the parameters  $m_{a_1}$ ,  $Z$ , and  $\Lambda$ , where  $\Lambda$  is of dimension energy and should not become smaller than  $\Lambda = m_\rho + m_\pi$ . The cut-off parameter was chosen to be 0.9 GeV. Then the results of the fit were stable and did not run to unphysical values.

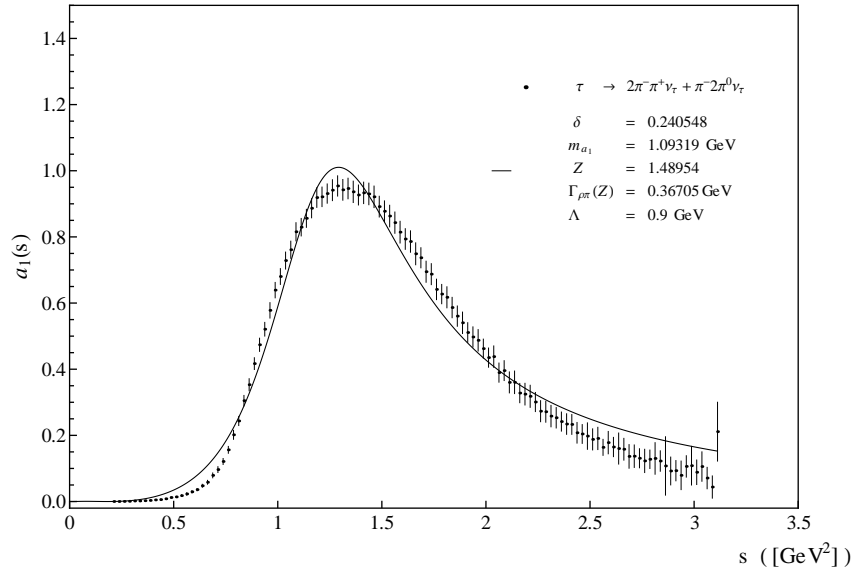


Figure 6.9: Fitted  $a_1(s)$  spectral density with  $s$ -dependent decay width  $\Gamma_{a_1 \rightarrow \rho\pi}(s)$  with cut-off  $\Lambda = 0.9$  GeV.

For the fit with cut-off  $\Lambda = 0.9$  GeV (Fig. 6.9) the results are:

$$\begin{aligned} \delta &= 0.2406, \\ Z &= 1.4895, \end{aligned} \quad (6.19)$$

$$\begin{aligned} m_{a_1} &= 1.09319 \text{ GeV}, \\ \Gamma(m_{a_1}, Z, \Lambda) &= 0.36705 \text{ GeV}. \end{aligned} \quad (6.20)$$

Both fits yield a value for the pion wave-function renormalisation constant  $Z$  of  $\sim 1.48$ . This is actually very well within the range that is necessary to describe the  $a_1 \rightarrow \rho\pi$  decay rate, the  $\sigma \rightarrow \pi\pi$  decay rate, and the axial-vector spectral density simultaneously without inconsistency problems. However,

therefore the vector channel coupling  $\delta$  would have to be approximately 18% larger.

The results for the  $a_1$  masses are almost of the same value and predict  $m_{a_1} \simeq 1.09$  GeV.

With the cut-off the converging contributions from the self energies are removed and  $\Gamma(m_{a_1}^2, Z, \Lambda)$  becomes smaller, but it still remains within the range given by the PDG.

However, if the larger vector-channel coupling  $\delta = 0.24055$  is applied to calculate the fully  $s$ -dependent vector-channel spectral density (Figure 6.10), it is clear that the exact value of  $\delta$  requires further investigation. The spectral function  $v_1(s, \delta = 0.24055)$  clearly exceeds the data. The remaining “free” parameters are to a certain extent the  $\rho$  mass and the  $\rho$  full width. However, a fit with fixed vector coupling,  $\delta = 0.24055$ , and free parameters  $m_\rho$  and  $\Gamma_{\rho \rightarrow \pi^- \pi^0} (m_\rho^2) = \Gamma_\rho^{\text{full}}$  yields a full decay with in the range  $\sim 0.22$  GeV which is definitely too large and does not reproduce the  $2\pi$  vector-channel data.

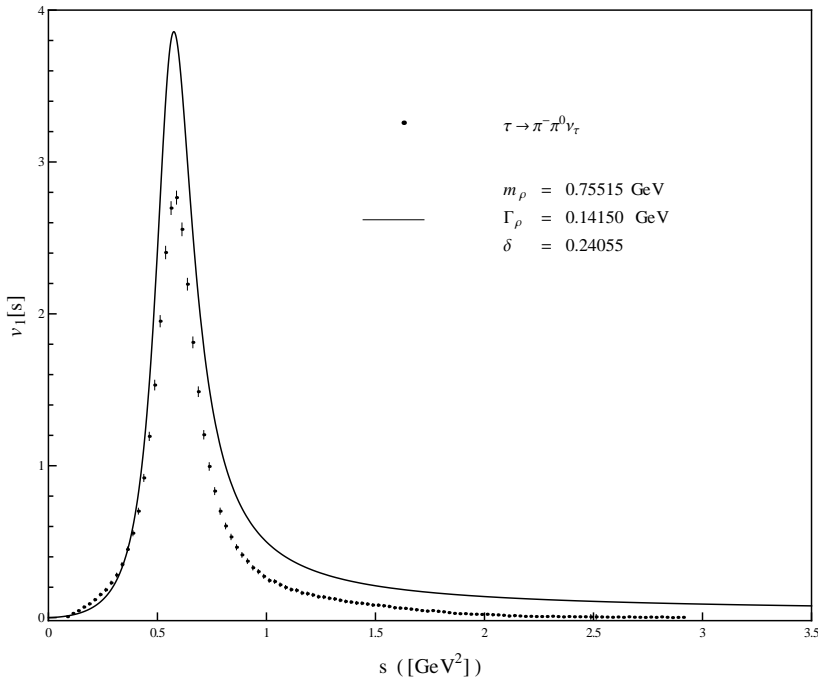


Figure 6.10: Vector channel spectral density with  $\delta = 0.24055$ ,  $\Gamma_{\rho \rightarrow \pi^- \pi^0} (m_\rho^2) = 0.14150$  GeV, and  $m_\rho = 0.75515$  GeV.

The objective of the current work was to describe on tree-level the  $\rho$  and  $a_1$  mesons as  $\bar{q}q$  states within an effective chiral model with electroweak interaction. The spontaneously broken chiral symmetry is reflected in the structure of the effective weak  $\tau \rightarrow a_1 \nu_\tau$  vertex  $g_{a_1} \sim \delta s - g_1 \phi_0^2$ . The coupling  $\delta$  was fixed in the vector channel. The vector-channel coupling  $\delta$  appears to be too small and the difficulties in the generalisation of the result from the vector channel to the axial-vector channel could not be resolved. Thus, vector and axial-vector spectral functions could not be described simultaneously by a common set of parameters.

It further needs to be investigated whether this is really a result of a modification of the vector coupling  $\delta$  by the direct  $W^- \rightarrow \pi^- \pi^0$  decay. Also, it is necessary to implement the other contributions in the axial-vector channel and to examine higher order contributions. Another possibility is to examine the Weinberg sum rules to obtain more insight into the nature of the relations between vector and axial-vector spectral densities within this model. If it proves to be not possible to describe vector and axial-vector spectral densities simultaneously it might as well have more fundamental reasons as, for instance, the question whether within a chiral model  $a_1$  and  $\rho$  can really be described as two  $\bar{q}q$  mesons that are chiral partners.

## Chapter 7

# Conclusions and Outlook

In order to describe the vector and axial-vector spectral functions of the  $\tau$  decay on the basis of an effective quantum field theory with hadronic degrees of freedom and weak interactions, the Linear Sigma Model with scalar, pseudoscalar, vector, and axial-vector mesons based on a global chiral  $U(2)_L \times U(2)_R$  symmetry was extended to a model which is now also invariant under local  $SU(2)_L \times U(1)_Y$  transformations. First, the quark fields were subjected to a  $U(1)_Y$  transformation, which led to the understanding of how the  $U(1)_Y$  transformation manifests itself on the hadronic level of the Linear Sigma Model. Second, it was shown that applying Vector Meson Dominance for the hypercharge gauge field to the Linear Sigma Model yields the same result as it was obtained from directly transforming the quark fields.

The result from applying VMD could then be further used to introduce weak interactions in a gauge-invariant way. Together with a new parameter  $\delta$ , an additional interaction term between the left-handed fields and the weak bosons was introduced into the model in order to generate a mixing term between the charged weak bosons  $W_\mu^\pm$  and  $\rho_\mu^\pm$ . From this extended Lagrangian the tree-level weak interaction vertices were extracted and used to derive effective vector and axial-vector channel couplings  $(g_\rho, g_{a_1})$ . The new mixing term also yielded an additional contribution to the  $W a_1$  mixing, which otherwise would only be proportional to the chiral condensate. The fact that  $\rho$  and  $a_1$  are chiral partners whose mass difference is generated by the spontaneously broken symmetry, is thus also clearly visible in the structure of  $g_{a_1}$ .

In a next step, the decay rate of the Standard Model  $\tau^- \rightarrow W^- \nu_\tau$  process was applied to the  $\tau^- \rightarrow \rho^- \nu_\tau (a_1^- \nu_\tau)$  decay width with an effective coupling that accounted for the  $W$  exchange by a point-like Fermi interaction. The



two couplings were now proportional to the newly introduced  $\delta$ , the Fermi coupling  $G_F$ , and for  $g_{a_1}$  to the chiral condensate  $\phi_0$ . Vector and axial-vector effective couplings were then used to derive a relation between the Källén-Lehmann representation and the ALEPH collaboration's spectral densities of the  $\tau$  decay.

Based on the assumption that the  $\rho$  resonance yields the dominant contributions to the vector channel, the vector-channel spectral function was calculated within several different parametrisations and compared to the experimental data given by the ALEPH collaboration. That way it was possible to obtain numerical results for the parameter  $\delta$ , which could then be used to determine the axial-vector spectral function as well. It was necessary to shift the PDG mass of the  $\rho$  meson to  $m_\rho = 0.76139$  GeV in order to obtain a good description of the data's lineshape. For all parametrisations the calculated vector-channel spectral function with shifted  $\rho$  mass agrees well with the experiment, for the vector channel coupling  $\delta \simeq 0.19$ . However, when this result was applied to the axial-vector spectral function, it was found that with the given parameter set the calculated spectral function describes approximately only half of the data.

The problem of the too small axial-vector spectral function turned out to be independent on whether one used the Breit-Wigner parametrisation or the spectral density based on the  $s$ -dependent decay width  $\Gamma_{a_1 \rightarrow \rho\pi}(s)$ . Since the range of the parameter  $Z$  is strongly limited by the  $a_1 \rightarrow \rho\pi$  decay width, one solution would be to further study the influence of the process  $W \rightarrow \pi\pi$  on the vector-channel coupling  $\delta$ . If  $\delta$  were about 25% larger, one could also describe the axial-vector spectral function very well.

Furthermore, for the axial-vector channel the assumption was made that the process  $a_1 \rightarrow \rho\pi$  dominates this decay channel, but there are further contributions such as  $a_1 \rightarrow \sigma\pi$  and  $a_1 \rightarrow f_0\pi$  that yield three-pion final states and might also contribute. Currently there are no reliable data for the  $a_1$  branching fractions and one should also take into account the results on their decay widths as calculated from the Lagrangian to see whether this improves the results.

It is also necessary to improve on the accuracy of the parameters  $\delta$ ,  $m_\rho$ ,  $\Gamma_\rho$  and  $Z$ . The spectral functions are very sensitive to the numerical values of the parameters, which in principle enables their determination with high precision, and thus it is also a good test of the model's validity. On the other hand, this raises the difficulty of how to fix all the parameters in a consistent way. Moreover because of finite width effects of the uncertainty in the  $a_1$  mass, which makes the study of its resonance difficult.

Calculating the spectral densities and comparing them to the ALEPH data,

allows for a precise determination of the parameters. Once the parameters are fixed consistently, the model can be further applied to make predictions of other physical observables, such as meson masses and decay widths.

Another possibility is the generalisation of the  $U(2)_L \times U(2)_R$  Linear Sigma Model with weak interaction to the case of  $N_f = 3$ . The extension of the model to  $N_f = 3$  is already in progress. Also, this work is based on considerations in the vacuum, one natural direction for further investigations is the application of the fixed parameters to in-medium effects and non-zero temperature processes.

If it is possible to resolve the inconsistencies between the parameters of the vector channel and the axial-vector channel, it would also yield strong evidence that the resonance which is observed at  $s \simeq 1.15 \text{ GeV}^2$  and whose nature has not yet been unambiguously identified can be understood as the  $J^{PC} = 1^{++}$  iso-triplet resonance of the  $U(N_f = 3)$  meson nonet.

# Appendix A

## Field Strength Tensors $L^{\mu\nu}$ and $R^{\mu\nu}$

The following explanation is based on Chapter 15.1 in Peskin and Schroeder's book on Quantum Field Theory [16]. In gauge theories the field strength tensors of the fields can be calculated from the commutator  $[D^\mu, D^\nu]$  of the covariant derivative. If a Lagrangian of a field  $\phi$  has a local symmetry under the transformation

$$\phi \rightarrow \phi' = U\phi \tag{A.1}$$

the commutator of the covariant derivatives  $[D_\mu, D_\nu]\phi$  must be invariant under the transformations itself, as it is only the product of two covariantly transforming factors. The commutator does not act on  $\phi$  as a derivative, but as a multiplicative factor, only. Since this proves the gauge invariance of the field strength tensors within the context of the globally  $SU(2)_L \times SU(2)_R$  invariant Linear Sigma Model the calculation will be performed explicitly.

In Chapter 2.2 the covariant derivative with the electroweak gauge bosons was defined as

$$D^\mu\Phi = \partial^\mu\Phi - ig_1(L^\mu\Phi - \Phi R^\mu) - igW^\mu\Phi + ig'B^\mu, \tag{A.2}$$

where the field  $\Phi$  is a tensor product on the space of left- and right-handed isospin with altogether 4 indices. The general chiral transformation then reads

$$(U_L \otimes U_R^*)\Phi \tag{A.3}$$

For mesons this reduces to the known transformation law  $\Phi' = U_L\Phi U_R$ . In order to calculate the field strength tensors from the commutator of the

covariant derivative one needs to factor out the field  $\Phi$  in (A.2). Therefore it is useful to write  $D^\mu\Phi$  explicitly as a four tensor, then one can also see on what spaces the gauge fields and  $L^\mu, R^\mu$  act on

$$(D^\mu\phi)_{ij} = \{(\mathbb{1} \otimes \mathbb{1})_{ik,jl}\partial^\mu - ig_1[(L^\mu \otimes \mathbb{1}) - (\mathbb{1} \otimes R^{\mu T})]_{ik,jl} - ig(W^\mu \otimes \mathbb{1})_{ik,jl} + ig'(\mathbb{1} \otimes B^{\mu T})_{ik,jl}\}\phi_{kl} . \quad (\text{A.4})$$

The commutator then yields the sum of all field strength tensors for the left- and right-handed mesons, as well as for the gauge bosons  $W^\mu$  and  $B^\mu$ . The calculation was performed assuming that chiral symmetry were local. The consequences with respect to the commutator for left- and right-handed fields, as well as for the coupling constant  $g_1$  from local symmetry were disregarded only later in the definition of the left- and right-handed field strength tensors.

In this context the field strength tensors  $L^{\mu\nu}$  for the left-handed fields will now be derived from

$$-ig_1L^{\mu\nu} = [D_L^\mu, D_L^\nu]. \quad (\text{A.5})$$

For simplicity the covariant derivative in the equation above has been defined as

$$D_L^\mu = \partial^\mu - ig_1L^\mu - igW^\mu . \quad (\text{A.6})$$

Since  $L^\mu$  and  $R^\mu$  act on different spaces, they commute with each other, as well as  $L^\mu$  with  $B^\mu$  and  $R^\mu$  with  $W^\mu$ , thus one can simply take those terms that act from the left on  $\Phi$ . This is also seen, when one uses the representation of  $D^\mu\Phi$  as a four tensor in the left- and right-handed product space. The commutator is obtained as

$$\begin{aligned} [D_L^\mu, D_L^\nu] &= [\partial^\mu - ig_1L^\mu - igW^\mu, \partial^\nu - ig_1L^\nu - igW^\nu] \\ &= -ig_1\partial^\mu L^\nu - ig\partial^\mu W^\nu - g_1^2L^\mu L^\nu - g_1gL^\mu W^\nu \\ &\quad - gg_1W^\mu L^\nu - g^2W^\mu W^\nu \\ &\quad - (-ig_1\partial^\nu L^\mu - ig\partial^\nu W^\mu - g_1^2L^\nu L^\mu - g_1gL^\nu W^\mu \\ &\quad - gg_1W^\nu L^\mu - g^2W^\nu W^\mu) \\ &= -ig_1\{\partial^\mu L^\nu - \partial^\nu L^\mu - ig_1[L^\mu, L^\nu] - ig[W^\mu, L^\nu] + ig[L^\mu, W^\nu]\} \\ &\quad - ig\{\partial^\mu W^\nu - \partial^\nu W^\mu - ig[W^\mu, W^\nu]\} . \end{aligned} \quad (\text{A.7})$$

In the global model the coupling constant of the commutator of the mesonic fields is not necessarily  $g_1$  anymore. The non-abelian contributions  $[L^\mu, L^\nu]$ , are therefore proportional to a new coupling constant  $g_2$  and are excluded from the definition of the field strength tensor

$$L^{\mu\nu} = \partial^\mu L^\nu - ig[W^\mu, L^\nu] - (\partial^\nu L^\mu - ig[W^\nu, L^\mu]) . \quad (\text{A.8})$$

The right-handed covariant derivative is defined as

$$D_R^\mu \Phi = \partial^\mu \Phi + ig_1 \Phi R^\mu + ig' \Phi B^\mu . \quad (\text{A.9})$$

In order to factor out  $\Phi$ ,  $D_R^\mu \Phi$  is written as a four tensor. In the product space the chiral transformations act on  $\Phi$  as

$$\Phi_{ij} \rightarrow \phi'_{ij} = (U_L)_{ik} \Phi_{kl} (U_R^\dagger)_{lj} = (U_L \otimes U_R^*)_{ik,jl} , \quad (\text{A.10})$$

where " $\otimes$ " denotes the tensor (dyadic) product.

Then the covariant derivative reads

$$\begin{aligned} (D_R^\mu \Phi)_{ij} &= (\partial^\mu \Phi)_{ij} + ig_1 (\Phi R^\mu)_{ij} + ig' (\Phi B^\mu)_{ij} \\ &= \delta_{ik} \partial^\mu \Phi_{kl} \delta_{lj} + ig_1 \delta_{il} \Phi_{lk} R_{kj}^\mu + ig' \delta_{il} \Phi_{lk} B_{kj}^\mu \\ &= \delta_{ik} \delta_{jl} \Phi_{kl} + ig_1 \delta_{il} R_{jk}^{\mu T} \Phi_{lk} + ig_1 \delta_{il} B_{jk}^{\mu T} \Phi_{lk} \\ &= (\mathbf{1} \otimes \mathbf{1})_{ik,jl} \Phi_{kl} + ig_1 (\mathbf{1} \otimes R^{\mu T})_{ik,jl} \Phi_{kl} + ig_1 (\mathbf{1} \otimes B^{\mu T})_{ik,jl} \Phi_{kl} . \end{aligned} \quad (\text{A.11})$$

Thus, one can write

$$D_R^\mu = \partial^\mu + ig_1 R^{\mu T} + ie B^{\mu T} . \quad (\text{A.12})$$

and follow the same steps as in the calculation for  $L^{\mu\nu}$ . The right-handed field strength tensor is obtained as

$$R^{\mu\nu} = \partial^\mu R^\nu - ig' [B^\mu, R^\nu] - (\partial^\nu R^\mu - ie [B^\nu, R^\mu]) . \quad (\text{A.13})$$

The non-abelian contributions for the left- and right-handed fields read

$$-2ig_2 \{ \text{Tr}[L_{\mu\nu}[L_\mu, L_\nu]] + \text{Tr}[R_{\mu\nu}[R_\mu, R_\nu]] \} \quad (\text{A.14})$$

and they are transferred to an additional term  $\mathcal{L}_3$  (see section 2.1).

## Appendix B

### $W\rho$ Vertex

The mixing term between the  $W$  boson and the  $\rho$  meson is given by

$$\frac{g \cos \theta_C \delta}{2} \partial_\mu W_\nu^- (\partial^\mu \rho^{\nu+} - \partial^\nu \rho^{\mu+}) + \text{h.c.} . \quad (\text{B.1})$$

Integration by parts yields

$$\int_V \partial_\mu W_\nu^- \partial^\mu \rho^{\nu+} dV = \int_V \partial_\mu (W_\nu^- \partial^\mu \rho^{\nu+}) dV - \int_V W_\nu^- \partial_\mu \partial^\mu \rho^{\nu+} dV \quad (\text{B.2})$$

and

$$\int_V \partial_\mu W_\nu^- \partial^\nu \rho^{\mu+} dV = \int_V \partial_\mu (W_\nu^- \partial^\nu \rho^{\mu+}) dV - \int_V W_\nu^- \partial_\mu \partial^\nu \rho^{\mu+} dV . \quad (\text{B.3})$$

Applying Gauss' theorem to the first integral over the surface of a large volume in (B.2) and (B.3), and the Proca condition  $\partial_\mu \rho^\mu = 0$  to the latter term in (B.3) yields

$$\partial_\mu W_\nu^- (\partial^\mu \rho^{\nu+} - \partial^\nu \rho^{\mu+}) = -W_\nu^- \partial_\mu \partial^\mu \rho^{\nu+} \quad (\text{B.4})$$

for the mixing term. After performing the derivative in (B.4) one obtains  $\partial^\mu \rightarrow iq^\mu$  and with  $q_\mu q^\mu = s$  the mixing term reads

$$-\frac{g \cos \theta_C \delta s}{2} W_\nu^- \rho^{\nu+} . \quad (\text{B.5})$$

## Appendix C

# Invariant Mass-Squared Distribution

The spectral function in [25] depends on the invariant mass-squared distribution

$$\frac{1}{N} \frac{dN}{ds} , \quad (\text{C.1})$$

which contains the information on the line shape of the experimental spectral function. In this chapter the relation between the invariant mass-squared distribution (C.1) and the theoretical spectral function  $\rho(s)$  is derived. The number of  $2\pi$  final states  $N_V$  in the vector channel of  $\tau$  decay can be written as

$$N_{2\pi} = B(\tau \rightarrow 2\pi\nu_\tau)N_\tau , \quad (\text{C.2})$$

with

$$B(\tau \rightarrow 2\pi\nu_\tau) = \frac{\Gamma_{\tau \rightarrow 2\pi\nu_\tau}}{\Gamma_\tau^{\text{tot}}} \quad (\text{C.3})$$

being the branching fraction of the respective decay channel normalised to  $\Gamma_\tau^{\text{tot}}$ . Now, the convolution (see (4.11)) of the spectral function in the respective channel  $\rho_V(s)$  with the decay width of  $\tau \rightarrow \rho\nu_\tau$  gives the decay rate for the vector channel

$$\Gamma_{\tau \rightarrow 2\pi\nu_\tau} = \int_0^\infty ds [\rho_V(s)\Gamma_{\tau \rightarrow \rho\nu_\tau}(s)] . \quad (\text{C.4})$$

Taking the derivative with respect to  $s$  on both sides of (C.2) yields

$$\frac{dN_{2\pi}}{ds} = \frac{N_\tau}{\Gamma_\tau^{\text{tot}}} \rho_V(s)\Gamma_{\tau \rightarrow \rho\nu_\tau}(s) . \quad (\text{C.5})$$

Multiplying the right-hand side of (C.5) with  $1 = \Gamma_{\tau \rightarrow 2\pi\nu_\tau} / \Gamma_{\tau \rightarrow 2\pi\nu_\tau}$  and using (C.2) again then yields the expression of the invariant mass-squared distribution in terms of the vector spectral function and the decay width in the respective channel

$$\begin{aligned} \frac{1}{N_{2\pi}} \frac{dN_{2\pi}}{ds} &= \frac{1}{\Gamma_{\tau \rightarrow 2\pi\nu_\tau}} \rho_V(s) \Gamma_{\tau \rightarrow \rho\nu_\tau}(s) \\ &= \frac{\rho_V(s) \Gamma_{\tau \rightarrow \rho\nu_\tau}(s)}{\int_0^\infty ds [\rho_V(s) \Gamma_{\tau \rightarrow \rho\nu_\tau}(s)]}. \end{aligned} \quad (\text{C.6})$$



## Appendix D

### $\tau \rightarrow W \nu_\tau$ Decay Width

The decay  $\tau \rightarrow W \nu_\tau$  is well known from the electroweak sector of the Standard Model. Bosons, as well as the  $a_1$  and  $\rho$  mesons are vector fields and thus yield the same amplitudes for decay processes. The decay width  $\tau \rightarrow W \nu_\tau$  is calculated in this chapter, under the assumption that the  $W$  boson were virtual and severely off-shell. Then the  $W$  propagator in the diagram depicted in Fig. D.1 will be replaced by a point-like interaction vertex proportional to the inverse mass of  $W$ . Because of the off-shell nature of the process  $\tau \rightarrow W \nu_\tau \rightarrow \rho \nu_\tau$  ( $a_1 \nu_\tau$ ) the  $W$  boson's mass  $M_W^2$  in the decay width is replaced by the running mass  $s$ . Thus, the result can be used as the energy-dependent decay width  $\Gamma(s)$  for the processes  $\tau \rightarrow \rho \nu_\tau$  ( $a_1 \nu_\tau$ ).

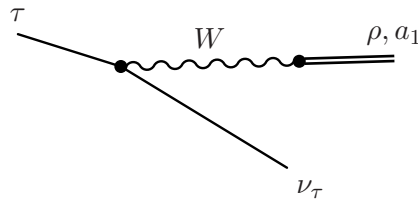


Figure D.1: The decay  $\tau \rightarrow W \nu_\tau \rightarrow \rho \nu_\tau$  ( $a_1 \nu_\tau$ ).

The charged weak interaction Lagrangian for leptons is given in Chapter 1.4 as

$$\begin{aligned} \mathcal{L}_{\tau \rightarrow W \nu_\tau} &= g \bar{\psi} (W_{\mu 1} t_1 + W_{\mu 2} t_2) \gamma^\mu (1 - \gamma^5) \psi \\ &= \frac{g}{2\sqrt{2}} \bar{\psi}_{\nu_\tau} W_\mu^- \gamma^\mu (1 - \gamma^5) \psi_\tau + h.c. . \end{aligned} \quad (\text{D.1})$$

The decay width is obtained from the squared S-matrix element of first order. The factor  $\frac{1}{2}$  considers the two possible directions of polarisation of the decaying  $\tau$  lepton, while summing over  $\lambda$  and  $s$ ,  $s'$  refers to the polarisations of all the fields that participate in the decay

$$\Gamma_{\tau \rightarrow W \nu_\tau} = \frac{1}{T} V \int \frac{d^3 k}{(2\pi)^3} V \int \frac{d^3 q'}{(2\pi)^3} \frac{1}{2} \sum_{\lambda=1}^3 \sum_{s', s=1}^2 | -i\mathcal{M} |^2 . \quad (\text{D.2})$$

The wave functions of the in- and outgoing particles are

$$W_\mu^- = \frac{\varepsilon_\mu}{\sqrt{2V}k_0} e^{ik \cdot x}, \quad \bar{\psi}_{\nu_\tau} = \frac{\bar{u}_{\nu_\tau}}{\sqrt{2V}q'_0} e^{iq' \cdot x}, \quad \psi_\tau = \frac{u_\tau}{\sqrt{2V}q_0} e^{-iq \cdot x}. \quad (\text{D.3})$$

Then the squared S-matrix element reads

$$\begin{aligned} | -i\mathcal{M} |^2 &= \left| -i \int d^4 x \frac{-g}{2\sqrt{2}} \bar{\psi}_{\nu_\tau} \gamma^\mu (1 - \gamma^5) \psi_\tau W_\mu^- \right|^2 \\ &= \left( \frac{-g}{2\sqrt{2}} \right)^2 \frac{1}{8V^3 q_0 q'_0 k_0} \left( \int d^4 x \varepsilon_\mu e^{ik \cdot x} \bar{u}_{\nu_\tau} e^{iq' \cdot x} \gamma^\mu (1 - \gamma^5) u_\tau e^{-iq \cdot x} \right)^2, \end{aligned} \quad (\text{D.4})$$

with  $k$  and  $q'$  describing the outgoing momenta,  $\lambda$  the directions of polarisation of the  $W$  boson, and  $s, s'$  the spin of  $\tau$  and  $\nu_\tau$ .

Integrating over space time then yields

$$(\delta^4(q' + k - q))^2 = \delta^4(q' + k - q) \delta^4(0) = \frac{VT}{(2\pi)^4} \delta^4(q' + k - q)$$

such that the decay width reads

$$\begin{aligned} \Gamma_{\tau \rightarrow W \nu_\tau} &= \frac{1}{8(2\pi)^2} \left( \frac{-g}{2\sqrt{2}} \right)^2 \times \\ &\quad \frac{1}{q_0} \int \frac{d^4 k}{k_0} \int \frac{d^4 q'}{q'_0} \delta^4(q' + k - q) \frac{1}{2} \sum_{\lambda, s, s'} |\varepsilon^\mu \bar{u}_{\nu_\tau} \gamma^\mu (1 - \gamma^5) u_\tau|^2. \end{aligned} \quad (\text{D.5})$$

The fermionic and bosonic projection operators are defined as

$$\sum_{\lambda=1}^3 \varepsilon_\mu(k, \lambda) \varepsilon_\nu(k, \lambda) = -g_{\mu\nu} + \frac{k_\mu k_\nu}{M_W^2} \quad (\text{D.6})$$

$$\sum_{s=1}^2 u_\alpha(q, s) \bar{u}_\beta(q, s) = (\not{q} + m)_{\alpha\beta}. \quad (\text{D.7})$$

With this relation for the sum over the spin directions and together with the assumption that the neutrinos are massless one obtains

$$\begin{aligned}
& \frac{1}{2} \sum_{\lambda=1}^3 \sum_{s',s=1}^2 |\varepsilon_{\mu} \bar{u}_{\nu\tau} \gamma^{\mu} (1 - \gamma^5) u_{\tau}|^2 \\
&= \frac{1}{2} \left( -g_{\mu\nu} + \frac{k_{\mu} k_{\nu}}{M_W^2} \right) \text{Tr}[(\not{q} + m_{\tau}) \gamma^{\mu} (1 - \gamma^5) \not{q}' \gamma^{\nu} (1 - \gamma^5)] \\
&= 8 \left( -g_{\mu\nu} + \frac{k_{\mu} k_{\nu}}{M_W^2} \right) (q^{\mu} q'^{\nu} + q^{\nu} q'^{\mu} - (q \cdot q') g^{\mu\nu}) \\
&= \frac{8}{M_W^2} \left[ \left( M_W^2 - \frac{k \cdot k}{2} \right) (q \cdot q') + 2(k \cdot q)(k \cdot q') \right]. \quad (\text{D.8})
\end{aligned}$$

The trace over the product of Dirac matrices has been calculated according to the identities

$$\begin{aligned}
\text{Tr}[\gamma^{\alpha} \gamma^{\beta} \gamma^{\gamma} \gamma^{\delta}] &= 4(g^{\alpha\beta} g^{\gamma\delta} + g^{\alpha\delta} g^{\beta\gamma} - g^{\alpha\gamma} g^{\beta\delta}) \\
\text{Tr}[\gamma^{\alpha} \gamma^{\beta} \gamma^{\gamma} \gamma^{\delta} \gamma^5] &= -4\varepsilon^{\alpha\beta\gamma\delta}.
\end{aligned}$$

Finally only the integral

$$\begin{aligned}
& \Gamma_{\tau \rightarrow W \nu_{\tau}} \\
&= \frac{1}{(2\pi)^2} \left( \frac{-g}{2\sqrt{2}} \right)^2 \frac{1}{m_{\tau} M_W^2} \otimes \\
& \int \frac{d^3 k}{k_0} \int \frac{d^3 q'}{q'_0} \delta^4(q' + k - q) \left[ \left( M_W^2 - \frac{k \cdot k}{2} \right) (q \cdot q') + (k \cdot q)(k \cdot q') \right] \quad (\text{D.9})
\end{aligned}$$

has to be calculated.

In the  $\tau$  centre-of-mass frame one obtains for the four momenta

$$\begin{pmatrix} m_{\tau} \\ \vec{0} \end{pmatrix} = \begin{pmatrix} |\vec{q}'| \\ \vec{q}' \end{pmatrix} + \begin{pmatrix} \sqrt{x^2 + \vec{k}^2} \\ \vec{k} \end{pmatrix}$$

where  $x$  refers to the mass of the off-shell  $W$  boson.

The four-dimensional delta function can be written as

$$\delta^4(q' + k - q) = \delta(q'_0 + k_0 - q_0) \delta^{(3)}(\vec{q}' + \vec{k}).$$

Then the integral reads

$$\int \frac{d^3 k}{k_0} \int \frac{d^3 q'}{q'_0} \delta(q'_0 + k_0 - q_0) \delta^{(3)}(\vec{q}' + \vec{k})$$

$$\begin{aligned}
&= 4\pi \int \frac{k^2 dk}{\sqrt{x^2 + k^2}} \int \frac{d^3 q'}{|\vec{q}_0'|} \delta(q'_0 + k_0 - q_0) \delta^{(3)}(\vec{q}' + \vec{k}) \\
&= 4\pi \int dk \delta\left(k - \frac{m_\tau^2 - x^2}{2m_\tau}\right) \frac{k}{\left(1 + \frac{k}{\sqrt{x^2 + k^2}}\right) \sqrt{x^2 + k^2}} \\
&= 4\pi \left(\frac{m_\tau^2 - x^2}{2m_\tau}\right) \frac{1}{m_\tau}. \tag{D.10}
\end{aligned}$$

Inserting the energy-momentum relation in the  $\tau$  centre-of-mass frame yields

$$\left(M_W^2 - \frac{k \cdot k}{2}\right) (q \cdot q') + (k \cdot q)(k \cdot q') = \frac{1}{2} m_\tau^3 \left(\frac{m_\tau^2 - x^2}{2m_\tau}\right) \left(1 + \frac{2M_W^2}{m_\tau^2}\right). \tag{D.11}$$

Finally, inserting (D.10) and (D.11) into the expression for the decay width (D.9) one obtains

$$\Gamma_{\tau \rightarrow W \nu_\tau}(x^2) = \frac{1}{8\pi} \left(\frac{-g}{2\sqrt{2}}\right)^2 \frac{m_\tau^3}{M_W^2} \left(1 - \frac{x^2}{m_\tau^2}\right)^2 \left(1 + \frac{2M_W^2}{m_\tau^2}\right). \tag{D.12}$$

With  $M_W^2, x^2 \rightarrow s$  and an effective Fermi coupling

$$G_F = \frac{g^2}{2\sqrt{2}M_W^2}, \tag{D.13}$$

the  $s$ -dependent decay width for  $\tau \rightarrow \rho(a_1)\nu_\tau$  can be written as

$$\Gamma_{\tau \rightarrow \rho(a_1)\nu_\tau}(s) = \frac{1}{8\pi} (g_{\rho/a_1})^2 \frac{m_\tau^3}{s} \left(1 - \frac{s}{m_\tau^2}\right)^2 \left(1 + \frac{2s}{m_\tau^2}\right), \tag{D.14}$$

with  $g_\rho$  and  $g_{a_1}$  being defined as the product of the Fermi coupling constant with the  $W\rho$  and  $W a_1$  couplings, from the results (3.25) and (3.26)

$$g_\rho = \frac{g^2 \cos \theta_C}{4\sqrt{2}M_W^2} \delta s, \tag{D.15}$$

$$g_{a_1} = \frac{g^2 \cos \theta_C}{4\sqrt{2}M_W^2} (g_1 \phi_0^2 + \delta s). \tag{D.16}$$

# Bibliography

- [1] J. C. Maxwell, *A Dynamical Theory of the Electromagnetic Field*, *Royal Society Transactions* **CLV** (1864).
- [2] M. Gell-Mann, *The Eightfold Way: A Theory of Strong Interaction Symmetry*, *California Institute of Technology, Report CTSL-20* (1961).
- [3] J. H. Christenson *et al.*, *Observation of Massive Muon Pairs in Hadron Collisions*, *Phys. Rev. Lett.* **25** (1970) 1523–1526.
- [4] D. H. Perkins, *Introduction to High Energy Physics*. Cambridge University Press, 4th ed., 2000.
- [5] A. S. Kronfeld and C. Quigg, *Resource Letter: Quantum Chromodynamics*, [arXiv:1002.5032](https://arxiv.org/abs/1002.5032).
- [6] Particle Data Group, K. Nakamura *et al.*, *Review of Particle Physics*, *J.Phys.* **G37** (2010) 075021.
- [7] J. Donoghue, E. Golowich, and B. R. Holstein, *Dynamics of the Standard Model*, vol. 2 of *Camb.Monogr.Part.Phys.Nucl.Phys.Cosmol.* 1992.
- [8] W. Greiner and B. Mueller, *Quantum Mechanics Symmetries*. Springer, 2008.
- [9] M. Gell-Mann and M. Levy, *The Axial Vector Current in Beta Decay*, *Nuovo Cim.* **16** (1960) 705.
- [10] 't Hooft, G., *Symmetry Breaking through Bell-Jackiw Anomalies*, *Phys. Rev. Lett.* **37** (1976) 8.
- [11] I. Aitchison and A. Hey, *Gauge Theories in Particle Physics 2*. Taylor & Francis, 3rd ed., 2004.
- [12] S. L. Adler, *Axial Vector Vertex in Spinor Electrodynamics*, *Phys. Rev.* **177** (1969) 2426–2438.

- [13] C. Bouchiat, J. Iliopoulos, and P. Meyer, *An Anomaly Free Version of Weinberg's Model*, *Phys.Lett.* **B38** (1972) 519–523.
- [14] V. Koch, *Introduction to Chiral Symmetry*, [nucl-th/9512029](#).
- [15] J. Goldstone, *Field Theories with Superconductor Solutions*, *Nuovo Cim.* **19** (1961) 154–164.
- [16] M. Peskin and D. Schroeder, *An Introduction to Quantum Field Theory*. Perseus Books, 1995.
- [17] A. Pich, *The Standard model of electroweak interactions*, [arXiv:0705.4264](#).
- [18] P. Ko and S. Rudaz, *Phenomenology of Scalar and Vector Mesons in the Linear Sigma Model*, *Phys.Rev.* **D50** (1994) 6877–6894.
- [19] S. Gasiorowicz and D. Geffen, *Effective Lagrangians and Field Algebras with Chiral Symmetry*, *Rev.Mod.Phys.* **41** (1969) 531–573.
- [20] M. Urban, M. Buballa, and J. Wambach, *Vector and Axial-Vector Correlators in a Chirally Symmetric Model*, *Nucl. Phys.* **A697** (2002) 338–371, [[hep-ph/0102260](#)].
- [21] S. Strüber and D. H. Rischke, *Vector and Axialvector Mesons at Nonzero Temperature within a Gauged Linear Sigma Model*, *Phys. Rev.* **D77** (2008) 085004, [[arXiv:0708.2389](#)].
- [22] D. Roder, J. Ruppert, and D. H. Rischke, *Chiral Symmetry Restoration in Linear Sigma Models with different Numbers of Quark Flavors*, *Phys. Rev.* **D68** (2003) 016003, [[nucl-th/0301085](#)].
- [23] D. Parganlija, *Pion-Pion-Streuung in einem geeichten linearen Sigma-Modell mit chiraler  $U(2)_L \times U(2)_R$  Symmetrie*. Johann Wolfgang Goethe-Universität, Diplomarbeit, 2006.
- [24] H. B. O'Connell, B. C. Pearce, A. W. Thomas, and A. G. Williams,  *$\rho - \omega$  mixing, Vector Meson Dominance and the Pion Form-Factor*, *Prog. Part. Nucl. Phys.* **39** (1997) 201–252, [[hep-ph/9501251](#)].
- [25] ALEPH Collaboration, S. Schael *et al.*, *Branching Ratios and Spectral Functions of Tau Decays: Final ALEPH measurements and physics implications*, *Phys.Rept.* **421** (2005) 191–284, [[hep-ex/0506072](#)].
- [26] F. Giacosa and G. Pagliara, *On the Spectral Functions of Scalar Mesons*, *Phys. Rev.* **C76** (2007) 065204, [[arXiv:0707.3594](#)].
- [27] <http://aleph.web.lal.in2p3.fr/tau/specfun.html>

- [28] D. Parganlija, F. Giacosa, and D. H. Rischke, *Vacuum Properties of Mesons in a Linear Sigma Model with Vector Mesons and Global Chiral Invariance*, *Phys. Rev.* **D82** (2010) 054024, [arXiv:1003.4934].
- [29] P. Lichard and M. Vojik, *An alternative Parametrization of the Pion Form Factor and the Mass and Width of Rho(770)*, hep-ph/0611163.
- [30] M. Wagner and S. Leupold, *Information on the Structure of the a(1) from Tau Decay*, *Phys.Rev.* **D78** (2008) 053001, [arXiv:0801.0814].
- [31] S. Leupold, *Different Nature of rho and a1*, *PoS* **CD09** (2009) 051.
- [32] CLEO Collaboration, D.M. Asner *et al.*, *Hadronic Structure in the Decay  $\tau \rightarrow \nu_\tau \pi^- \pi^0 \pi^0$  and the Sign of the Tau-Neutrino Helicity*, *Phys.Rev.* **D61** (2000) 012002, [hep-ex/9902022].